

Modeling Satellite Formations In The Presence Of Perturbations

2005

Robert Cannaday
University of Central Florida

Find similar works at: <https://stars.library.ucf.edu/etd>

University of Central Florida Libraries <http://library.ucf.edu>

 Part of the [Aerospace Engineering Commons](#)

STARS Citation

Cannaday, Robert, "Modeling Satellite Formations In The Presence Of Perturbations" (2005). *Electronic Theses and Dissertations*. 537.
<https://stars.library.ucf.edu/etd/537>

This Masters Thesis (Open Access) is brought to you for free and open access by STARS. It has been accepted for inclusion in Electronic Theses and Dissertations by an authorized administrator of STARS. For more information, please contact lee.dotson@ucf.edu.

MODELING
SATELLITE FORMATIONS
IN THE PRESENCE
OF PERTURBATIONS

by

ROBERT L.CANNADAY
B.S. Florida State University, 1969

A thesis submitted in partial fulfillment of the requirements
for the degree of Master of Science in Aerospace Engineering
in the Department of Mechanical, Materials, and Aerospace Engineering
in the College of Engineering and Computer Science
at the University of Central Florida
Orlando, Florida

Fall Term
2005

© 2005 Robert L. Cannaday

ABSTRACT

The potential benefits of autonomous satellite formation flying in such areas as high-resolution remote sensing, and sparse aperture radar, has stimulated interest in modeling the satellite environment for feasibility and simulation studies to help explore and define the technical challenges that must be solved in order to achieve successful autonomous satellite formations. The purpose of this paper is to develop and describe a numerical simulation of the orbital environment including central force field perturbations and atmospheric drag effects which will be a useful analytical tool for investigating issues relating to maintaining satellite formations in low-earth-orbit. Many of the studies done in this area confine their research to circular orbits, with and without perturbation effects. This study will investigate apply orbital dynamic equations to the problem of maintaining satellite formations in both circular and elliptical orbits, with and without the presence of J_2 gravity perturbation effects and atmospheric drag. This effort is primarily focused on modeling the orbital mechanics of one and two satellites in the presence of J_2 and drag perturbations This effort is being performed as part of a multi-disciplined University of Central Florida KnightSat project, sponsored by the Air Force, to develop a two-satellite formation in the nanosatellite class, for investigating issues related to using formation satellites for remote earth sensing, to develop three-dimensional mapping.

ACKNOWLEDGMENTS

To God who brought me through this,

"The heavens declare the glory of God;

And the firmament shows His handiwork." Psalm 19:1

To my wife, Linda, who supported me in this endeavor, and

To Dr Roger Johnson, my thesis advisor, who provided

challenges, direction, and invaluable insight.

TABLE OF CONTENTS

LIST OF FIGURES	vi
LIST OF TABLES	viii
LIST OF ACRONYMS/ABBREVIATIONS/SYMBOLS	ix
CHAPTER ONE: INTRODUCTION.....	1
CHAPTER TWO: LITERATURE REVIEW.....	6
CHAPTER THREE: METHODOLOGY	12
CHAPTER FOUR: FINDINGS	24
CHAPTER FOUR: FINDINGS	24
CHAPTER FIVE: CONCLUSIONS	65
APPENDIX: ANALYSIS PROGRAM IN MATLAB.....	67
APPENDIX: ANALYSIS PROGRAM IN MATLAB.....	68
LIST OF REFERENCES.....	90

LIST OF FIGURES

Figure 1: Reference Axis System	13
Figure 2: Satellite Axis Reference System- Deputy At (x y, z) Relative To Chief.	14
Figure 3: Circular Orbit Case With Deputy In 1 km Trail, No Perturbations (Case1- 1/5).....	27
Figure 4: Circular Orbit-No Perturbation Effects (Case 1-2/5).	28
Figure 5: Circular Orbit With No Perturbations So Constant 1 km Separation. (Case 1- Plot 3/5).	29
Figure 6 Polar Plot Of Deputy Total Separation From Chief (Case 1- Plot 4/5).....	30
Figure 7: No Velocity Differences For Circular Orbit With No Perturbations. (Case 1-plot 5/5)	31
Figure 8: Elliptical Orbit-No Perturbations. (Case 2-plot 1/5)	33
Figure 9: Elliptical Orbit No Perturbations Check Case (Case 2 -plot 2/5).....	34
Figure 10: Elliptical Orbit Check-Case With No Perturbations. (Case 2-plot3/5)	35
Figure 11: Elliptical Orbit, No Perturbations, Along-Track vs. Radial. (Case 2 - plot 4/5).....	36
Figure 12: Elliptical Orbit X-, Y-, Z- Relative Velocities (ref.8 case)(Case 2-5/5).	37
Figure 13: J ₂ Perturbation Effects On Chief And Deputy Satellites. (Case 3 -1/6).....	39
Figure 14: Elliptic Case With J ₂ Effects On Inclination And Angular Momentum (Case 3- 2/6)	40
Figure 15: J ₂ Induced Precession Rates For Selected Orbit. (3/6).....	41
Figure 16: Chief And Deputy Lateral Precession Due To J ₂ . (Case 3- 4/6).	42
Figure 17: Separation Magnitude Between Chief And Deputy. Case 3-plot 5/6.....	43
Figure 18: Velocity Component Differences Between Chief And Deputy. Case 3 - plot 6/6.....	44
Figure 19: Elliptical Orbit With J ₂ And Drag Effects Included, Showing Lateral Drift. (Case 4).	45

Figure 20: Chief-Deputy Separation During Elliptic Orbit With J2 And Drag. Case 4 -plot 2/2.	46
Figure 21: Elliptic Case J2 And Drag, With Deputy In 200m. Trail.	47
Figure 22: Elliptic Polar Plot Showing Separation In Km- Deputy Initialized At 200m. Trail. ..	48
Figure 23: Elliptical Orbit With J2 And Drag, Deputy Initialized At 200m.	49
Figure 24: Polar Plot Of Deputy Circular Orbit With J2 & Drag. (Case 6- 1/6)	50
Figure 25: Circular Orbit Radial Difference Between Chief And Deputy. (Case 6 -plot 2/6).	51
Figure 26: Circular Orbit J2 Effect On Orbit Inclination And Momentum. (Case 6 -plot3/6)	52
Figure 27: Test Case 6 For Two Orbits Shows Repition In J2 Distrubance Pattern. (plot 4/6) ...	53
Figure 28: Polar Plot Of Differences Vs. True Anom. In Along-Track Spacing. (Case 6-plot 5/6)	54
.....	
Figure 29: Deputy Relative Velocity Component Differences For Two Orbits. (Case 6 -plot6/6).	55
.....	
Figure 30: Deputy Attempt Decel And Hold Three Km.	59
Figure 31: Relative Velocity Components For 3 Km Hold Manuever.	60
Figure 32: Three Km Sep. & Hold Maneuver With Radial Thrust.	61
Figure 33: Thruster Input Profile That Resulted In Formation Separation Of Figure 32.	62
Figure 34: Launch From Cape Kennedy Deputy Trail 3 Km.	63

LIST OF TABLES

Table 1:Orbital Test Cases Investigated. Orbital Test Cases Investigated Using MATLAB-Based Program.....	26
Table 2: Results of Cases Investigated. Orbital Test Cases Investigated.	53

LIST OF ACRONYMS/ABBREVIATIONS/SYMBOLS

A	cross-sectional area of satellite for drag purposes, m^2
a	semi-major axis for ellipse, km
a_{drag}	acceleration on satellite due to atmospheric drag, km/s^2
C_D	drag coefficient of satellite
e	orbit eccentricity, non-dimensional
G	Universal Gravitation Constant
\underline{H}	angular momentum vector, km/sec^2
H	scale height for computing density from reference (7), km
i	orbit inclination angle relative to equatorial plane, radians
\underline{i}_h	unit vector, in direction of angular momentum vector
\underline{i}_v	unit vector, in direction of velocity vector.
I, J, K	unit vectors of Geocentric Equatorial Coordinate System.
J_2	second zonal harmonic coefficient, 1.08263×10^{-3}
M	mean anomaly, radians
m	mass of each satellite, 8.0 kg
\underline{p}	perturbation acceleration vector, km/sec^2
P_h	perturbation component normal to orbit plane due to J_2
P_r	perturbation in radial direction due to J_2
P_{\perp}	perturbation cross-track due to J_2
r	orbit radius, km
R_{eq}	radius of Earth, 6,378.137 km

<u>u</u>	control input vector
v	orbital velocity, km/sec
w	defined as $\underline{r} \cdot \underline{r\dot{}}$, km ² /sec
x	relative x-distance along track, km
y	relative y-distance across track, km
z	relative z-distance along radial, km
δ	small variation from chief orbit reference value
ρ	atmospheric density, kg/m ³
v	true anomaly, radians
ω	argument of perigee, radians
μ	gravitational parameter, 3.986 x 10 ⁵ km ³ /sec ²
Ω	longitude of ascending node, positive east from I, radians

SUBSCRIPTS

chf	identifies a chief satellite variable
dep	identifies a deputy satellite variable
h	specifies component in direction of <u>H</u>
v	specifies component in direction of <u>v</u>
o	reference value
r	radial direction

ACRONYM

Definition of Acronym

AFOSR

Air Force Office of Scientific Research

ION-F	Ionosphere Observation Nanosatellite Formation
KnightSat	University of Central Florida nanosatellite project sponsored by AFOSR, includes a two-nanosatellite formation for three-dimensional topographic mapping.
LEO	low earth orbit
LQR	linear quadratic regulator
MATLAB	MATLAB v. 6.5, copyrighted by The Math Works

CHAPTER ONE: INTRODUCTION

Background

With the development of inexpensive, lightweight, yet rugged micro-electronic components, it has become feasible in recent years to realistically consider the advantages offered by making use of formations of small orbiting satellites. These satellites would be equipped with sensors, processors, algorithms, and actuators sufficient to autonomously maintain desired orientation and spacing required to accomplish the intended tasks, and communicate key information back to ground stations for further processing. This class of small satellites has become known as "nanosatellites", with a typical mass per individual satellite of less than 15 kg. according to reference(1). Optimum formation orientation and spacing may vary with the particular sensing task, and thus might require the orbit to shift orientation or spacing, through a command from ground control. Examples of formation satellite use under consideration include sparse-aperture radar, interferometry, atmospheric observations, and three-dimensional earth surface mapping using digital cameras and multi-spectral imaging, to name a few.

The Air Force Office of Scientific Research (AFOSR) has awarded the University of Central Florida (UCF) a grant to pursue technical issues related to using satellite formations as camera platforms for three-dimensional digital mapping of the earth surface. Sensor or camera spacing is an important parameter to maintain within tight tolerances, for the success of the mapping mission. The University is developing both the hardware and software required to perform this mission, including modeling and simulation studies to identify problems and develop solutions, long before the hardware actually flies.

Most Keplerian two-body analyses assume a spherical mass distribution for modeling a gravitational force field, whereas, for maintenance of real-world low earth-orbits, the earth's oblateness must be accounted for, often requiring the use of on-board thrusters to periodically provide orbit corrections. When attempting to maintain satellite relative spacing, fuel and weight limitations dictate that the controller-commanded correction requires careful planning, to help minimize fuel expenditure while maximizing useful payload.

In the past much of the previous modeling and analysis of satellite formations has made use of the relatively simple Hill or Clohessy-Wiltshire equations, developed for circular orbits with no perturbations present, but recent efforts as described in references (2) and (3) have attempted to expand the solution to include J_2 perturbation effects in the form of a linearized solution, while maintaining a Hill equation format, for ease of formation analysis. Reference (4) has attempted to solve formation equations using an eccentric reference orbit.

Objective

The present thesis effort is intended as part of the development of the UCF engineering simulation tools necessary to help research and define formation satellite orbital issues. Specifically, this study will focus on developing a program to simulate two independent satellite orbits to study the problems of maintaining a two-satellite formation subjected to the effects of earth gravity perturbations, and atmospheric drag in low-earth-orbit (LEO). . This thesis describes development of an orbital simulation which includes two independent orbiting satellites using a model structure that appears to support a Hill-like analysis when the satellite orbits are in close proximity, approximating formation spacing. To these two independent satellite models, standard text-book J_2 perturbation and drag models were added. The integrated

models were then initialized and operated from simple to more complex cases, including circular and eccentric orbits, to verify general results of various relative orbit and perturbation combinations. In addition to examining the orbits of two closely orbiting passive satellites, a rudimentary three-axis thrust capability was added to the follower or deputy satellite model providing the ability to exercise the models in an open-loop formation adjustment maneuver, and to observe the resulting dynamics when the delicate orbital balance is upset.

The orbital equations of motion used for the development of this simulation model were based on equations of motion presented in reference (5). These equations were developed and expressed in polar coordinates, and offer some advantages over other approaches, including the ability to compute multiple orbits without quadrant concerns, true anomaly computed directly for circular or eccentric orbits, and straight-forward incorporation of perturbation vector components and control input vectors. These perturbation vectors included J_2 -gravity perturbation acceleration components from reference (6) and drag perturbation vector from equations and data provided in reference (7). A two-satellite formation was modeled, one called the "leader" or "chief" and the other called "follower" or "deputy". From properly designed open-loop studies, control strategies will be determined, based on resulting "delta-v" observations gained from this and subsequent studies using this program as an analysis tool. "Delta-v" is a cumulative measure of the velocity differences between formation members, specifically the chief may be used as the reference satellite, and the deputy, as the satellite orbit requiring correction with-respect-to the reference orbit.

The model components were verified individually, and also as they were integrated together. The formation model verification process included trivial check cases along with an elliptic case from reference (8). Once the basic spherical two-body model was verified, the J_2

perturbation model was added, which included perturbation acceleration terms added for each satellite, as well as inclusion of precession drift effects being added to the argument of perigee, longitude of the ascending node, and mean anomaly. Then an atmospheric drag perturbation model was added from reference (7).

The analysis approach used in the development of this thesis-related program is described as follows. The model was programmed in the MATLAB environment and verified against available check-case data or readily apparent simple-case results. The model was then initialized with user defined test conditions, and set up to run integration loops until the desired loop or time-count was achieved. Usually the cases were run for one orbit, although two-orbit cases were run. Orbital test cases could be set up for any combination of initial conditions, which included defining the chief orbital parameters, and perturbations, as well as deputy independent orbit parameters and perturbations. From these orbital test runs, variables of interest were indexed for post plotting and subsequent analysis. Of particular interest were Hill-like relative velocity and positional components. From the chief and deputy orbital test runs, with J_2 gravity perturbations, and drag perturbation present, as desired, the data were analyzed for circular and elliptical orbits, making observation of any position or velocity divergence between deputy and chief that might provide insight into any delta-v implications or requirements. In addition delta-v was computed directly from the model structure by subtracting the two "velocity dot" terms for each satellite and integrating the result with respect to time.

Statement Of Work

The purpose of this thesis work was to provide separation analysis of a two-satellite passive formation in low-earth orbit, in the presence of central force field and drag perturbations,

in support of the University of Central Florida KnightSat project. This present effort includes the development of an engineering simulation program to be used for modeling two independent orbiting nanosatellites. The orbital mechanics equations used for this analysis are structured to provide ease of computation and analysis, and facilitate integration of perturbation and control components from other sources. The integrated model was programmed in MATLAB, and partially verified against independent test cases. The validation process presented in this paper included running six-test cases ranging from the simple leader-follower case to out-of-plane elliptical cases, first without perturbations and then with perturbations, to help isolate perturbation effects. Also some simple thrust examples are included, and a simulated direct to orbit launch from Cape Kennedy with various initialized formation array positions.

CHAPTER TWO: LITERATURE REVIEW

The following references were used as the basis for this thesis work:

- 1) Campbell and Schetter, "Formation Flying Mission for the UW Dawgstar Satellite", University of Washington, Seattle, WA, IEEE 0-7803-5846-5/00, 2000.

This reference provides a description of the University of Washington formation flying nanosatellite project called ION-F, awarded by AFRL/DARPA/NASA as part of the University Nanosatellite joint program with some other universities. The objectives of the project include the use of a three-satellite formation to make ionospheric measurements and formation flight management. The satellite design included full attitude and position control capability. In addition the intended thruster system was described as "the integration of pulsed plasma thrusters". One project goal was to "demonstrate autonomous formation maneuvering with no ground communications, except high-level commands". This reference provides a brief high level description of the UW simulation, and discusses some of the results of simulation studies and implications. Some interesting delta-v estimates are provided for various tasks and total 22.0 m/sec. for phase I and 45.0 m/sec for phase II.. These estimates include formation keeping, formation maneuvering, and least is attitude control with about 15 percent, of the total for each phase, for a two-month mission period.

- 2) Schweighart & Sedwick, "High-Fidelity Linearized J_2 Model For Satellite Formation Flight", Massachusetts Institute of Technology, Cambridge, MA, May 2002.

This reference addresses the need to incorporate "the effect of J_2 potential" into the equations of relative motion in order to improve formation satellite research modeling. Within

this reference is derived a set of linearized constant-coefficient differential equations, which include the J_2 effects, and also manage to retain the form of the Hill equations. However from these extended equations a new formation satellite mode has been observed, called "tumbling". This is the name given to describe an effect observed in the revised model in which the formation cluster rotates about the velocity vector as it progresses along in the track direction.. Although this reference adds the effects of J_2 potential, the solution does not go beyond a circular orbit. Numerical simulation results are also presented.

- 3) Roberts & Roberts, "The Development of High Fidelity Linearized J_2 Models For Satellite Formation Flying Control.", AAS 04-162, Cranfield University, UK, 2004.

This reference verifies the J_2 modified Hill equations developed in reference (2), against the Satellite Tool Kit (STK) numerical orbit propagator. The gradient of J_2 terms are then implemented as time varying coefficients in the state matrix, performance of the time varying model is evaluated. Once verified then the developed model was to be used to design a Linear Quadratic Regulator (LQR) for use in a controller algorithm. Only circular orbits are considered.

- 4) Inalhan, Tillerson, & How, "Relative Dynamics and Control of Spacecraft Formations In Eccentric Orbits", Stanford and MIT, February 2002.

"This paper generalizes previous aperture design approaches and presents a complete initialization procedure for a fleet of vehicles with an eccentric reference orbit. The main result of the paper is derived in two ways. The primary analysis uses the solutions of linearized equations of relative motion with respect to an eccentric reference orbit. These solutions are used to find the necessary and sufficient conditions on the initial states that produce periodic

solutions, that is vehicles return to the initial relative states at the end of each orbit. In the second method, the orbital elements are used to derive the exact nonlinear condition that ensures periodic relative motion from the differential energy matching condition."

5) Roger Johnson, etal "Guidance and Control for Aerospace Vehicles", Hanford House Publishing, London, NATO AGARDograph 131, June 1969.

The equations used to describe the basic orbital equations of motion for this study were obtained from this reference. These equations are used to describe both a leader and follower satellite, to constitute a complete independent model for each satellite, capable of modeling both circular and eccentric orbits. See the symbol list for value of μ used in this study and definition of variables contained in the equations. These equation are listed below, with additional descriptions contained in the Methods section.

$$d^2\mathbf{r}/dt^2 + (\mu/r^3)\mathbf{r} = \mathbf{p} + \mathbf{u} , \quad \text{equation (1)}$$

where $\mu = G(m_1 + m_2)$, where G is the universal gravitational constant and m_1 and m_2 are mass of the earth and satellite respectively in this case. The vector quantities \mathbf{p} and \mathbf{u} represent a perturbation vector and control vector respectively.

$$dv/dt = -\mu w/vr^3 + (\mathbf{i}_v \cdot \mathbf{p}) + (\mathbf{i}_v \cdot \mathbf{u}) \quad \text{equation (2)}$$

$$dr/dt = w/r \quad \text{equation (3)}$$

$$dw/dt = v^2 - \mu/r + (\mathbf{r} \cdot \mathbf{p}) + (\mathbf{r} \cdot \mathbf{u}) \quad \text{equation (4)}$$

$$dv/dt = ((v^2 - (w/r)^2)^{1/2})/r \quad \text{equation (5)}$$

Equations (2) through (5) describe motion in the orbital plane. In addition the following two equations add the capability to describe motion outside the plane, allowing changes in orbit inclination and angular momentum vector as appropriate to the situation being modeled.

$$di/dt = v_h/r(\sin(\omega + \nu)) \quad \text{equation (6)}$$

$$dH/dt = \underline{1}_h \cdot (\underline{r} \times \underline{p}) + \underline{1}_h \cdot (\underline{r} \times \underline{u}) \quad \text{equation (7)}$$

- 6) Curtis, Orbital Mechanics for Engineering Students, Embry-Riddle Aeronautical University, Elsevier Aerospace Engineering Series, Elsevier Butterworth-Heinemann, Oxford, UK, 2005.

The J_2 perturbation equations used in this study were obtained from this reference. This reference is a textbook on mechanics of space systems and includes the following J_2 perturbation component equations, structured in polar coordinate format, with the subject satellite located at the tip of the radius vector. P_r is the radial perturbation in acceleration experienced by at satellite at the prescribed location (r, i, ω, ν) , P_\perp is the transverse component in direction of \underline{v} , and P_h is the cross-track or out of plane component:

$$P_r = -\mu/r^2 \ 3/2 \ J_2 \ (R/r)^2 \ [\ 1 - 3\sin^2(i)\sin(\omega + \nu)^2 \] \quad \text{equation (8)}$$

$$P_\perp = -\mu/r^2 \ 3/2 \ J_2 \ (R/r)^2 \ [\ \sin^2(i)\sin(2(\omega + \nu)) \] \quad \text{equation (9)}$$

$$P_h = -\mu/r^2 \ 3/2 \ J_2 \ (R/r)^2 \ [\ \sin(2i)\sin(\omega + \nu) \] \quad \text{equation(10)}$$

These components from this source were integrated with the orbital equations of motion listed as equations (2) through (7) above by taking the indicated dot products.

- 7) David A. Vallado, Fundamentals of Astrodynamics and Applications (second edition) , Microcosm Press, El Segundo, CA, 2001.

This source used to help provide overall background and confirmation for parts of this effort. This reference is used as a graduate textbook and provides a broad background on many of the fundamental disciplines required to understand the field of orbital mechanics. With regard to formation satellite modeling, this reference contains a brief but comprehensive description of the development of the Hill or Clohessy-Wiltshire equations in Section 6.8 on Relative Motion, pages 374-399. This reference also provided good description of perturbations in Chapter 8, specifically in Section 8.6.1 Gravity Field of a Central Body, on pages 511-524, of the J_2 "zonal harmonics" perturbation, including a statement that " J_2 is almost 1000 times larger than the next largest coefficient (J_3)".

Atmospheric drag is also considered as a perturbation in Section 8.6.2 of the same chapter, pages 524 through 542. Therefore the drag perturbation equation can be stated as the following:

$$\underline{a}_{\text{drag}} = -1/2 \rho (C_D A/m) \underline{v}\underline{v} \quad \text{equation (14)}$$

- 8) Schaub and Junkins, Analytical Mechanics of Space Systems, AIAA Education Series, 2003.

This reference is intended as a text-book and overall reference on the subject of Space Systems. Chapter 14 of this reference is dedicated to Spacecraft Formation Flying. The first part of the chapter develops the Hill or Clohessy-Wiltshire equations and provides solutions for a circular, no perturbation case, as an example. Then a method called the "orbit element difference description" is developed to include both circular and eccentric orbits, although perturbations again are not included. However the last half of this chapter provides some insight into strategies for the design of J_2 -invariant relative orbits. This reference does provide the equations for describing secular drift in the mean longitude of the ascending node, mean argument of perigee, and mean anomaly, due to J_2 gravitational perturbation.

CHAPTER THREE: METHODOLOGY

To study the problems of satellite formation flying, such as how best to maintain the formation at minimal fuel and weight cost, requires the ability to model dynamic satellite orbits that include the relatively minor effects known as perturbations which can, over the long term, have drastic effects on satellite formation spacing. So the methodology used in this study included identifying a convenient set of equations of motion for describing satellite orbital dynamics, and also identifying and adding the perturbation equations of interest at the appropriate point in the model. In addition required axis systems need to be defined for reference, when developing the satellite formation model.

I. Satellite Model Development.

A. Axis Systems.

The earth fixed-inertial system, IJK, was used as the reference coordinate-axes for this study and are presented in Figure 1. According to reference (7) this system is most commonly used. Also for chief-deputy relative analysis, a body-fixed coordinate system fixed at the chief center of mass, was used and is depicted in Figure 2. Unlike the Hill system, this system is defined as positive "x" along the track, positive "y" to the right of an on-board observer or chief, and positive "z" along the radial axis pointed toward the center of the Earth. This system can be described as similar to an aircraft body-axis, however its primary purpose is to provide a convenient reference frame for defining deputy motion relative to the chief.

B. Numerical Integrators.

Once the orbital equations of motion including perturbations were determined then an integration routine was selected to provide acceptable accuracy. In this study the fourth-order

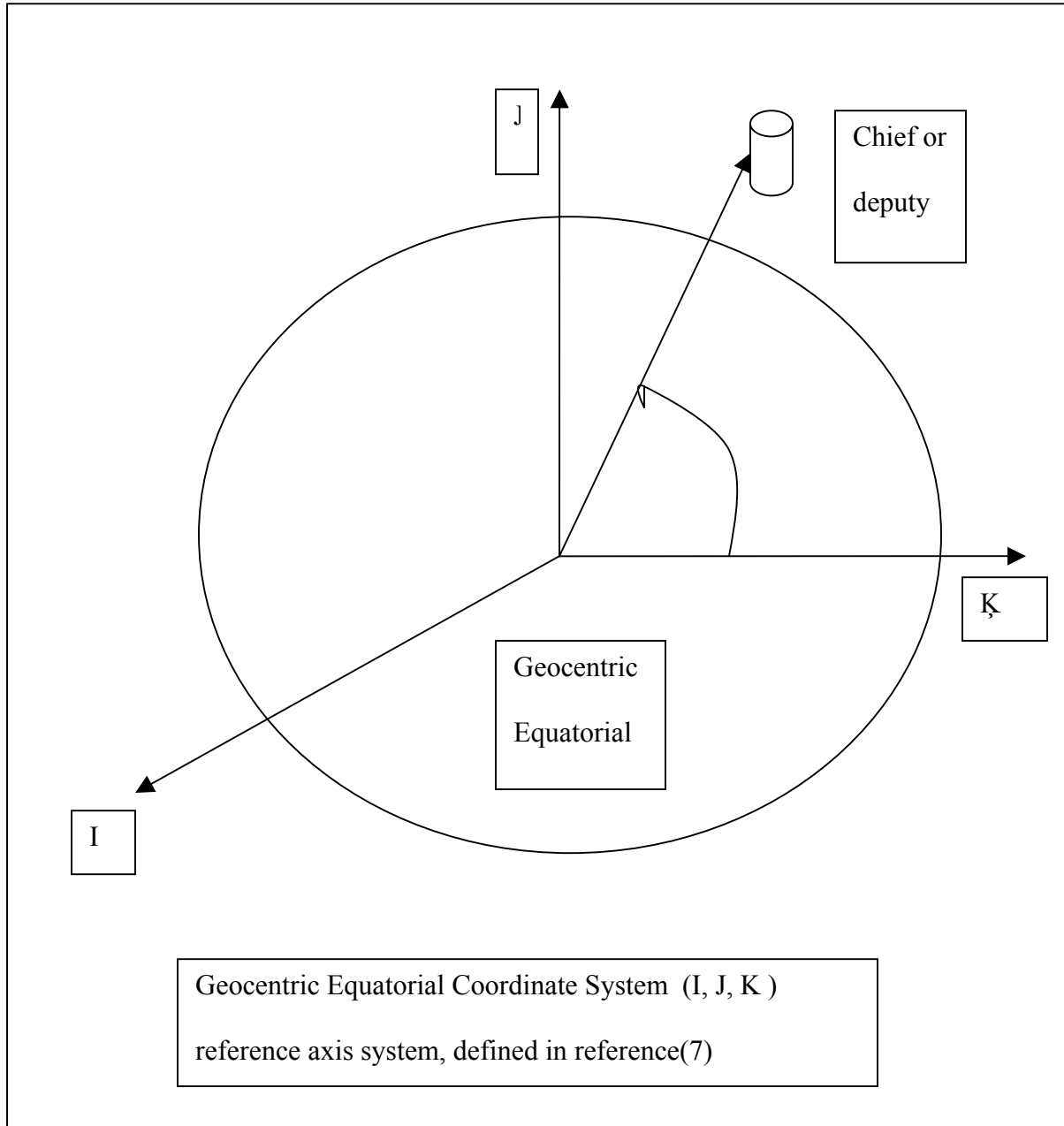


Figure 1: Reference Axis System

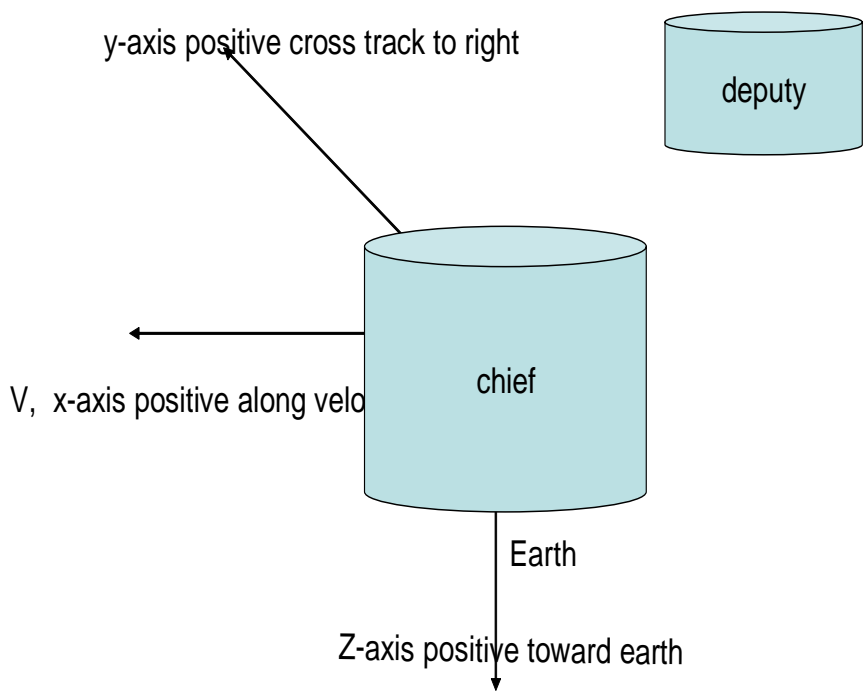


Figure-2- Satellite axis system

Figure 2: Satellite Axis Reference System- Deputy At (x y, z) Relative To Chief.

Runge-Kutta algorithm was used for integrating rapidly changing variables such as dr/dt , dv/dt , and dw/dt , otherwise a first-order Euler integrator was used for slower variables such as Euler angle updates..

C. Orbital Equations of Motion.

The baseline orbital equations selected for this study were obtained from reference (5), in which the equations of motion were derived using basic principles. These first order nonlinear differential equations may be used for either ballistic missile trajectories or orbiting satellite orbits; they include terms already representing perturbation vectors and control input vectors, so simply substituting and taking the indicated dot or cross-products resulted in the perturbation terms being integrated with the basic equations. The perturbations of interest for this study were the J_2 gravitational perturbations and the atmospheric drag. It is recognized that there are other sources of perturbation forces on orbiting satellites including other gravitational effects, and solar radiation, and third-body, gravitational effects, however the effects being included in this study are considered the major sources.

The following equations, from reference (5), were used as the basis for this thesis work:

(1) The equations are easily derived using Newton's laws and standard vector relationships such as dot and cross product rules. Key equations used as the starting point are provided below:

$\mu = G(m_1 + m_2)$, where G is the universal gravitational constant and m_1 and m_2 are mass of the earth and satellite respectively in this case. The μ parameter is used to quantify the gravitational attraction force between earth and other known masses of interest. Using this parameter, the first orbital equation of motion is provided below from reference (1) as:

$$\underline{d^2\mathbf{r}}/dt^2 + \mu/r^3 \underline{\mathbf{r}} = \underline{\mathbf{p}} + \underline{\mathbf{u}} , \quad \text{equation (1)}$$

where the underline represents vector quantities and $\underline{\mathbf{p}}$ and $\underline{\mathbf{u}}$ represent a perturbation vector and control vector respectively. It can be shown that by taking \underline{dr}/dt dotted with vector equation (1), and recognizing the \underline{dr}/dt equals \underline{v} , results in the following scalar equation:

$$dv/dt = -\mu w/vr^3 + (\underline{i}_v \cdot \underline{\mathbf{p}}) + (\underline{i}_v \cdot \underline{\mathbf{u}}) \quad \text{equation (2)}$$

Also, since \underline{w} is defined as $\underline{\mathbf{r}}$ dotted with \underline{dr}/dt , it can be shown that,

$$dr/dt = w/r \quad \text{equation (3)}$$

Also, it can be shown that

$$dw/dt = v^2 - \mu/r + (\underline{\mathbf{r}} \cdot \underline{\mathbf{p}}) + (\underline{\mathbf{r}} \cdot \underline{\mathbf{u}}) \quad \text{equation (4)}$$

Recognizing that the vertical and horizontal components of \underline{v} , the velocity vector, are \underline{dr}/dt and $\underline{\mathbf{r}}$ times \underline{dv}/dt respectively, in polar coordinates, the range angle rate or true anomaly rate (dv/dt) may be solved for by using the properties of a right triangle to arrive at

$$dv/dt = (1/r) (v^2 - (w/r)^2)^{1/2} \quad \text{equation (5)}$$

Equations (2) through (5) describe motion in the orbital plane. In addition the following two equations add the capability to describe motion outside the plane, adding the possibility of changes in orbit inclination (i) and angular momentum vector ($\underline{\mathbf{H}}$).

$$di/dt = v_h/r(\sin(\omega + v)) \quad \text{equation (6)}$$

describes inclination rate of the orbital plane, where v_h describes the out-of-plane (cross-track) velocity component, and the rate of change in angular momentum is described by

$$\underline{dH}/dt = \underline{1}_h (\underline{\mathbf{r}} \times \underline{\mathbf{p}}) + \underline{1}_h (\underline{\mathbf{r}} \times \underline{\mathbf{u}}) \quad \text{equation (7)}$$

D. J₂ Perturbation Equations.

In the present study appropriate equations for J₂ gravity perturbations were identified in reference (6) and these were added to the orbital models of both the chief satellite and the deputy satellite. These are listed below in spherical coordinate format. The subject satellite is located at the tip of the radius vector and the J₂ perturbation components are P_r, the radial perturbation acceleration experienced by at satellite at the prescribed location (r, i, ω, ν), P_⊥, the transverse component in direction of \underline{v} , and P_h, the cross-track or out of plane component:

$$P_r = -\mu/r^2 \ 3/2 \ J_2 \ (R/r)^2 \ [\ 1 - 3\sin^2(i)\sin(\omega + \nu)^2 \] \quad \text{equation (8)}$$

$$P_{\perp} = -\mu/r^2 \ 3/2 \ J_2 \ (R/r)^2 \ [\ \sin^2(i)\sin(2(\omega + \nu)) \] \quad \text{equation (9)}$$

$$P_h = -\mu/r^2 \ 3/2 \ J_2 \ (R/r)^2 \ [\ \sin(2i)\sin(\omega + \nu) \] \quad \text{equation (10)}$$

These components listed in equations (8), (9), and (10) can be integrated with orbital equations (2), (4) and (7) above by taking the indicated dot products.

Also since J₂ gravity perturbation is known to cause satellite orbit precession with respect to a fixed-earth reference, these effects described by equations from reference (6), were included in the model and are described in the equations (11) through (13) following:

$$d\Omega/dt = -1.5 \ J_2 \ n \ (R_{eq}/p)^2 \ \cos(i) \quad \text{equation (11)}$$

$$d\omega/dt = 0.75 \ J_2 \ n \ (R_{eq}/p)^2 \ \sqrt{1 - e^2} \ (5 \ \cos(i)^2 - 1) \quad \text{equation (12)}$$

$$dM/dt = 0.75 J_2 n (R_{eq}/p)^2 \sqrt{1 - e^2} (3 \cos(i)^2 - 1) \quad \text{equation (13)}$$

E. Atmospheric Drag.

The drag perturbation simulation used in this study is based on information presented in reference (7). On page 555 of reference (7) the following equation is provided along with the knowledge that it is based on three assumptions, using an exponential atmosphere (for density), ignoring complex interactions with the winds in the relative-velocity calculations, and assuming \underline{v}_{rel} is the same as the velocity of the satellite. Therefore the drag perturbation equation can be stated as the following:

$$\underline{a}_{drag} = -1/2 \rho (C_D A/m) \underline{v} \underline{v} \quad \text{equation (14)}$$

where ρ is atmospheric density, and C_D is the drag coefficient, given a value of 2.2 as is often assumed for satellites in the upper atmosphere. Again from reference (7) equation (8-34), an expression is provided for determining the density and is shown below:

$$\rho = \rho_0 \text{EXP}[-(h_{elip} - h_0)/H], \quad \text{equation (15)}$$

where ρ_0 is reference density used with the reference altitude h_0 , and where h_{elip} is the actual altitude above the ellipsoid (earth), and H is defined as scale height, and changes with altitude range.

F. Data Analysis Methods.

Based on reviewing most of the technical references listed in this report, it became apparent that structuring the formation satellite model in Hill equation form ($x, y, z, dx/dt, dy/dt, dz/dt$) is desirable from a data analysis viewpoint. The variables x, y, z , and their derivatives are deputy coordinates relative to the chief, and this format enhances the ability to determine

"delta-v" directly between the reference or chief satellite. Analysis of these data then provide a means to estimate fuel and thrust requirements as well as required design features of the satellite formation feedback controller.

To help with the analyses of the KnightSat formation, it was observed that the dynamic model structure used for this analysis lends itself to similar information as provided by the Hill equations. Since true anomaly is being computed for each satellite, and the radius of each satellite is nearly equal, then the along track "x-component" distance between satellites may be computed from the known radius and true anomaly differences. The following relationships were used to compute "x", "y" and "z" relative Hill-like component positions:

$$x_{\text{chf-dep}} = ((r_{\text{dep}} + r_{\text{chf}})/2) \sin(0.5(v_{\text{chf}} - v_{\text{dep}})) \quad (\text{from geometric considerations})$$

$$y_{\text{chf-dep}} = ((r_{\text{dep}} + r_{\text{chf}})/2) (\text{inc}_{\text{chf}} - \text{inc}_{\text{dep}}) \sin(\omega + v_{\text{chf}}) \quad (\text{from geometric considerations})$$

$$z_{\text{chf-dep}} = (r_{\text{chf}} - r_{\text{dep}}) \quad (\text{from geometric considerations})$$

In addition, to obtain relative Hill-like relative velocity components the following relations were used where the subscript "veldiff" indicated velocity differences:

$$x_{\text{veldiff}} = v_{\text{chf}} - v_{\text{dep}}$$

$$y_{\text{veldiff}} = v_h - v_{\text{hdp}}$$

$$z_{\text{veldiff}} = (dr/dt)_{\text{chf}} - (dr/dt)_{\text{dep}}$$

These relations were obtained through geometric considerations and with the desire to be consistent with the following sign conventions described below and shown in Figure 2. The positive x-axis is defined to be aligned with the chief velocity vector, through the chief center-of-mass, with positive in front of the chief and negative as behind the chief. Also, for the positive y-axis, the origin is at the chief center of mass, and positive direction is to the right. That is, if the

deputy is on the right of the chief , it is at "positive-y". The positive z-axis is defined as positive downward, or earthward, and negative above the chief, with the z-axis origin located again through the center of mass.

G. X-, Y-, Z-, Thruster Addition

Since one purpose of this study is to provide a simulation tool to perform formation maintenance "delta-v" studies when the satellite formation is subjected to "real-world" gravity and drag perturbations, an additional three-axis thrust capability was added to the follower or deputy model. The thrusters are configured in a mutually perpendicular triad located on the center-of-mass, with one thruster aligned along the "x-axis" to provide direct pro-v or retro-thrust, one thruster to provide a radial thrust component, and one thruster to provide cross-plane, or cross-track thrust, in the direction of the angular momentum vector, \underline{H} . The thrust might be considered as a specific thrust since its acceleration capability is stated in km/secs, with no scaling up or down for satellite mass size. These thrust components are integrated with the model through the equations of motion. Specifically equations (2), (4), and (7) provide a means for introducing the input vector, \underline{u} , where \underline{u} is defined arbitrarily as

$$\underline{u} = a_r \hat{i}_r + a_v \hat{i}_v + a_H \hat{i}_h$$

where the three thrust components are modeled as either on, or off , with the acceleration value to be determined during delta-v studies. The acceleration value may be positive or negative depending on the combination needed to accomplish the task.

For equation (2) the resulting thruster addition is $(\hat{i}_v \cdot \underline{u}) = a_v$, which results in a term added directly to the programmed deputy equation. Similarly for equation (4) the $(\underline{r} \cdot \underline{u})$ term becomes $(\underline{r} \cdot a_r)$. For equation (7) the $(\underline{r} \times \underline{u})$ term results in $(a_r \hat{i}_h - a_H \hat{i}_v)$. Dotting this with \hat{i}_h results in adding a_r to the deputy program model. Since the a_r acceleration term is affected,

for the sign convention and axis system used in this program, this translated to adding and "x-axis" rocket term to the dh/dt equation. During the thrust maneuver the following constraint equation can be used to maintain steady-state relationship between the two orbiting vehicles:

Energy level(E_c) of chief = energy level(E_d) of deputy; at all times.

H. Delta-V Calculations.

Delta-v, is a measure of the difference in velocity magnitude between the satellite state of interest and the velocity required for a desired orbit or of a target satellite. Delta-v in the case of formation satellites may be determined by taking the differences in "vdot" between the follower and chief satellites, integrating with time over an orbital period or other time of interest. So the delta-v computed in this study resulted from differences in "vdot" times the time-step, dt, and summed over an orbit period.

I. Programming Considerations.

To perform a research study such as this, requires a programming environment and analysis tools to allow for convenient numerical graphical observations. MATLAB was selected for much of this effort because of ease of programming and plotting capabilities, and the relative inexpense of the commercially available program, Student Version Release 13.

Once the component system equations were identified or developed, they were programmed in the MATLAB environment for solving the resulting first order, nonlinear, differential-equations using a fourth-order Runge-Kutta integration scheme developed within the program, for ease of time-step adjustment. Time-steps were varied between 1 and 5 seconds for most of this analysis.

See the Appendix for a listing of the MATLAB code used here.

I. Model Verification Process.

Prior to using the model for satellite formation studies, such as predicting when and where a formation might diverge, or the effects of thrusters, the model, including perturbation sub-models, must be verified and validated as much as possible. One approach to this is to test the model initially against simple cases and adding additional levels of complications to help build up confidence in the analysis or simulation program. This type of approach was taken with this program and the test matrix is listed in Table 1 of Section 4. For example the first test case listed was the simple circular orbit "leader-follower" formation, for a 1 km. separation distance. For the next case, the model was checked against an elliptical orbit check-case presented in reference (8), which had been generated using reference (8) equations. Next, the J_2 perturbation effects were added to the elliptical case just ran. Then atmospheric drag was added on top of this, so that this model build-up test method might help to isolate a significant effect due to perturbations additions. Finally a circular case just like the simple leader-follower case was run but with J_2 and drag active.

The variables monitored were selected to try to isolate effects are for relative satellite positions in "Hill-like" coordinates, and relative "Hill-like" velocities. The reason the term "Hill-like" is used is due to the fact that these results were not obtained by solving the Hill differential equations, but were obtained from performing relative simple operations described in the Data Analysis Methods section above.

CHAPTER FOUR: FINDINGS

This section is divided into three sections, the general formation test cases to demonstrate the model overall ability to simulate a two-satellite formation in low-earth-orbit for both circular and elliptical orbits, and with and without drag and J_2 gravitational perturbations. The specific testing approach and test conditions are described in the General Model Demonstration section below. This is followed by a section describing the Addition Of A Thruster Model, and a section on Delta-V Computation, along with a specific demonstration case of a formation satellite launch from a direct orbit launch from the Kennedy Space Center in Florida

I. General Model Demonstration.

As a means of validating the integrated model sample check runs were conducted using the orbital simulation program. The initial conditions and set-up parameter values for these test runs are listed in Table I. Selected portions of these test results are contained in Figure 3 through Figure 29. These figures contain MATLAB plots of orbital parameters such as radius and velocity verses time for one orbit, or true anomaly for one orbit, generally expressed in radians. The following sections contain discussion about each particular test case.

Table 1:Orbital Test Cases Investigated.

Orbital Test Cases Investigated Using MATLAB-Based Program

Test Conditions	Orbit Parameters					(Perturbations)		
	a,km	e	i,rad	Ω ,rad.	ω ,rad.	Mo,rad.	J2	Cd
1- Chief Orbit (circular).	6678.	0.0	0.837	0.349	0.1745	0.0	0.0	0.0
- Deputy Orbit (1 km. trail)	6678.	0.0	0.837	0.349	0.1745	-0.00015	0.0	0.0
2- Chief Orbit (ellipse)	7555	0.03	0.837	0.349	0.1745	0.0	0.0	0.0
- Deputy Orbit	7555.	0.03*	0.837*	0.349*	0.1745*	0.0*	0.0	0.0
3- Chief Orbit (ellipse)	7555	0.03	0.837	0.349	0.1745	0.0	1	0.0
- Deputy Orbit	7555.	0.03*	0.837*	0.349*	0.1745*	0.0*	1	0.0
4- Chief Orbit (ellipse/J2/Cd)	7555	0.03	0.837	0.349	0.1745	0.0	1	2
- Deputy Orbit	7555.	0.03*	0.837*	0.349*	0.1745*	0.0*	1	2
5- Chief Orbit(ellipse/J2/Cd)	7555	0.13	0.837	0.349	0.1745	0.0	1	2
- Deputy Orbit(200m trail)	7555.	0.13*	0.837*	0.349*	0.1745*	0.0*	1	2
6- Chief Orbit(circular/J2/Cd)	6678.	0.0	0.837	0.349	0.1745	0.0	1	0.0
- Deputy Orbit(1 km. trail)	6678.	0.0	0.837	0.349	0.1745	-0.00003,.	1	0.0

*

Note- 1. When J2 effects are active, J2 = 0.00108263.

2. When drag perturbation active, Cd =2.2

* indicates deputy orbits are chief orbits plus small added delta's (examples from reference(4))

See specific Figures for test case conditions.

Case 1: Circular Orbit, No Perturbations, With Deputy In 1 km. Trail.

Case 1 was considered to be a simple check case to verify that the model is providing correct results for the basic case of the "leader-follower" satellite formation. For this case the chief satellite is initialized in a circular orbit with the deputy initialized at the same orbital parameters except displaced 1 km. aft of or trailing the chief. This translates to setting the deputy at the chief anomaly (M_0) "minus" 0.00015 radians, at the orbit radius.

In Figure 3, the orbit radius is plotted versus true anomaly in radians, and is a constant 6678 km, or 300 km above spherical earth altitude of 6378 km. The next trace is velocity in km/sec. versus true anomaly. The third trace is true anomaly versus time in seconds. It is noted that for the circular orbit true anomaly is linear with time, or the orbit angular rate is constant, unlike eccentric orbits. Also on Figure 3 under the figure number, the test set-up values are presented for both the chief satellite and deputy. The deputy initial values are shown as "delta's" from the chief orbit, and the simulation program is set up to convert these delta's to deputy orbit parameters. Reference (8) used this "delta" structure when setting up their example formation problems contain in Chapter 14, in the "orbit element difference vector". In Figure 4 are presented the orbit inclination rate the derivative of angular momentum value, both of which have "zero" value when no perturbations are present, which is the case here. The middle trace is the orbit inclination in radians. .

Case 1 was considered to be a simple check case to verify that the model is providing correct results for the basic case of the "leader-follower" satellite formation. For this case the chief satellite is initialized in a circular orbit with the deputy initialized at all the same orbital

parameters except for being displaced 1 km. rearward, which translates to setting the deputy at the chief anomaly (M_0) "minus" 0.00015 radians, at the orbit radius

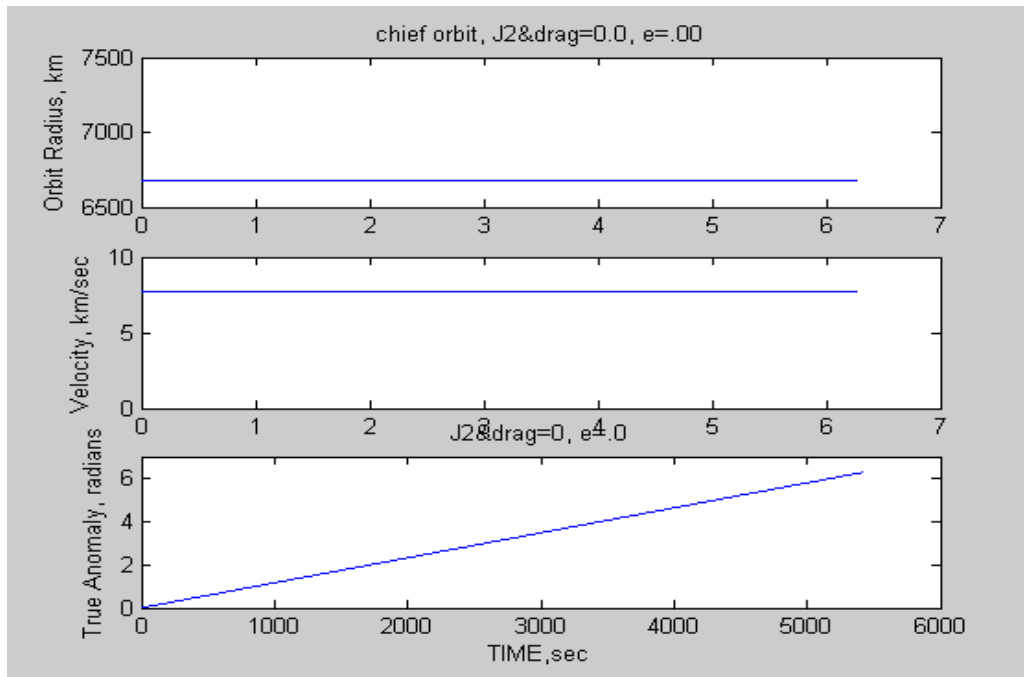


Figure 3: Circular Orbit Case With Deputy In 1 km Trail, No Perturbations (Case1- 1/5).

Chief Satellite Initial Conditions:

Circular Orbit, $e = 0.0$, $a = 6678$. km, $i = 48$. deg., $\Omega = 20$. deg.

$\omega = 10.0$ deg., $M_0 = 0.0$, J_2 effects = 0., atmospheric drag = 0.

Deputy Satellite Initial Conditions(Chief plus follwing δ 's)

Elliptical Orbit, $\delta e = 0.0$, $\delta a = 0$. km, $\delta i = 0.0$ deg., $\delta \Omega = 0.0$ deg.

$\delta \omega = 0.0$ deg., $\delta M_0 = -0.00015$ rad (deputy 1 km behind chief)

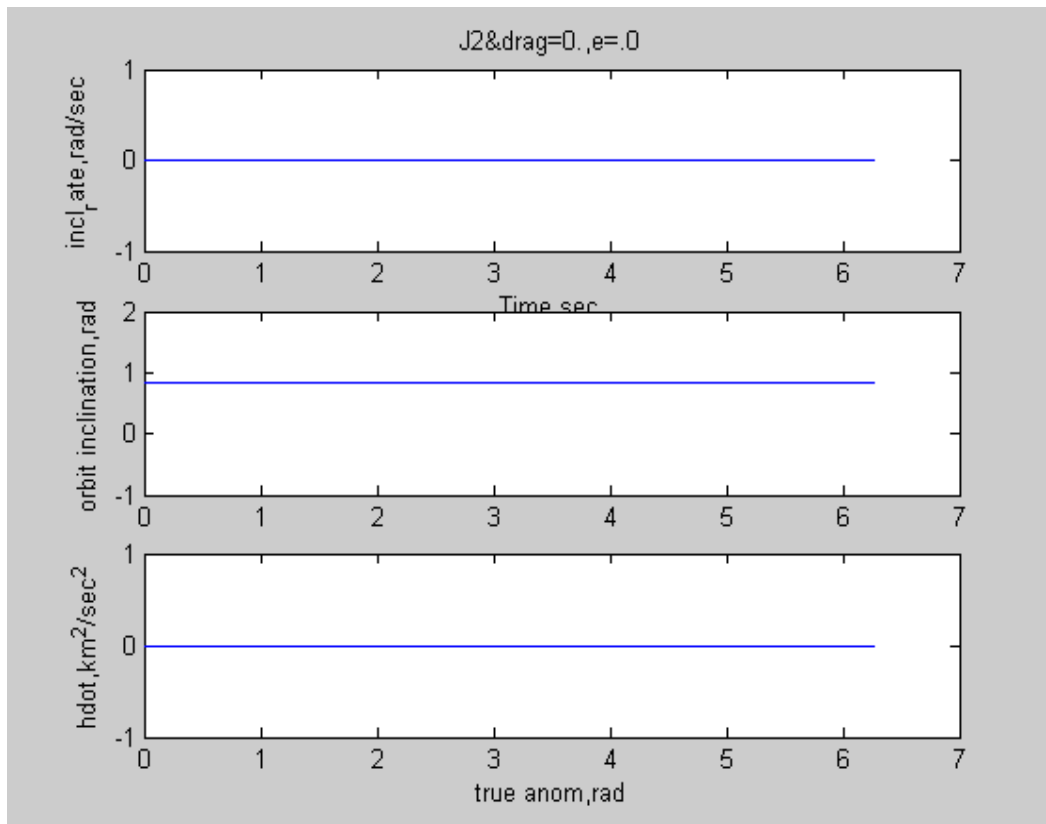


Figure 4: Circular Orbit-No Perturbation Effects (Case 1-2/5).

In Figure 4 are presented the orbit inclination rate the derivative of angular momentum value, both of which have "zero" value when no perturbations are present, which is the case here. The middle trace is the orbit inclination in radians.

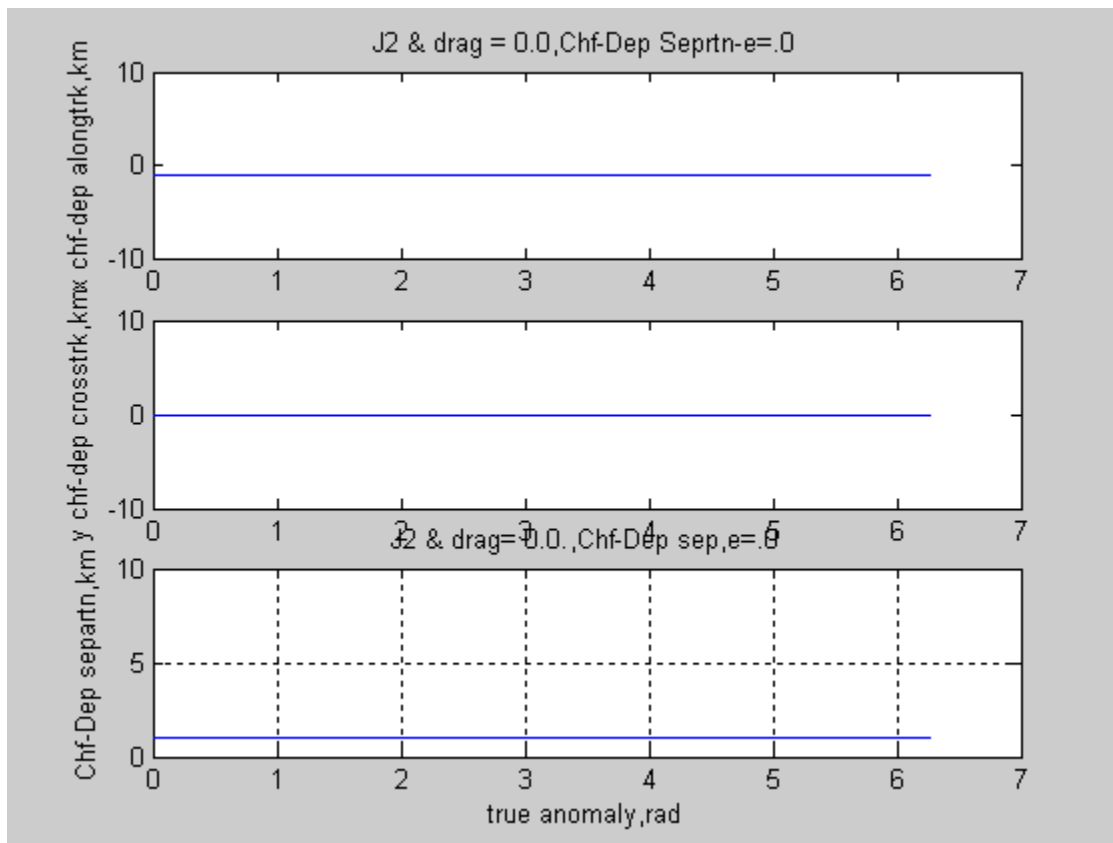


Figure 5: Circular Orbit With No Perturbations So Constant 1 km Separation. (Case 1- Plot 3/5).

It can be observed from the above figure that the "along-track" separation is a constant negative 1 km. indicating that the deputy is 1 km behind ($x = -1.0$ km) the chief as they perform a complete orbit. This is as expected since the effective gravitational model is a Keplerian two-body central force field with no perturbations, at this point.

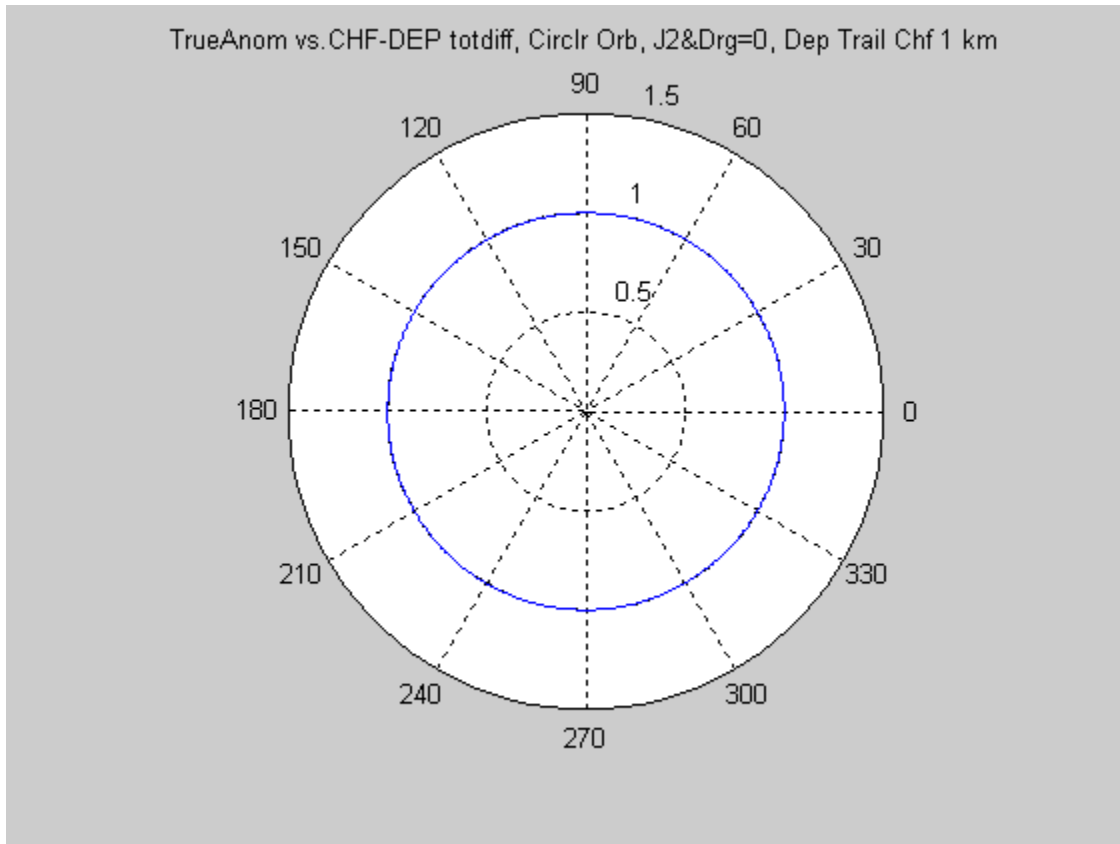


Figure 6 Polar Plot Of Deputy Total Separation From Chief (Case 1- Plot 4/5)

Figure 6 shows the chief-deputy separation distance vector magnitude verses true anomaly for a complete orbit. Note that the separation is again a constant for the complete orbit. The polar plot provided the same information as shown in the bottom trace of Figure 5, displayed in a different format to help interpret the results when perturbations are added.

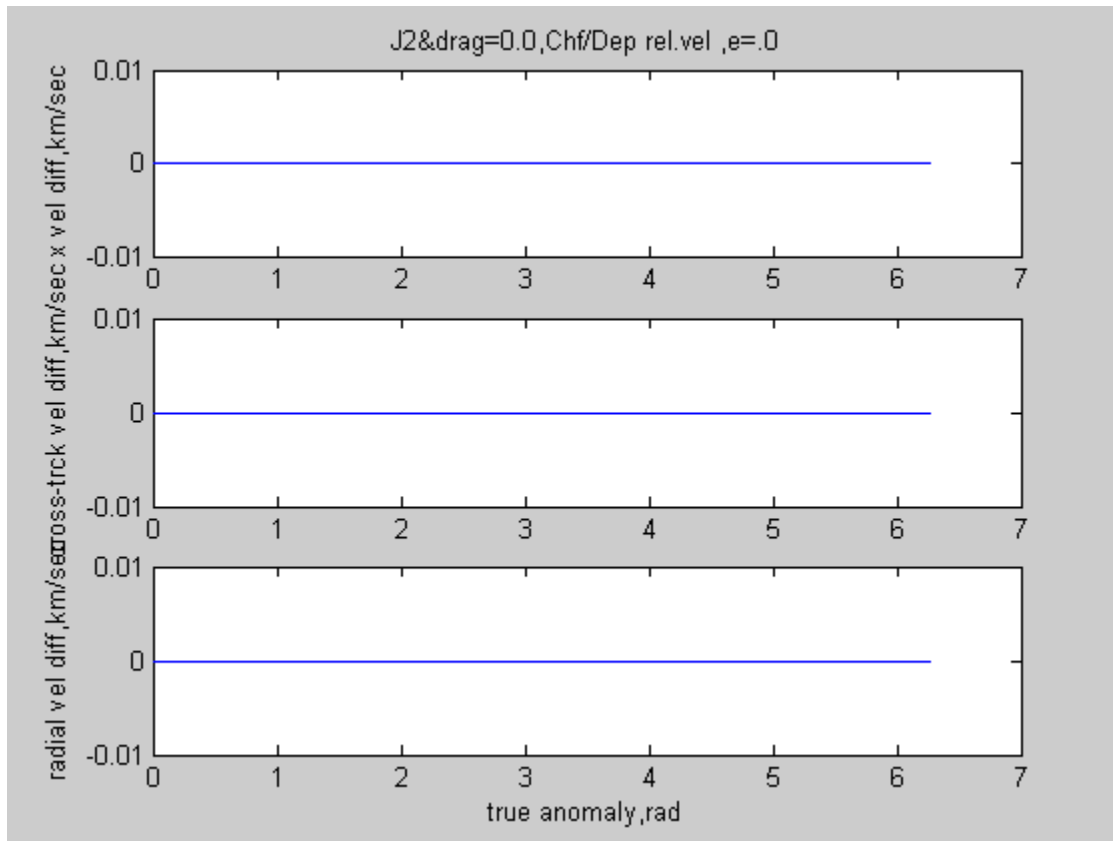


Figure 7: No Velocity Differences For Circular Orbit With No Perturbations. (Case 1-plot 5/5)

In Figure 7 it is noted that there are no relative velocity differences between the chief and deputy as would be expected for this case. For the simple case shown, these velocity differences are "zero" as the satellites orbit, indicating no tendency to drift apart or towards each other, thus requiring no correction to maintain the 1.0 km spacing, while they continue on at the same radius and velocity magnitudes.

Case 2- Elliptic Orbit, No Perturbations, Deputy Offset In Three Axes (ref.(8))

Case 2 was selected from reference (8) as a check-case of the model, prior to the activation of the perturbation effects models. This case provided a situation where the deputy satellite was to be initialized at slightly different offset values from the chief orbit to exercise an additional degree-of-freedom, out-of-plane or cross-track variations of the deputy relative to the chief reference orbit. Also this case included "delta's" for all orbital states except "a", the semi-major axis. This is because the orbital period is a function of this parameter, through the relationship below:

$$\text{Orbital Period} = 2\pi[a^3/\mu]^{1/2} \text{ from reference (7).}$$

If the semi-major axis for each member of the formation are not identical, then they will either drift apart or possibly collide. This is a practical application of the orbital constraint requirement for satellite formations.

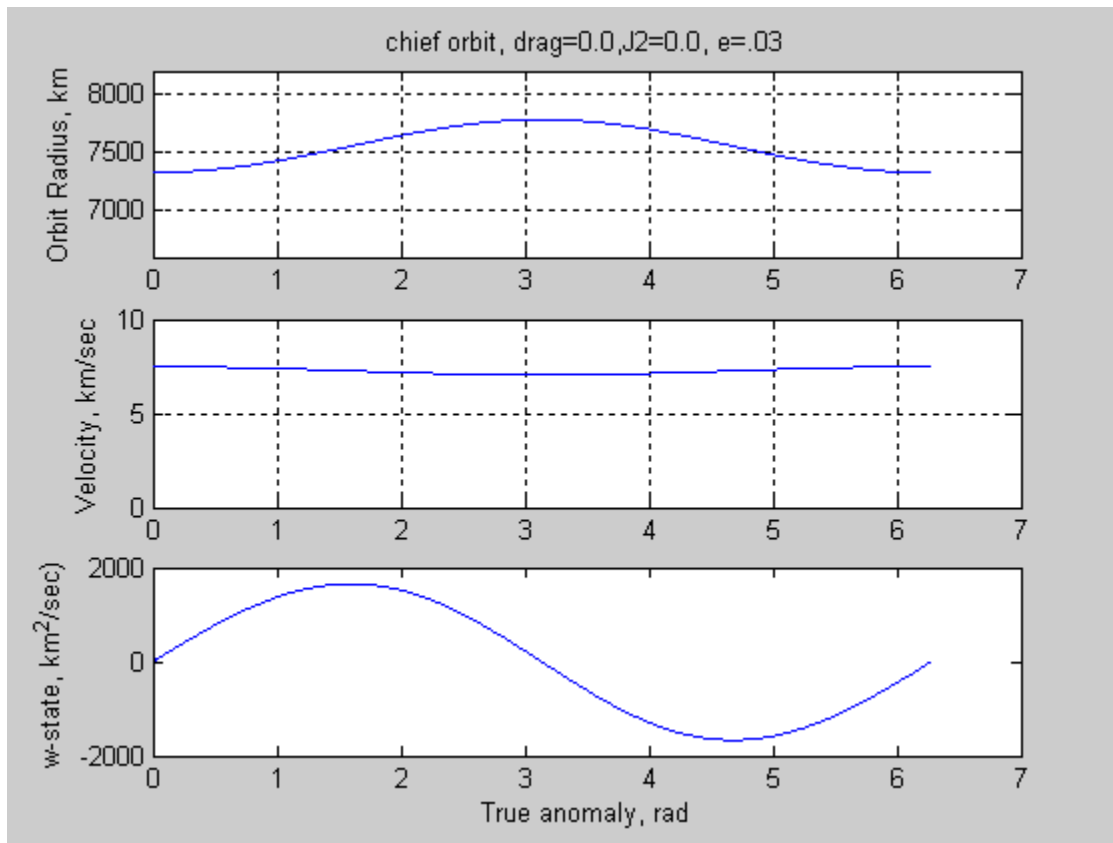


Figure 8: Elliptical Orbit-No Perturbations. (Case 2-plot 1/5)

Chief Satellite Initial Conditions:

Elliptical Orbit, $e = 0.03$, $a = 7555$. km, $i = 48$. deg., $\Omega = 20$. deg.

$\omega = 10.0$ deg., $M_0 = 0.0$, J_2 effects = 0., atmospheric drag = 0.

Deputy Satellite Initial Conditions(Chief plus follwing δ 's)

Elliptical Orbit, $\delta e = 0.00095316$., $\delta a = 0$. km, $\delta i = 0.006$ deg., $\delta \Omega = 0.100$ deg.

$\delta \omega = 0.100$ deg., $\delta M_0 = -0.100$

Note: Orbital parameters from Table 14.1 of reference (8), used as check-case against reference (8) results.

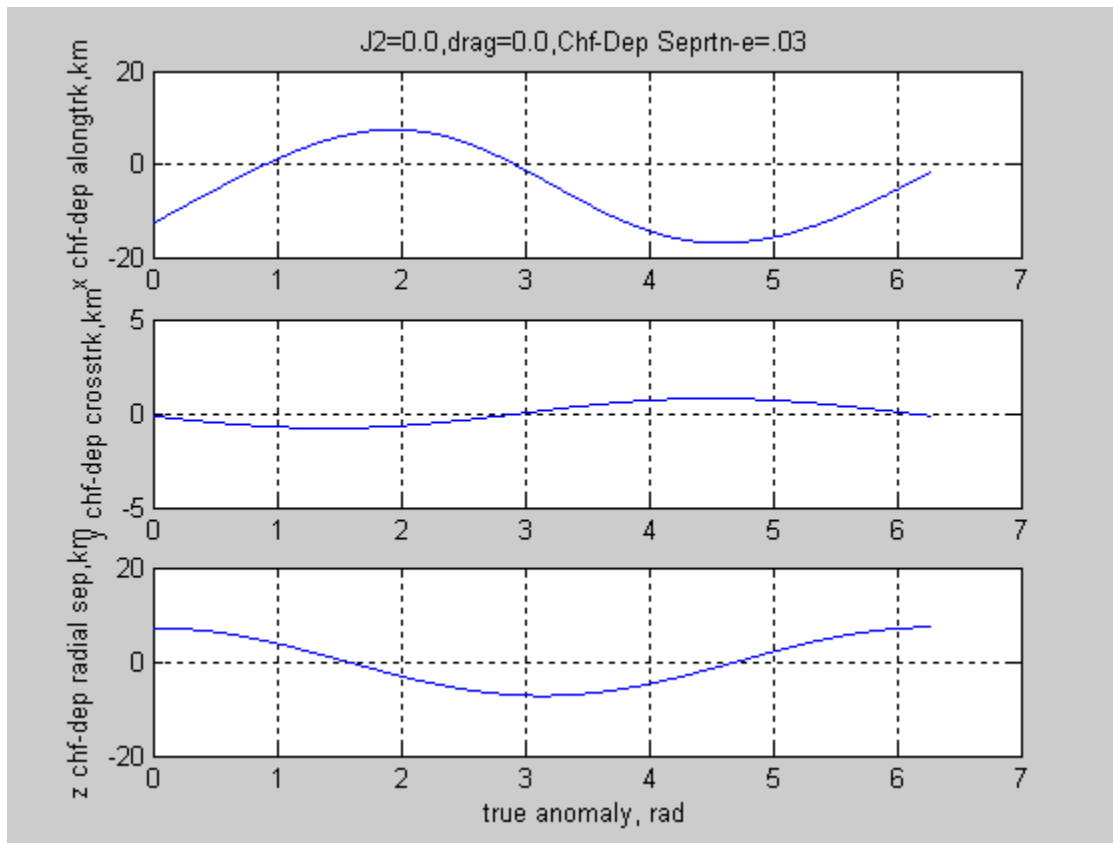


Figure 9: Elliptical Orbit No Perturbations Check Case (Case 2 -plot 2/5)

The values shown in Figure 9, indicate the x,y, and z-distance between the chief satellite at the origin, and the deputy satellite. Note that with the chief body fixed axis system and sign convention chosen, that the along track x-direction indicates the deputy starts approximately 12 km. behind the chief. This amount of the deputy trailing distance, corresponds to the deputy being initialized at M_0 of -0.100 deg., at this orbit radius. Also note that the deputy is about 7 km below the chief (downward being positive). Also, with a slight inclination angle offset (0.006 deg), note that the resulting motion appears to the chief as the deputy crisscrossing the chief track periodically, at one cycle per orbit revolution.

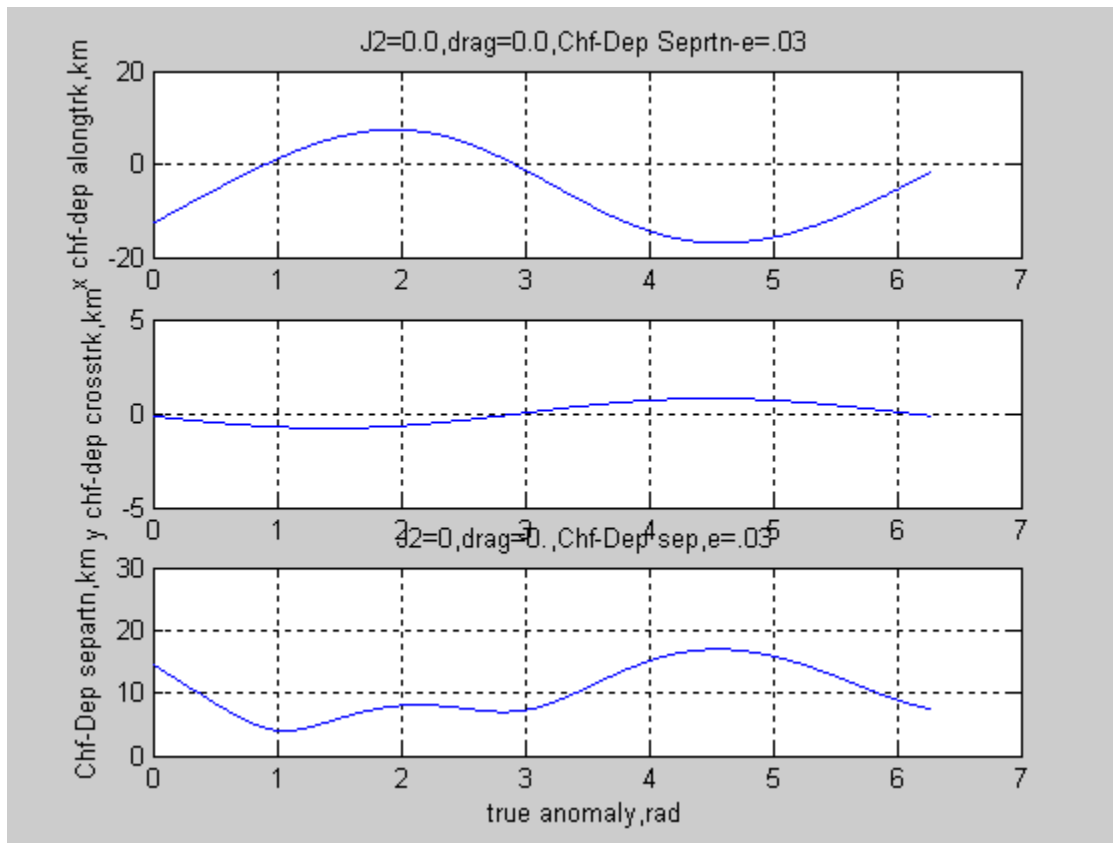


Figure 10: Elliptical Orbit Check-Case With No Perturbations. (Case 2-plot3/5)

From Figure 10 the magnitude of the separation vector vs. true anomaly, can be observed in the bottom third of the figure as the satellite formation of chief and deputy orbit according to the initial conditions.

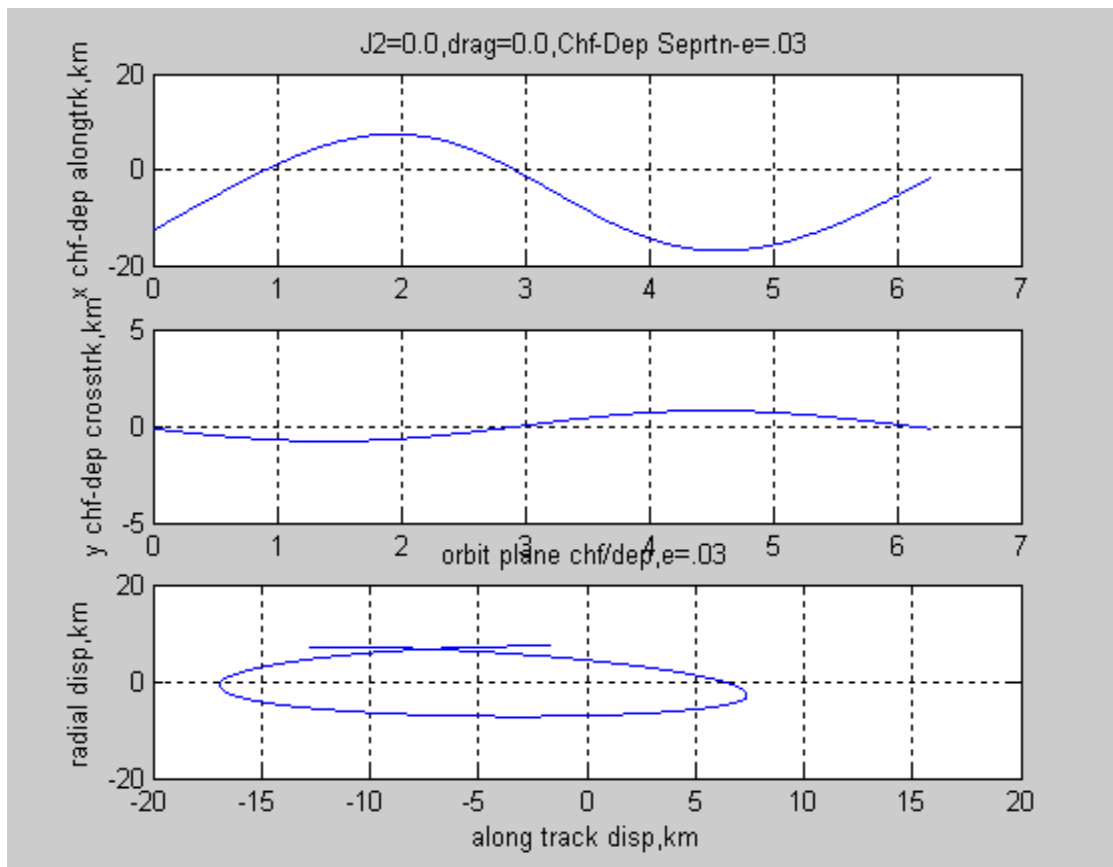


Figure 11: Elliptical Orbit, No Perturbations, Along-Track vs. Radial. (Case 2 - plot 4/5).

From Figure 11, it can be observed that the deputy orbit appears as an ellipse when projected in the orbital plane (plane containing the radius vector and velocity vector). The peak-to-peak amplitude along-track of about 25 km appears to agree with results presented in reference (8) Figure 14.6. Also the radial variation observed with the thesis model was about 15 km, vs. about 15-20 km in reference 14.6.

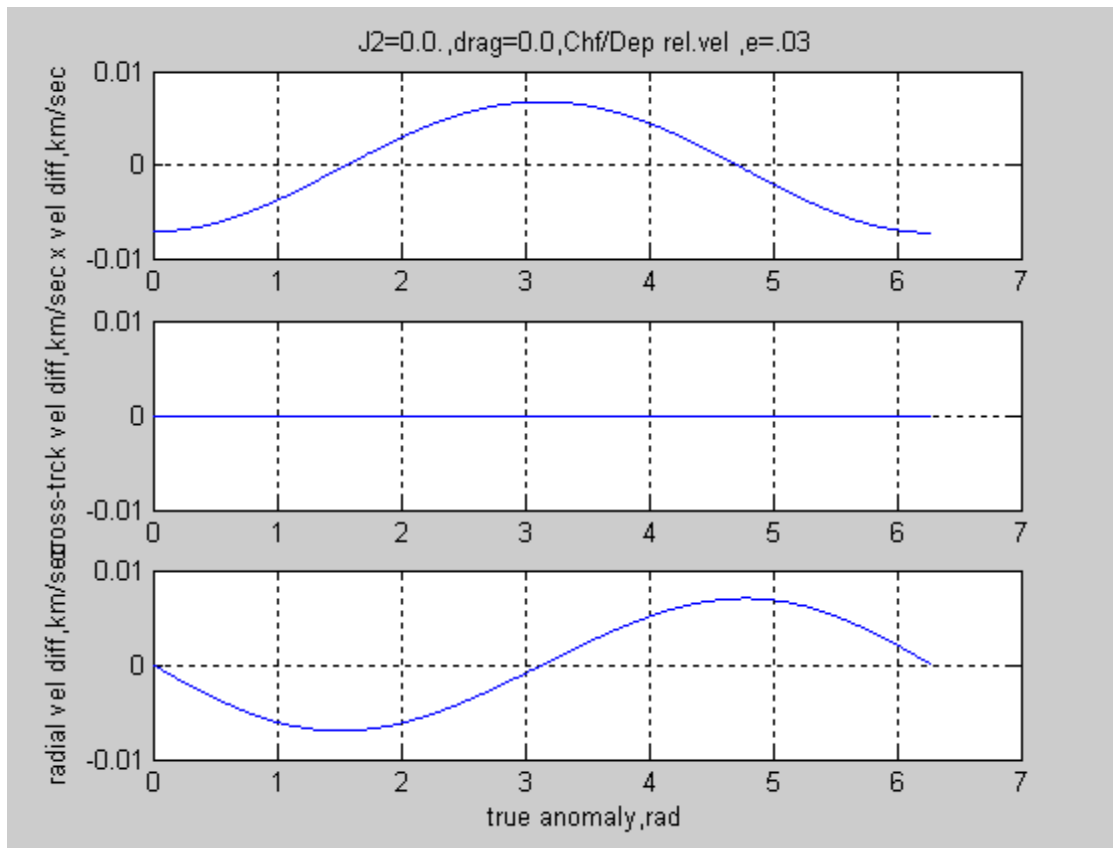


Figure 12: Elliptical Orbit X-, Y-, Z- Relative Velocities (ref.8 case)(Case 2-5/5).

In Figure 12 the relative velocity components between the chief and deputy are shown, as the satellite pair orbit the Earth. If a lateral offset such as a chevron is required to be held constant for some period of time then, some form of thrust will be required to provide the necessary "delta-v" to maintain desired spacing. These are among the items that must be considered in designing the control algorithm and control system.

Case 3- Elliptic Orbit, J₂ Perturbation, Deputy Offset In Three Axes.

The next test case, Test Case 3, continues with the same elliptical orbit test case but adds the J₂ perturbation effects to each satellite model, along with the precessions in mean anomaly, argument of perigee, and right ascension of the ascending node, according to the equations described previously. The radius and velocity verses true anomaly plots for this case are not presented here, since they are nearly duplicates of Figure-7. However two new plots are added showing effects of J₂ gravity perturbations on orbit inclination angle and rate, due to perturbations in the angular momentum vector \underline{h} . Under Figure-13 is listed the test conditions for Test Case 3, which is essentially Test Case 2, plus J₂ perturbation components from reference (6). From equations for these components it can be noted that they are functions of radius, orbit inclination, and true latitude (argument -of-perigee plus true anomaly) from reference(6).

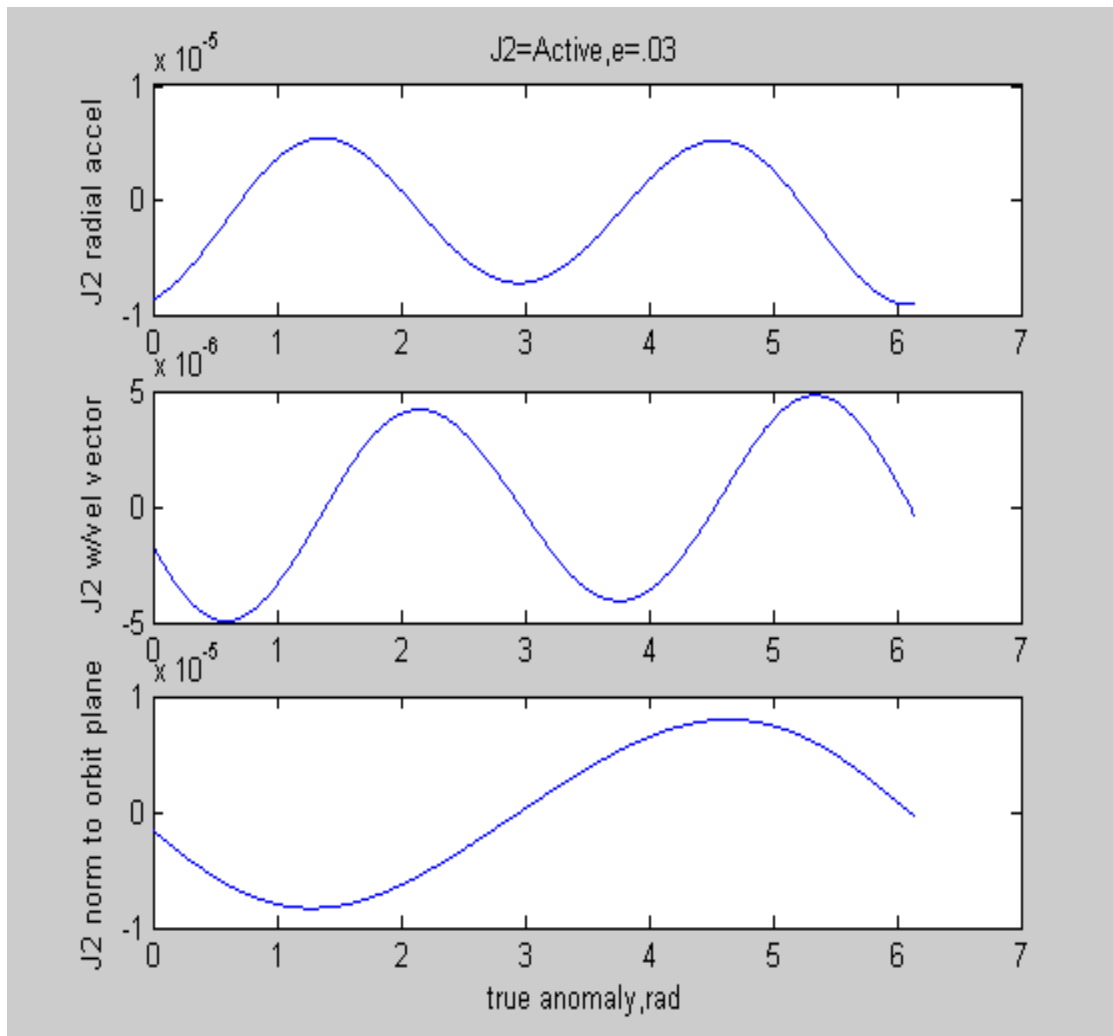


Figure 13: J_2 Perturbation Effects On Chief And Deputy Satellites. (Case 3 -1/6).

Chief Satellite Initial Conditions for Test Case 3:

Elliptical Orbit, $e = 0.03$, $a = 7555$. km, $i = 48$. deg., $\Omega = 20$. deg.

$\omega = 10.0$ deg., $M_0 = 0.0$, J_2 effects = Active, atmospheric drag = 0.

Deputy Satellite Initial Conditions(Chief plus follwing δ 's)

Elliptical Orbit, $\delta e = 0.00095316$, $\delta a = 0$. km, $\delta i = 0.006$ deg., $\delta \Omega = 0.100$ deg.

$\delta \omega = 0.100$ deg., $\delta M_0 = -0.100$ deg., J_2 effects = Active, atmospheric drag = 0.

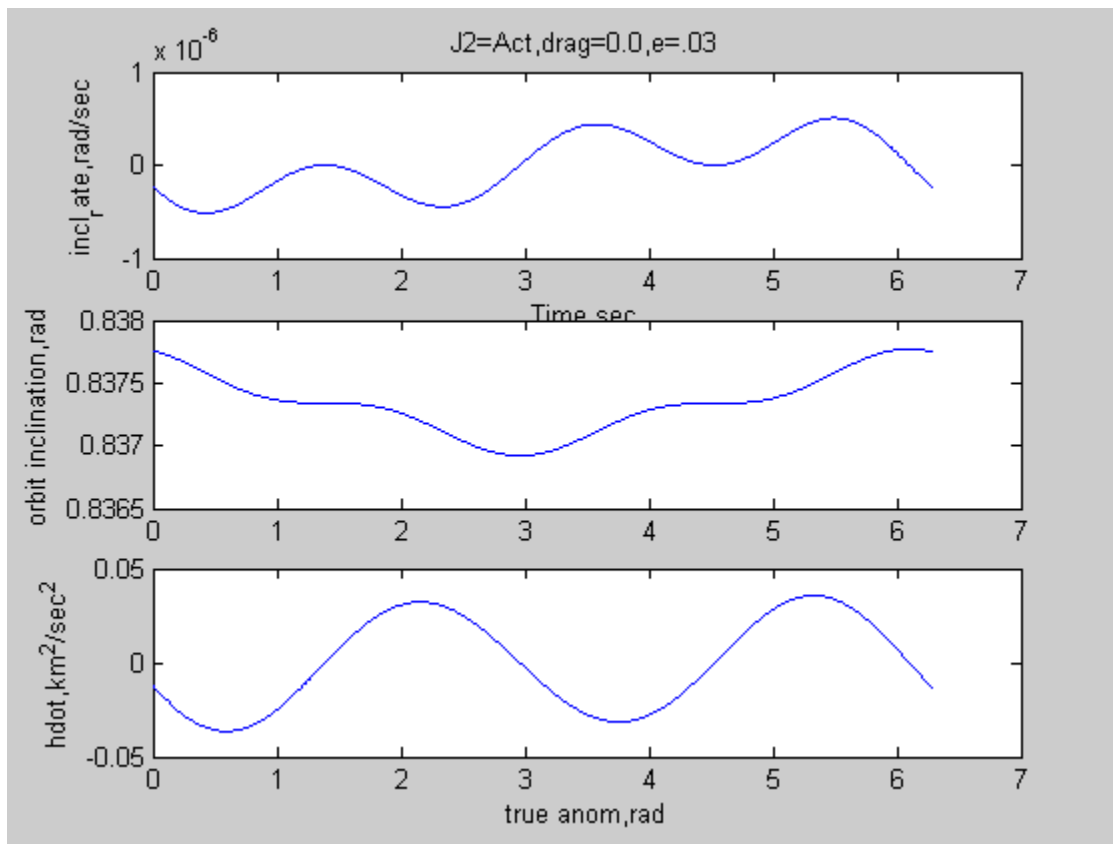


Figure 14: Elliptic Case With J_2 Effects On Inclination And Angular Momentum (Case 3- 2/6)

In Figure 14 the effects of J_2 on orbit inclination rate, and angular momentum can be observed, in contrast to the non-perturbation case shown in Figure 4.

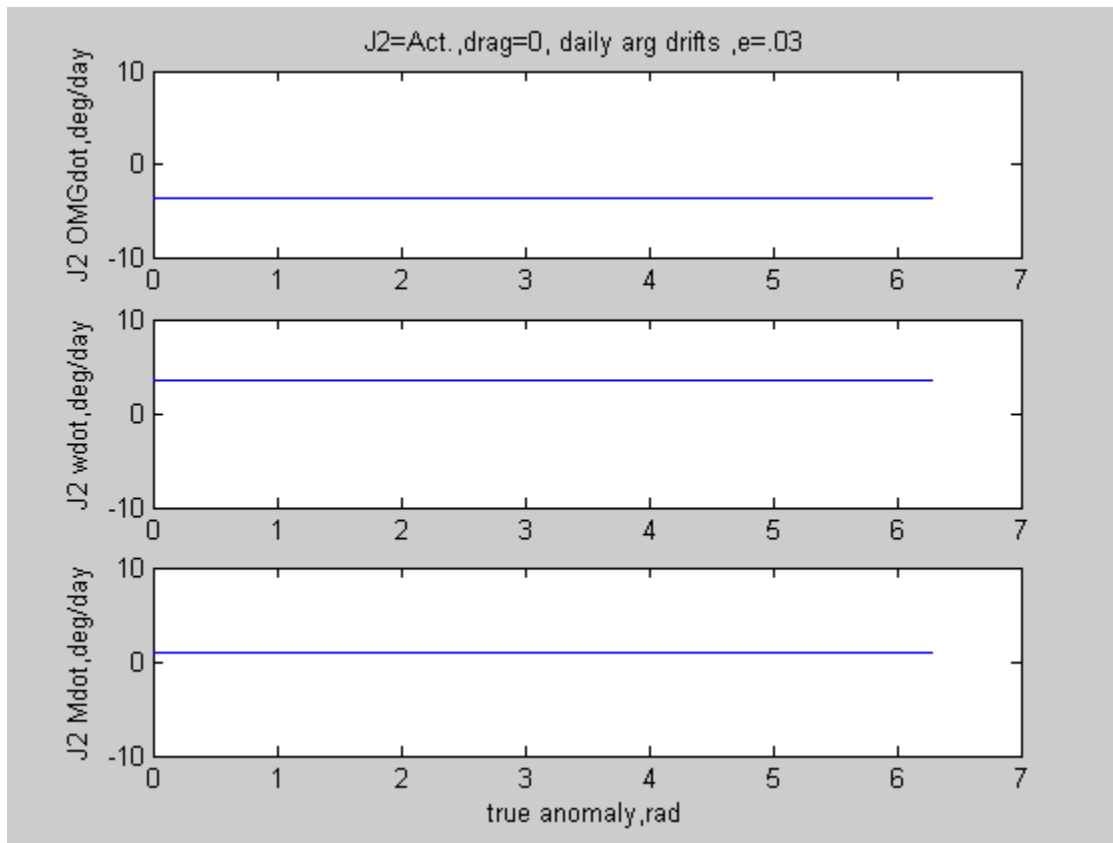


Figure 15: J_2 Induced Precession Rates For Selected Orbit. (3/6).

Figure 15 shows the effects of J_2 induced daily precession rates on right ascension of the ascending node, Ω , and argument of perigee, ω , as well as mean anomaly, M_0 . These precession rates are functions of the inclination angle, so care is needed when planning a formation satellite orbit, to consider orbit inclination. In Figure 16 the lateral drift due to J_2 perturbation can be observed, and it was computed independently for both the chief and deputy, based on the amount of angular momentum perturbation, "hdot", experienced by each satellite based on its orbital location and state. Since these two satellites were within 20 km. at all times during the orbit, the amount of perturbation on each satellite was computed to be numerically nearly identical, with Figure 16 showing a plot of the difference in this lateral drift rate, between the two satellites.

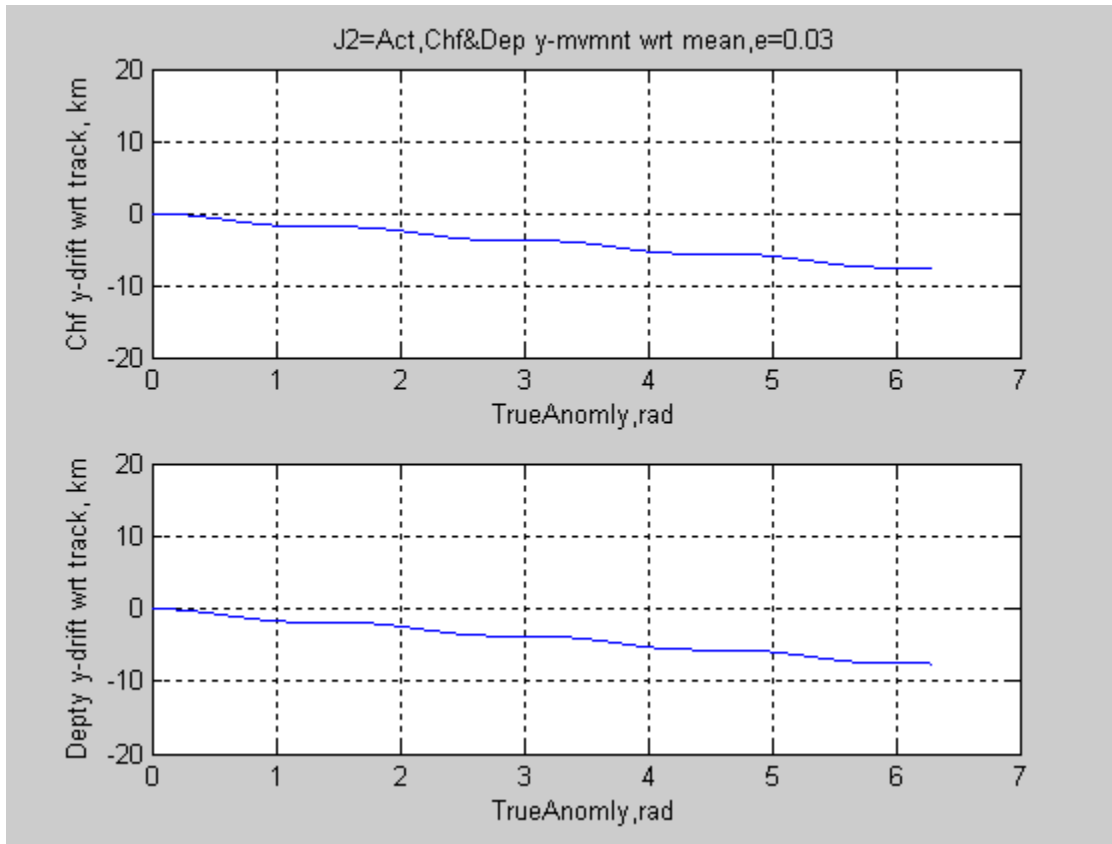


Figure 16: Chief And Deputy Lateral Precession Due To J_2 . (Case 3- 4/6).

The differences between lateral drifts for the chief and deputy were computed, and it was noted that the differences in lateral drift for a whole orbit don't exceed 0.005 km, or about 5 meters. Care is needed in interpreting results due to lack of accuracy and precision in these calculations. However it may be noted that all members of a formation might be affected by a perturbation in the same general manner, so that maintaining desired ground track may be a larger concern than maintaining spacing, in some situations.

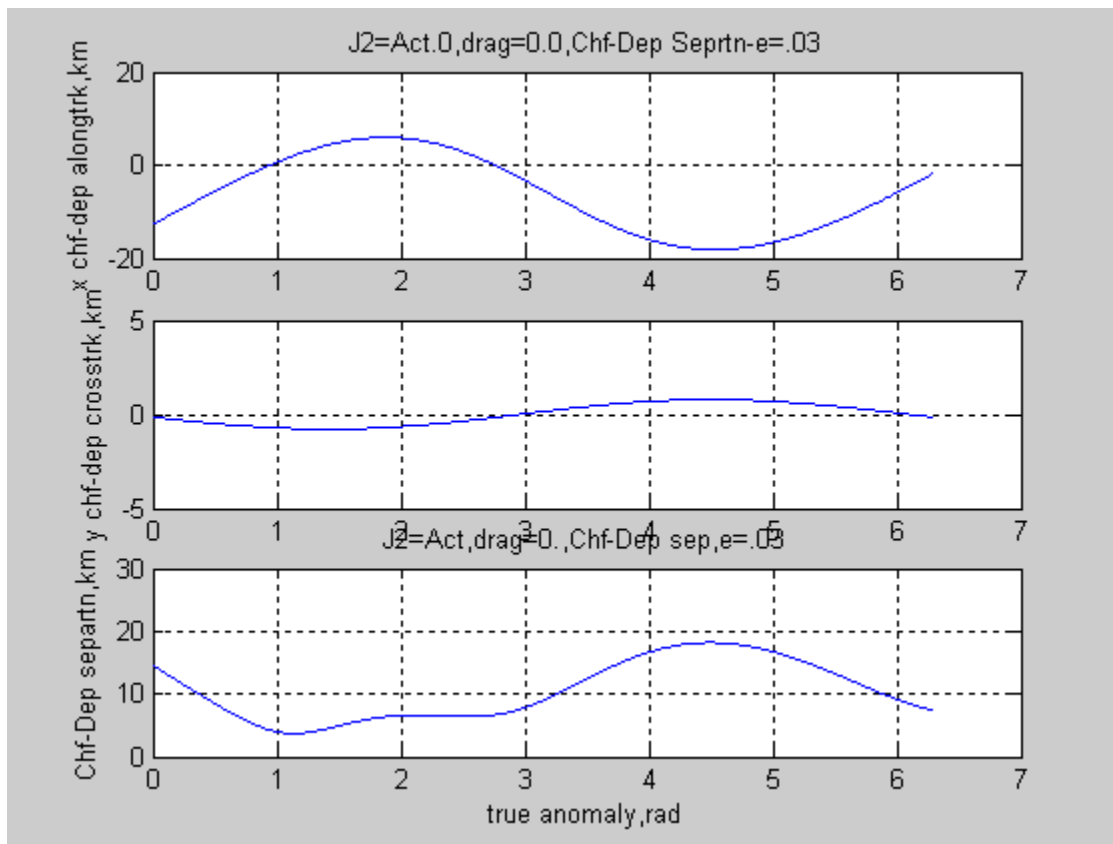


Figure 17: Separation Magnitude Between Chief And Deputy. Case 3-plot 5/6.

In Figure 17 deputy relative movement appears very similar to Case 2, with no perturbation however, as noted earlier, a lateral drift has been added to the above for both satellites.

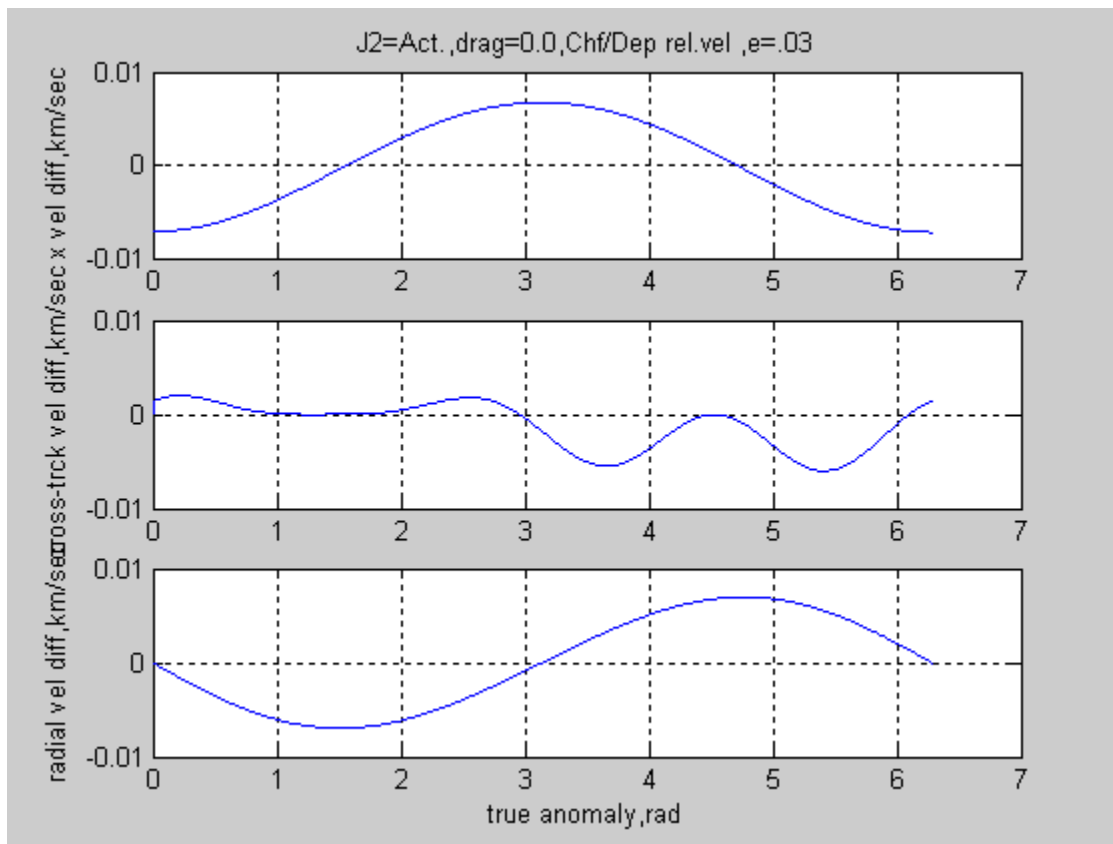


Figure 18: Velocity Component Differences Between Chief And Deputy. Case 3 - plot 6/6.

Comparing Figure 18 to Figure 12, the main noticeable difference is the difference in cross-track velocity, with Figure 18 showing not only a disturbance, but a bias in the negative direction, leftward. However since this was obtained by taking differences in out-of-plane velocity components by subtracting one from the other, then the parallel left drift is not the contributor here, since it would have been roughly equal for both satellites.

Case 4- Elliptic Orbit, w/J2 and Drag, Deputy Offset In Three Axes

For Test Case 4, the initial conditions are like Case 3, but with the addition of atmospheric drag perturbation. For this case the radius and velocity plots again looked the same as in Figure 7, so will not be repeated here. Also the y lateral drift or precession due to J2 (about -7.5 km per orbit revolution) appears unchanged by the addition of drag, however this plot is still presented as Figure 19.

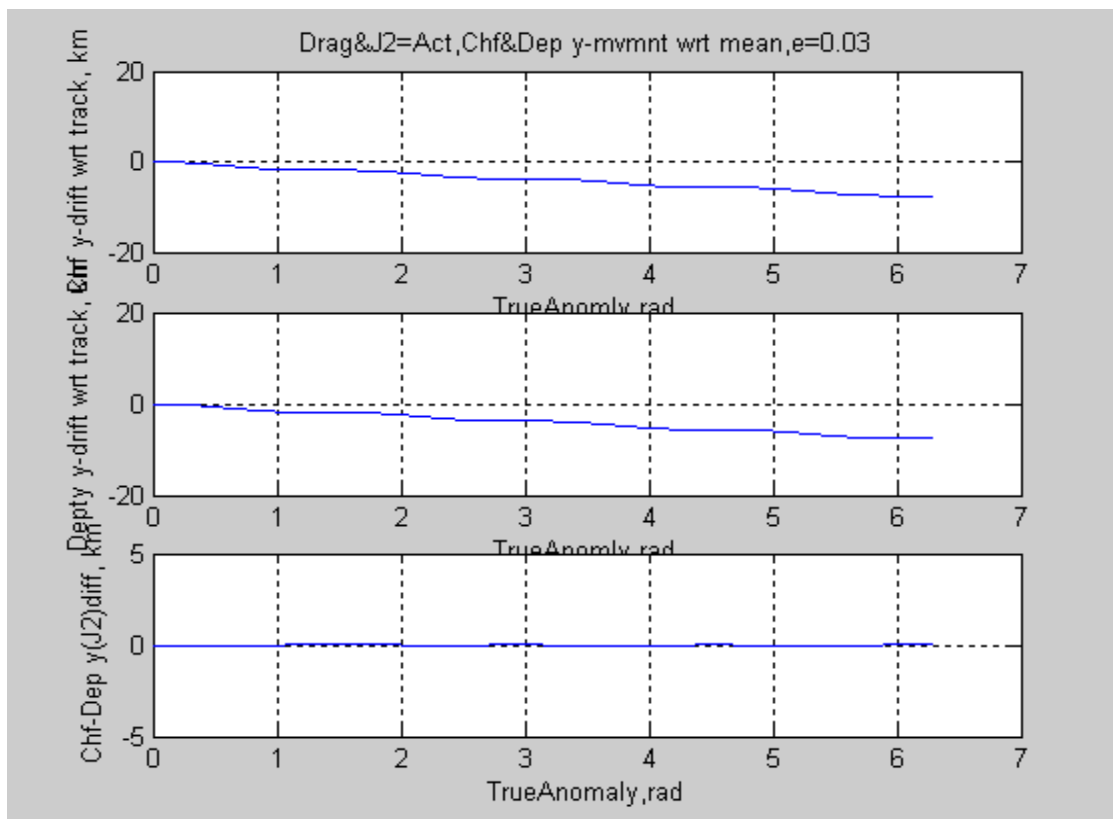


Figure 19: Elliptical Orbit With J2 And Drag Effects Included, Showing Lateral Drift. (Case 4).

Chief Satellite Initial Conditions for Test Case 4:

Elliptical Orbit, $e = 0.03$, $a = 7555$ km, $i = 48$ deg., $\Omega = 20$ deg.

$\omega = 10.0$ deg., $M_0 = 0.0$, J2 effects = Active, Atmospheric drag = Active.

Deputy Satellite Initial Conditions(Chief plus follwing δ 's)

Elliptical Orbit, $\delta e = 0.00095316$, $\delta a = 0$ km, $\delta i = 0.006$ deg., $\delta \Omega = 0.100$ deg.

$\delta \omega = 0.100$ deg., $\delta M_0 = -0.100$ deg., J2 effects = Active, Atmospheric drag = Active

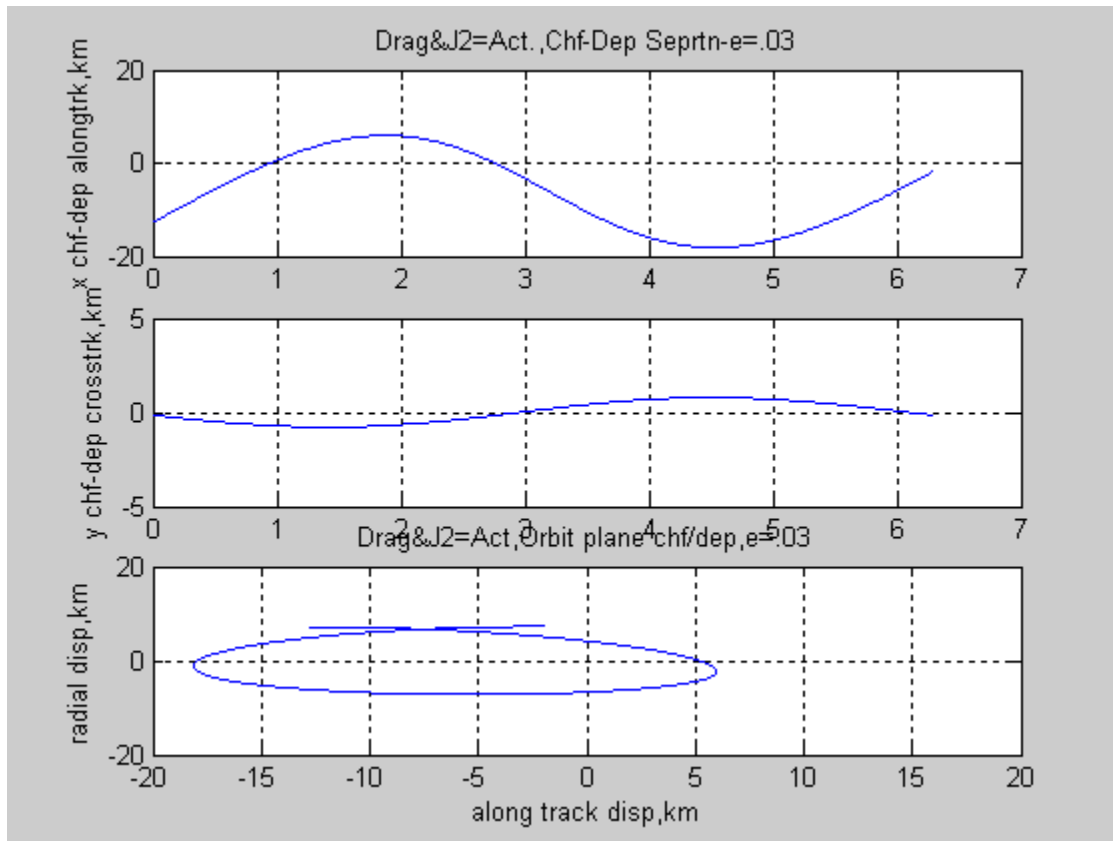


Figure 20: Chief-Deputy Separation During Elliptic Orbit With J2 And Drag. Case 4 -plot 2/2.

The addition of drag perturbation was undetectable for one orbit, since no significant numerical differences could be observed within the accuracy of these computations. However real-world experience has obviously taught that orbits erode with time due to atmospheric drag will have to be considered as a long term effect.

Case 5- Elliptic Case w/J2 and Drag- Deputy in 200 m. Trail.

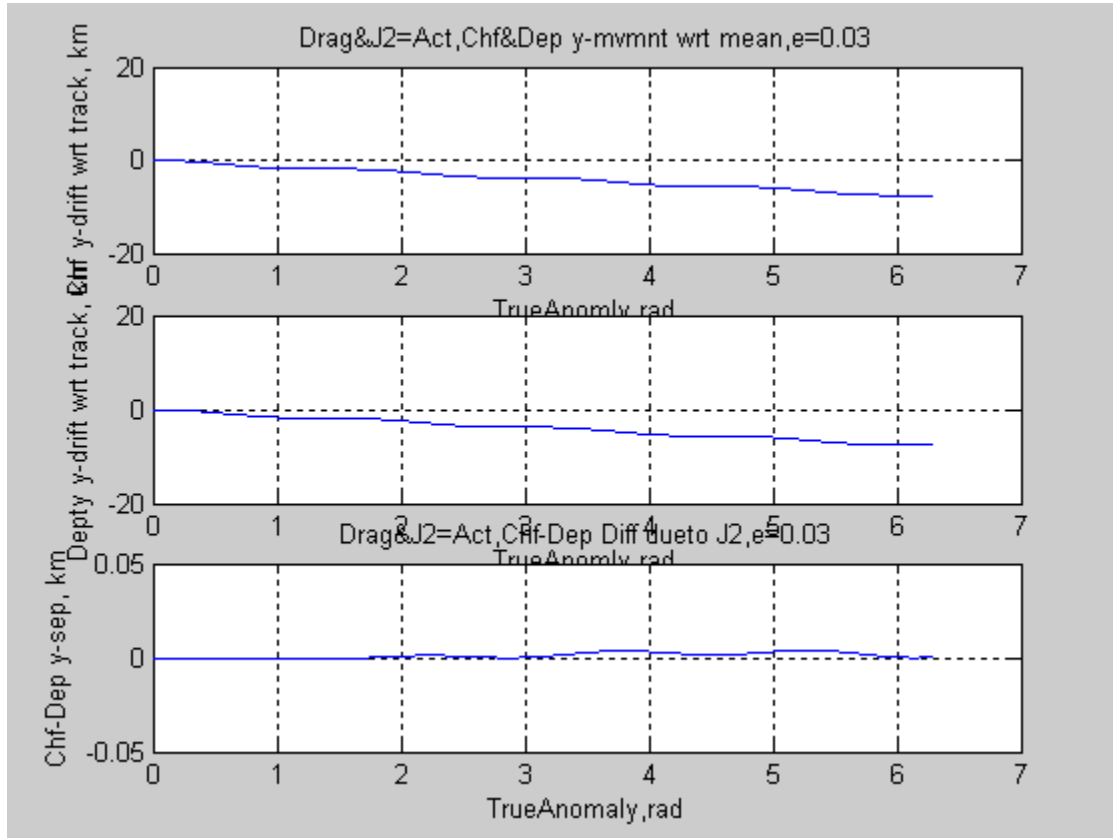


Figure 21: Elliptic Case J2 And Drag, With Deputy In 200m. Trail.

Chief Satellite Initial Conditions for Test Case 5 (plot 1/5):

Elliptical Orbit, $e = 0.03$, $a = 7555$. km, $i = 48$. deg., $\Omega = 20$. deg.

$\omega = 10.0$ deg., $M_0 = 0.0$, J2 effects = Active, atmospheric drag = Active

Deputy Satellite Initial Conditions(Chief plus following δ 's)

Elliptical Orbit, $\delta e = 0.0$, $\delta a = 0$. km, $\delta i = 0.0$ deg., $\delta \Omega = 0.0$ deg.

$\delta \omega = 0.0$ deg., $\delta M_0 = -0.0000265$ rad. (trail 200 km.), J2 eff. = Act., Atmospheric drag = Act.

To investigate the tendency for a closely spaced formation in the same orbit to collide, the follower satellite was placed in a relatively close orbit of 200 m. trailing orbit, with J_2 and drag active. Such orbits might be of interest for monitoring radio frequencies, where each satellite would act as a node for a particular wavelength. From Figure 21 it is seen that the leftward lateral drift, or precession component is still present, roughly equal for both satellites. In Figure 22 the trajectory of the deputy relative to the deputy is shown in the orbital plane in polar plot format, as the formation makes a complete orbit in true anomaly.

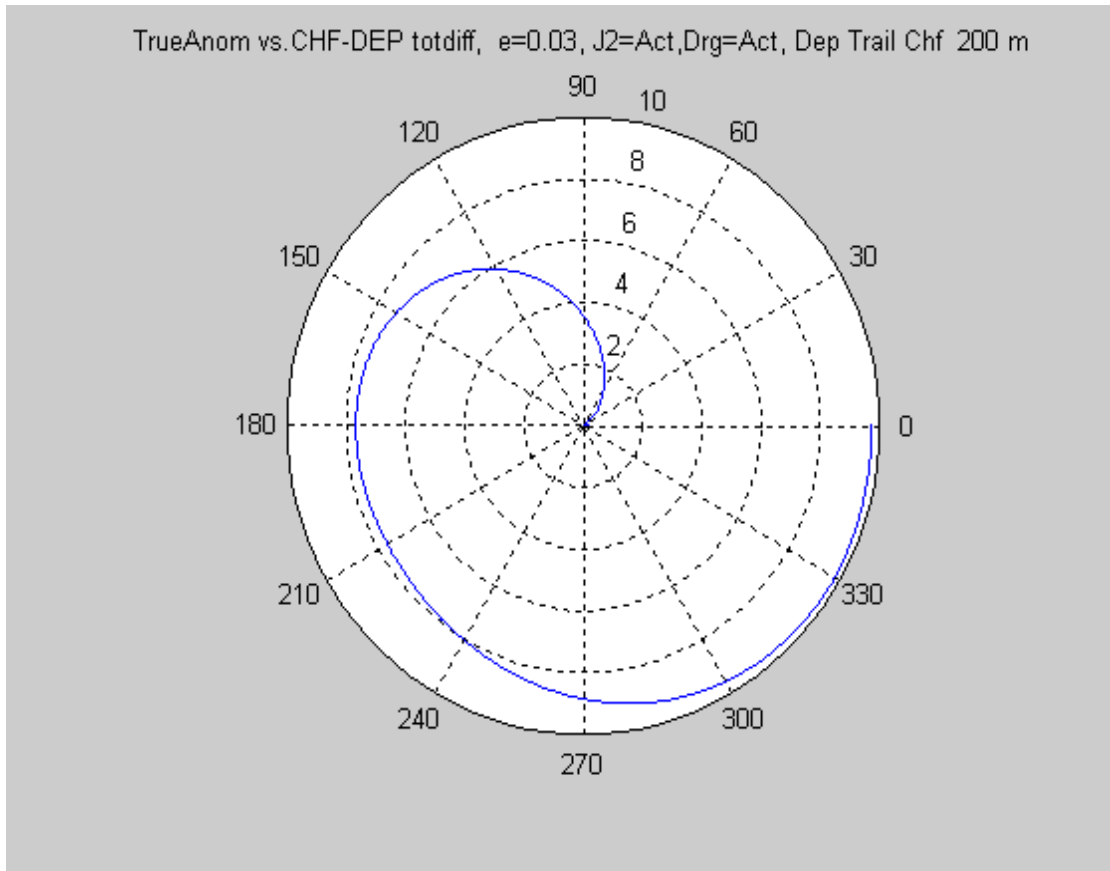


Figure 22: Elliptic Polar Plot Showing Separation In Km- Deputy Initialized At 200m. Trail.

At least in this case there is a distinct tendency for the formation to separate in the orbital plane, being almost 10 km. separation distance between them by the end of just one orbit. Of course it must be remembered that this is an elliptic orbit, however, with the addition of perturbations, the separation path is not as predictable or uniform as with no perturbations.

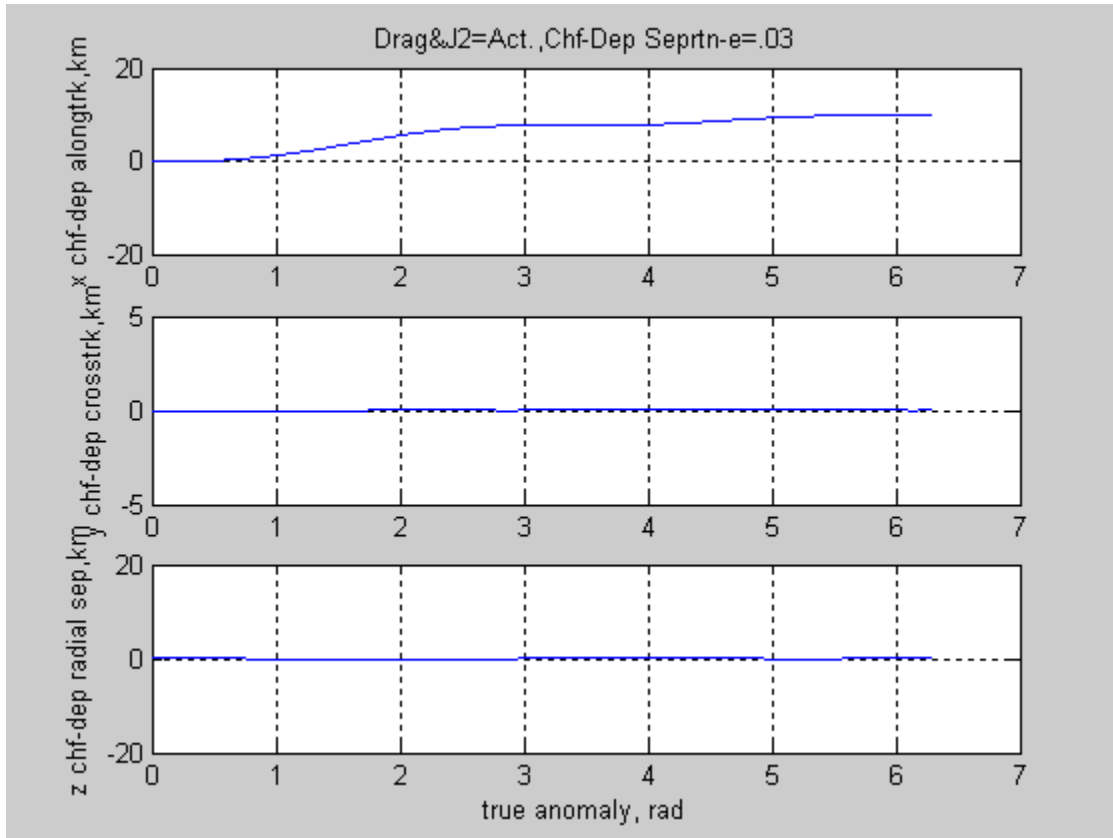


Figure 23: Elliptical Orbit With J2 And Drag, Deputy Initialized At 200m.

Figure 23 shows the x,y, and z positions verses true anomaly for Case 5, for one orbit. There appears to be a tendency for along-track divergence for elliptic orbit with perturbation. The other axes appear to remain together, so control algorithms may need to focus on providing "x-along track" compensation.

Case 6- Circular Orbit With J_2 and Drag- Deputy in 1 km. Trail.

This is the last case considered from the Table 1 list. It consists of a circular orbit with the deputy initialized in a 1 km. along-track trailing position, just like Case 1. However, drag and J_2 perturbation effects were added to the conditions of Case 1. The chief orbit and velocity plots look identical to Case for the accuracy shown here, so will not be included in these Figures.

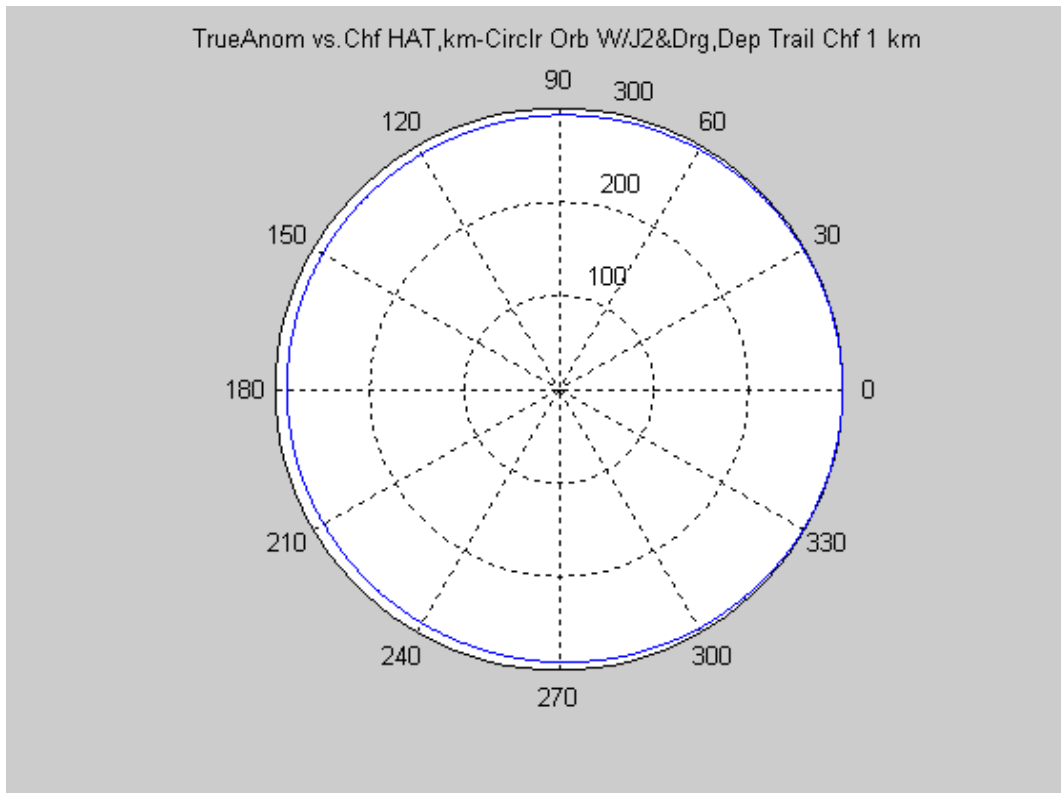


Figure 24: Polar Plot Of Deputy Circular Orbit With J_2 & Drag. (Case 6- 1/6)

Chief Satellite Initial Conditions:

Circular Orbit, $e = 0.0$, $a = 6678$. km, $i = 48$. deg., $\Omega = 20$. deg.

$\omega = 10.0$ deg., $M_0 = 0.0$, J_2 effects =Active, Atmospheric drag =Active.

Deputy Satellite Initial Conditions(Chief plus follwing δ 's)

Elliptical Orbit, $\delta e = 0.0$, $\delta a = 0$. km, $\delta i = 0.0$ deg., $\delta \Omega = 0.0$ deg.

$\delta \omega = 0.0$ deg., $\delta M_0 = -0.00015$ rad (trailing chief 1 km)

J_2 effects =Active, Atmospheric drag =Active.

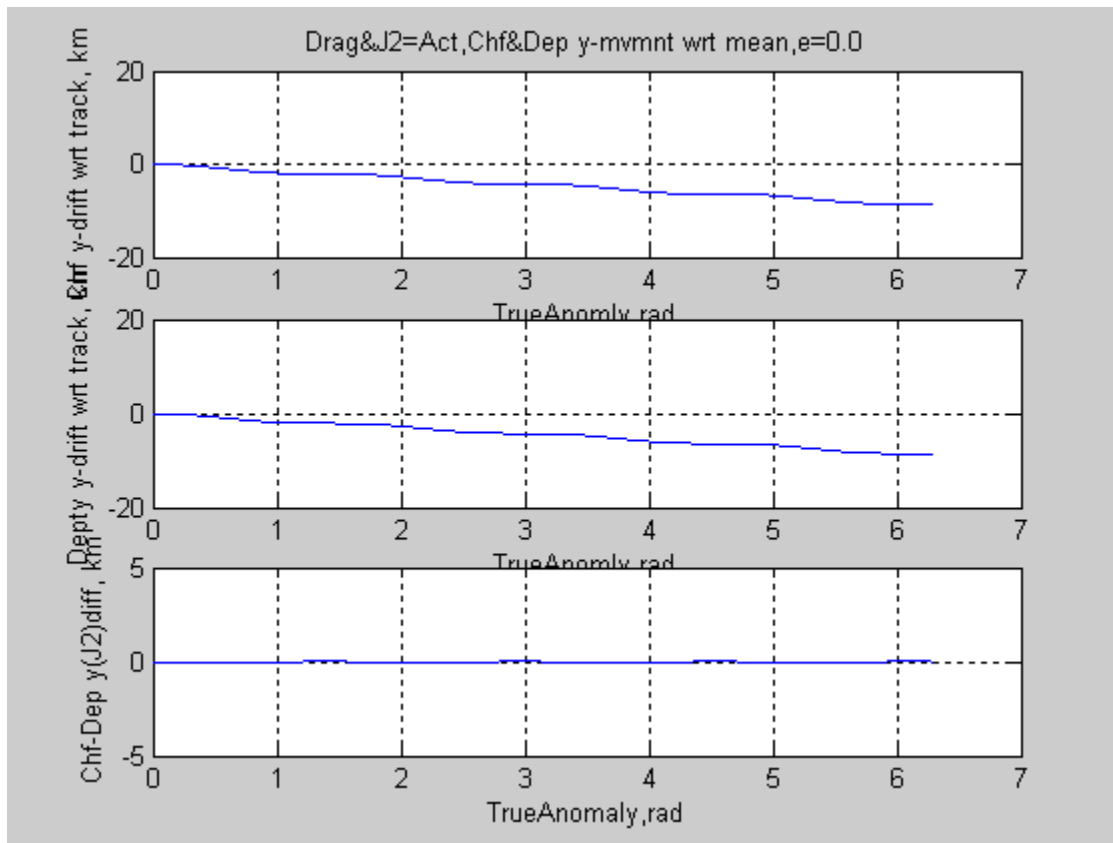


Figure 25: Circular Orbit Radial Difference Between Chief And Deputy. (Case 6 -plot 2/6).

From Figure 25 it can be noted that the J_2 induced lateral drift and difference in lateral drift between the two satellites is essentially like the elliptic case within the accuracies of these calculations. However it is suspected that as eccentricity is increased beyond the $e = .03$ case investigated that the relative drifts may diverge more, especially near apogee and perigee.

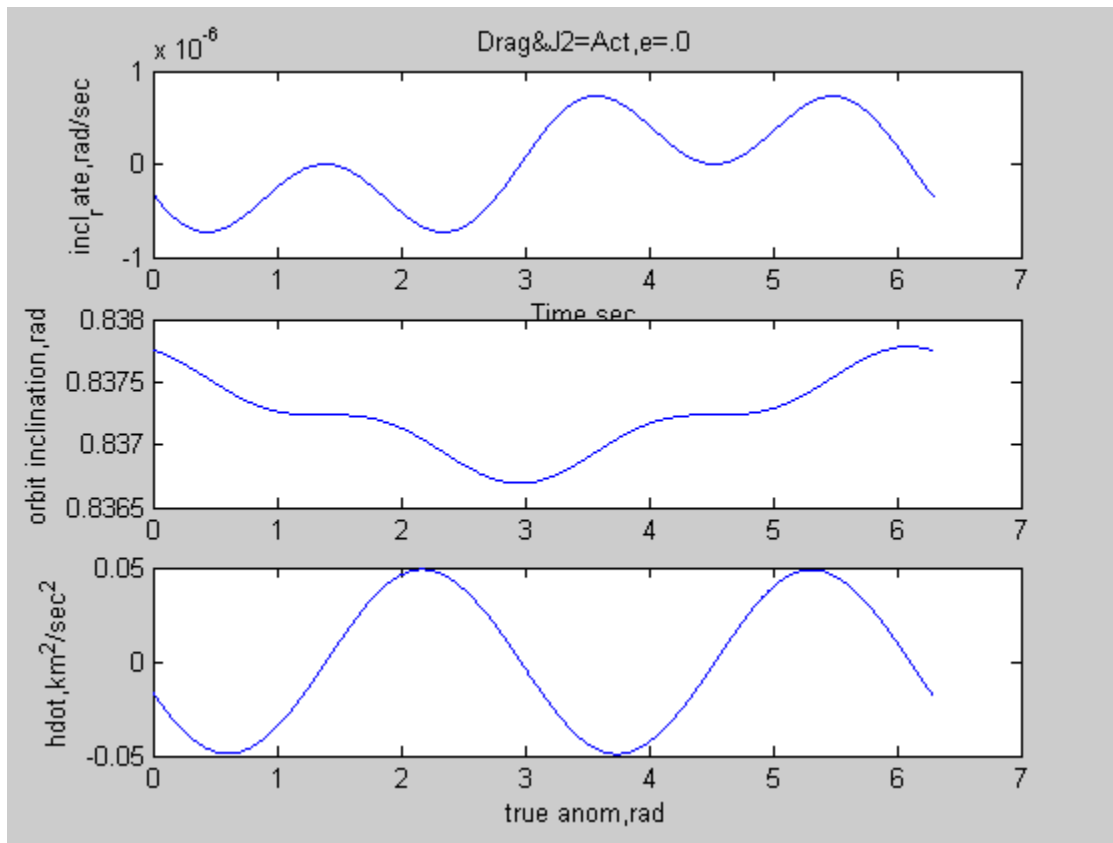


Figure 26: Circular Orbit J2 Effect On Orbit Inclination And Momentum. (Case 6 -plot3/6)

Comparing Figure 26 to Figure 14, it appears that the orbital inclination variations and angular momentum perturbations due to J2 effects are slight higher for the circular orbit than for the elliptical orbit, although this may be due in part to the fact that $a = 6678$ km for the circular orbit and $a = 7555$ km for the elliptical orbit, the larger orbit having a higher angular momentum to overcome, in order to cause an inclination change.

To determine whether the above pattern repeats for each orbit, or diverges, an additional run was made of Test Case 6 to go for two orbits. The results are presented in Figure 27 on the

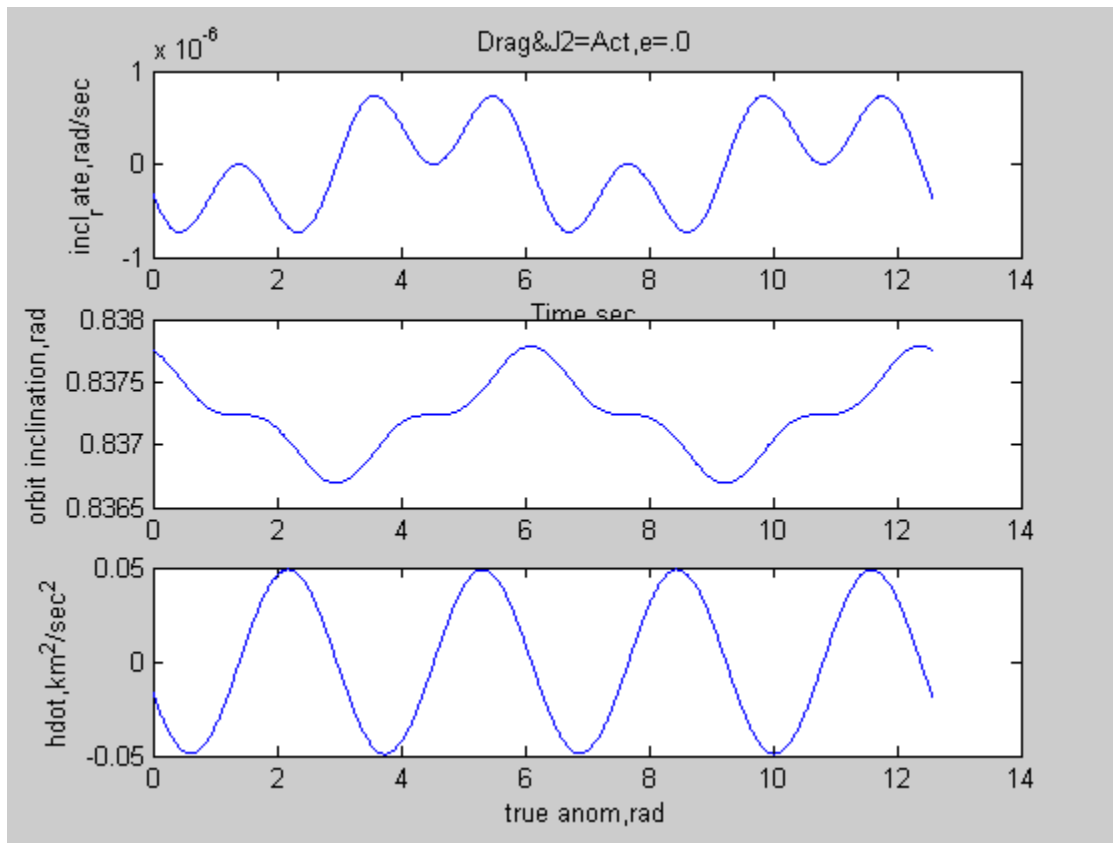


Figure 27: Test Case 6 For Two Orbits Shows Repitition In J2 Distrubance Pattern. (plot 4/6)

next page, and shows the pattern of Figure 26 repeating for the next orbit. This was also true of the other variables examined, but not plotted in this report. Although not plotted in this report, the J_2 precession rates computed in the analysis program used for this study, agree well with the charts presented in reference (6).for the right ascension of the ascending node , argument of perigee, and mean anomaly for both the chief and deputy satellites. These precession rates appear nearly constant during the orbit which agrees with expected results.

From Figure 6, circular orbit with no perturbation, that the deputy remained a constant 1 km. behind chief. However note in the Figure 28, a polar plot for the deputy to chief along-track separation, that the relative orbit spacing is not constant, but varies from about 1 km. at true anomaly of 180 degrees to about 1.2 km at 0 degrees. This variation in spacing appears to range up to 200 m. beyond the initial 1 km. separation, for a circular orbit. This variation in along-track spacing is the result of including the J_2 perturbation components in the model.

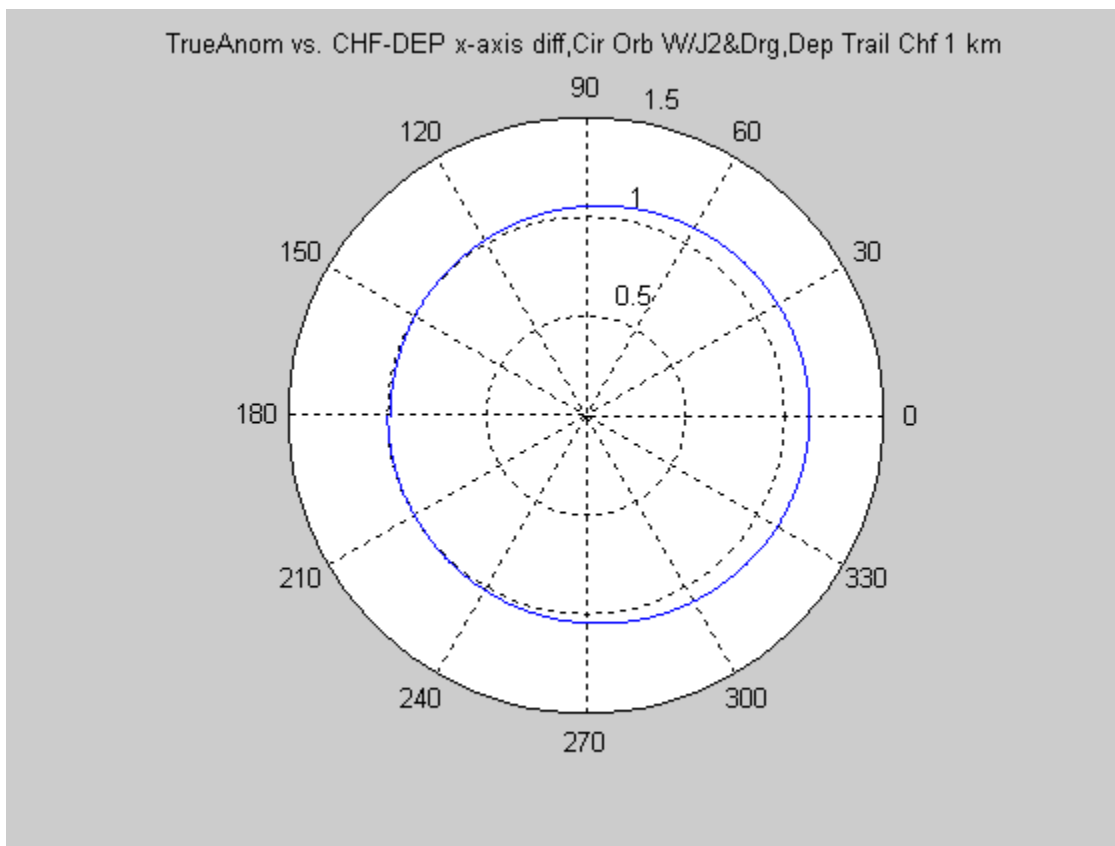


Figure 28: Polar Plot Of Differences Vs. True Anom. In Along-Track Spacing. (Case 6-plot 5/6)

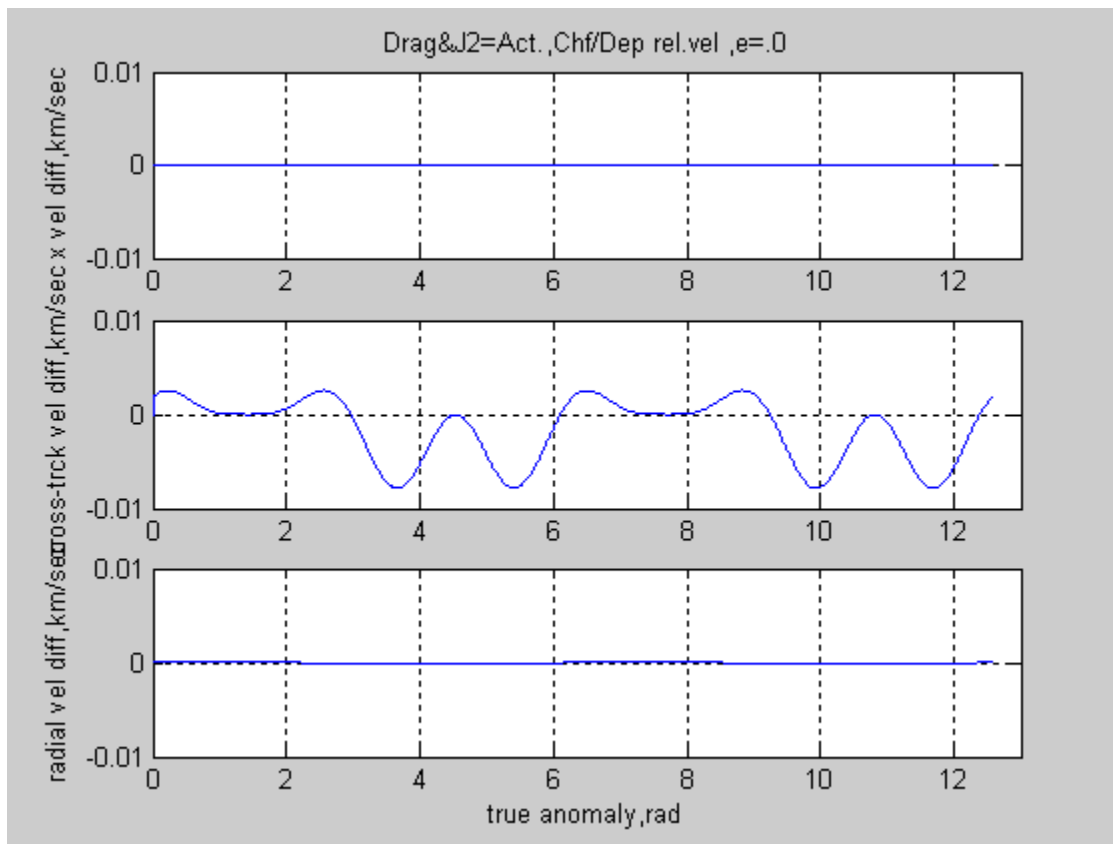


Figure 29: Deputy Relative Velocity Component Differences For Two Orbits. (Case 6 –plot6/6).

In Figure 29 the three dimensional velocity component differences between the two satellites may be seen. For the x (along-track) and z (radial) there appear to be no significant velocity differences so only small corrections or delta-v's would be required in these axes for the circular case, to maintain a satellite formation. However for the cross-track direction or y-axis it appears that there are noticeable differences in the velocity components and it can be observed that the area under the velocity curve appears to be biased in the negative direction such that a net negative y-velocity would result, if left uncompensated. This may account for the negative

velocity drift or precession portrayed in Figure 25 and elsewhere for both elliptic and circular orbits. It may be noted by comparison with Figure 6, that the cross-track velocity variation is the result of adding the J_2 perturbation effects. As far as the effects of drag perturbation on this case, it was not readily observable.

These tests were intended to provide a level of confidence that program is useful simulation of the low-earth-orbit gravitational and atmospheric environment, so far as it pertains to the the study of a two-satellite formations. However to provide some additional functionality to the program, a three-axis rocket thruster was added to the deputy or follower model. The next section provides some limited cases of thruster inputs and and resulting dynamics.

Table 2: Results of Cases Investigated Using Program In MATLAB-Environment..

Orbital Test Cases Investigated and Summary of Results.

Test Conditions	Orbit Parameters					(Perturbations)		
	a,km	e	i,rad	Ω ,rad.	ω ,rad.	Mo,rad.	J2	Cd
1- Chief Orbit (circular).	6678.	0.0	0.837	0.349	0.1745	0.0	0.0	0.0
- Deputy Orbit (1 km. trail)	6678.	0.0	0.837	0.349	0.1745	-0.00003	0.0	0.0
- Results - Orbits tracked exactly- maintained 1 km. spacing.								
2- Chief Orbit (ellipse)	7555	0.03	0.837	0.349	0.1745	0.0	0.0	0.0
- Deputy Orbit	7555.	0.03*	0.837*	0.349*	0.1745*	0.0*	0.0	0.0
- Results- Model produced results much like check-case of reference(4) with no perturbations.								
3- Chief Orbit(ellipse w/J2)	7555.	0.0	0.837	0.349	0.1745	0.0	1	0.0
- Deputy Orbit (same as 2-)	7555.	0.0	0.837	0.349	0.1745	-0.00003,	1	0.0
- Results - Both orbits added similar cross-track drift component. (~ 7.5 km y-drift/orbit)								
4- Chief Orbit (ellipse)	7555	0.03	0.837	0.349	0.1745	0.0	1	2
- Deputy Orbit (same as 2-)	7555.	0.03*	0.837*	0.349*	0.1745*	0.0*	1	2
- Results – Same as for case 3, with no noticeable affects due to drag.								
5- Chief Orbit (ellipse/J2/Cd)	7555	0.03	0.837	0.349	0.1745	0.0	1	2
- Deputy Orbit (1 km trail)	7555.	0.03*	0.837*	0.349*	0.1745*	0.0*	1	2
- Results – Dep. drifted from 1 to 10 km along track distance during orbit also same lat. drift.								
6- Chief Orbit(circular/J2/Cd)	6678	0.0	0.837	0.349	0.1745	0.0	1	2
- Deputy Orbit(1 km trail)	6678.	0.0	0.837*	0.349*	0.1745*	0.0*	1	2
- Results – Chf-dep cross-track velocity variations due to addition of J ₂ . compared to Case 1. -- Ran case for two orbits and perturbation patterns repeated.								

*

Note- 1. When J2 effects are active, J2 = 0.00108263.

2. When drag perturbation active, Cd = 2.2 for each satellite.

* indicates deputy orbits are chief orbits plus small added delta's (examples from reference (4))

II. Addition Of A Three-Axis Thruster Model.

In order to introduce rocket-like thrust forces into the formation satellite simulation, a three-axis, on-off, thrusting capability was added to the deputy satellite model at points in the equations designated for control input vectors. The purpose of the thrusters was to provide a means to incorporate thrust into the model and observe model behavior in response to these inputs. The three thrust directions included were "x-rocket" along the track, for directly assisting or retarding velocity; "y-rocket" axis for cross-track accelerations to left or right, and "z-rocket" to provide forces in the radial direction. The rocket thrust effects were simulated as constant accelerations, either positive or negative, for the duration of the rocket firing. Also each rocket was either at full thrust, or "off".

Two sample cases are provided in this thesis as Figures 30 and 31. In Figure 30, while in a circular orbit initially together, the deputy rocket attempts a deceleration of 0.00008 km/sec^2 .

Figure

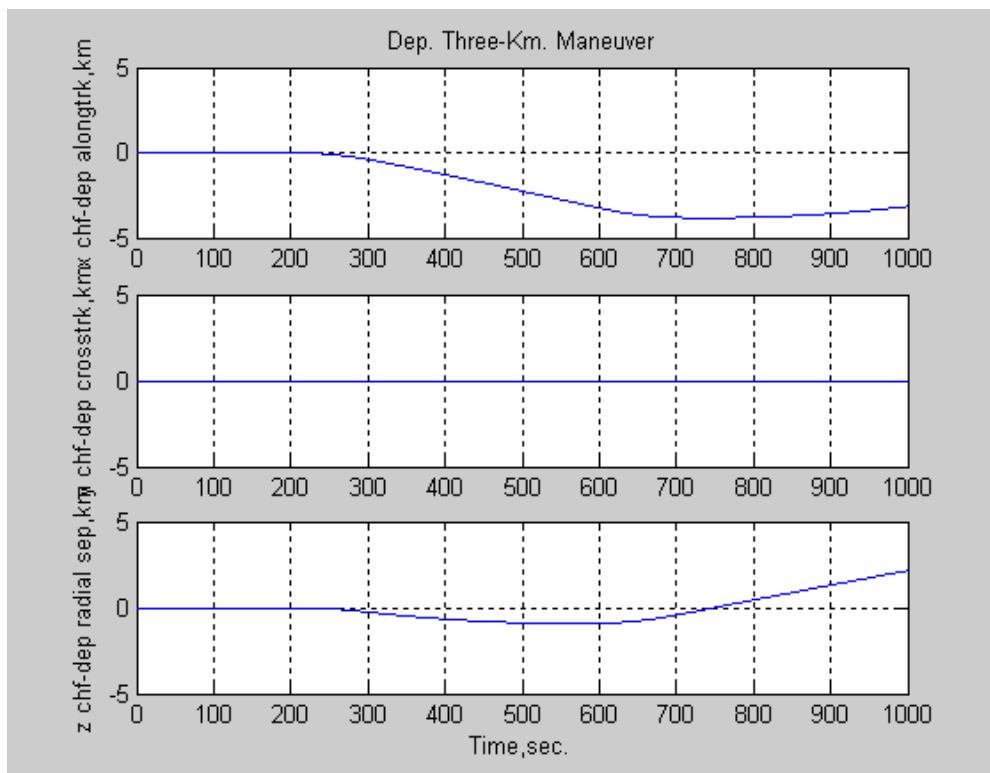
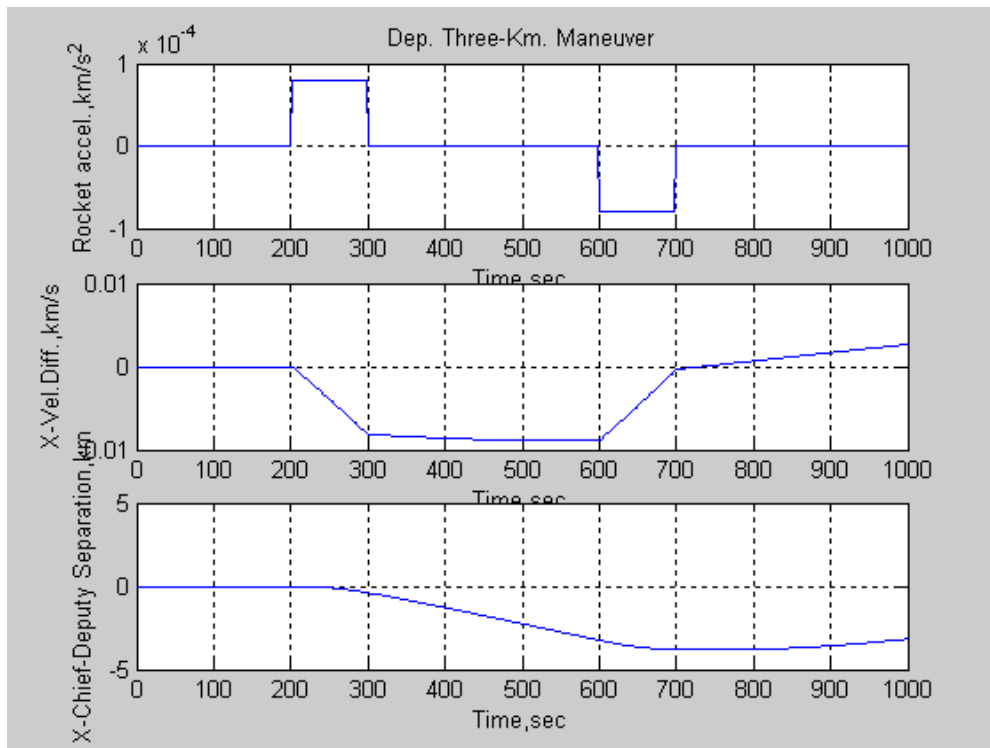


Figure 30: Deputy Attempt Decel And Hold Three Km.

for 100 seconds, to drift rearward until a 3 km. separation is achieved, and then arrest backward drift with a like magnitude firing in the opposite direction. However, without any radial thrust compensation orbital mechanics dictates that when the deputy slows up, it also moves upward, at least initially, changing it's radius relative to the chief reference track. This velocity-radial coupling will require compensation during formation corrections and repositioning. However control algorithms are easily designed to include these effects.

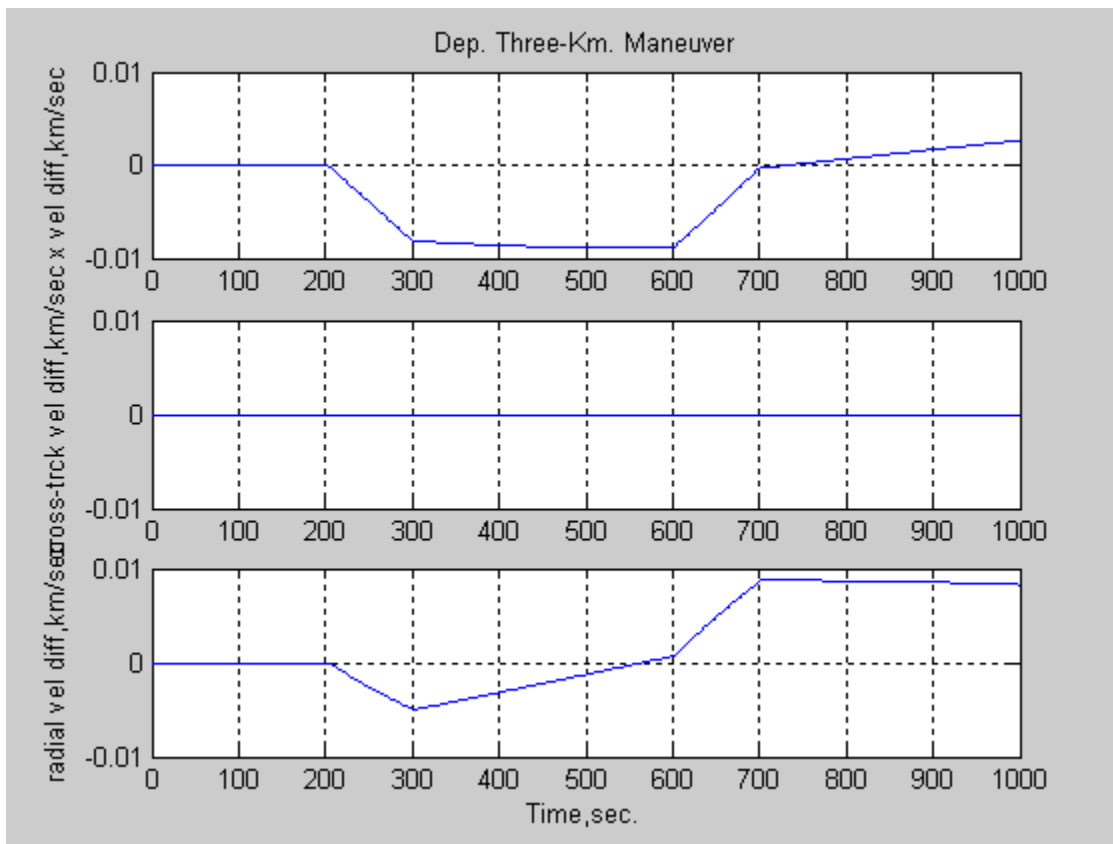


Figure 31: Relative Velocity Components For 3 Km Hold Maneuver.

In Figure 31 the relative velocity profile for each component is shown, resulting from the accelerations shown in Figure 30. In Figure 32 is an attempt to add a radial

thrust component to the "3 km separate and hold maneuver" and observe the orbit for two revolutions.

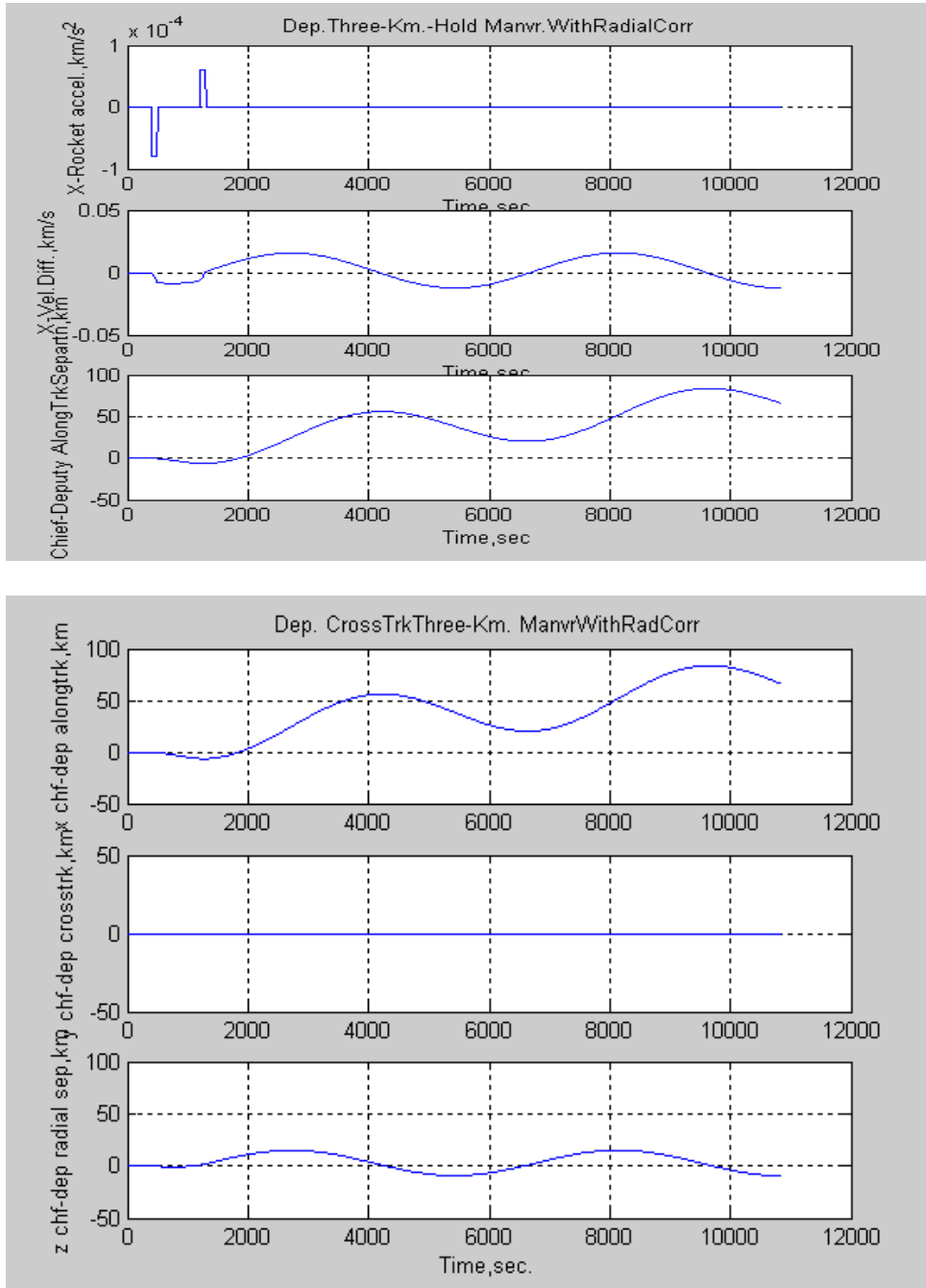


Figure 32: Three Km Sep. & Hold Maneuver With Radial Thrust.

It may be noted that the result of this input over two orbits was to cause

a large "along-track separation." In Figure 33 is shown the thrust component profiles that produced the responses shown in Figure 32.

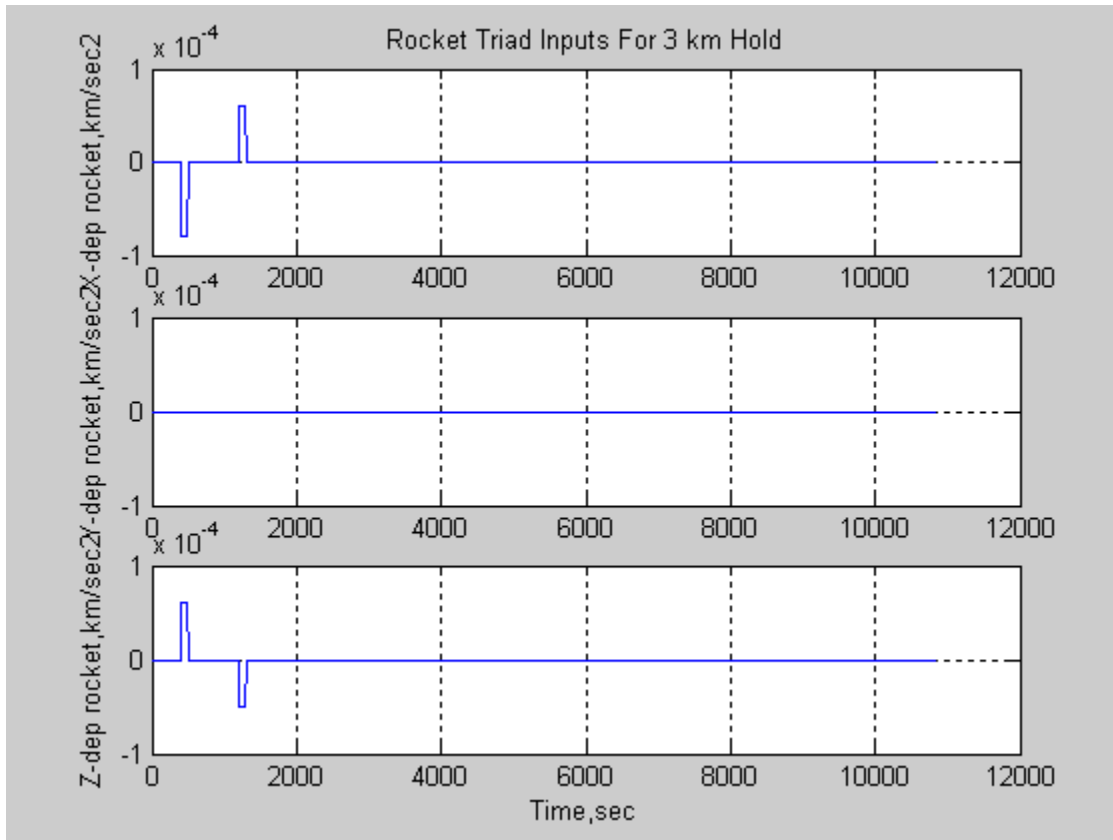


Figure 33: Thruster Input Profile That Resulted In Formation Separation Of Figure 32.

III. Direct Launch To Orbit From Cape Kennedy

As an example of the possible use of the satellite formation simulation program, the situation of a launch directly into orbit case is considered. From reference (7) is provided the launch site longitude and latitude. Also for this type of launch directly to the east, with no other maneuvering, defines the orbit inclination as the launch site latitude. The satellite formations to

be considered for this example are 1 km trail, 3 km trail, 1 km chevron, and 3 km chevron. Also for these cases, delta-v calculations were added, to demonstrate its utility. In Figure 34 the relative positions of the deputy relative to the chief are presented. It is noted that the chief long-track (x-distance) varies around the orbit from 3.0 to 3.22 km, or roughly 80 m. This variation happens once per orbit, and is definitely the result of the presence of J_2 perturbations in the simulation. So even a relative circular orbit may present unexpected variations with the presence of J_2 effects.

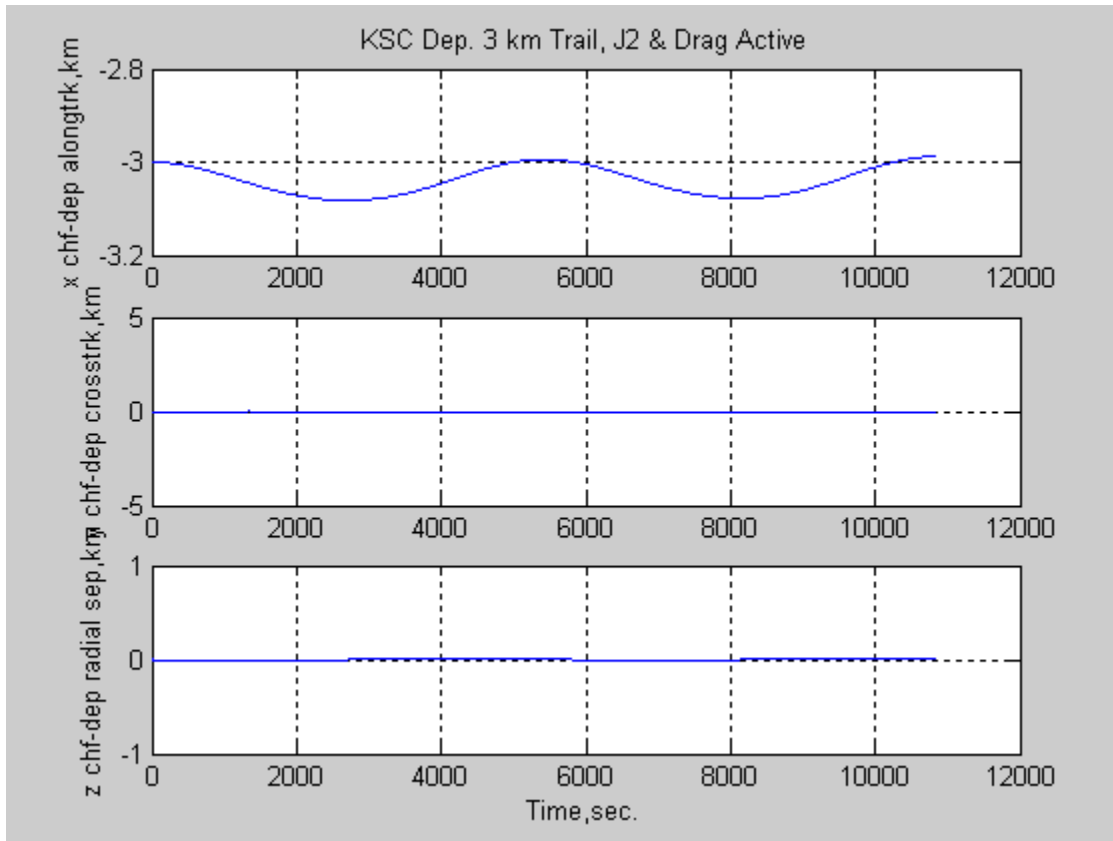


Figure 34: Launch From Cape Kennedy Deputy Trail 3 Km.

The following formations were simulated for a circular orbit with J_2 and drag present, using the Cape Kennedy launch conditions from reference (7):

Kennedy Launch Orbital Test Cases Investigated and Summary of Results.

Test Conditions	Orbit Parameters					(Perturbations)			
	a,km	e	i,rad	Ω ,rad.	ω ,rad.	Mo,rad.	J2	Cd	
1- Chief Orbit (circular).	6678.	0.0	0.4974	3.3	1.57	0.0	Active	Active	
- Deputy Orbit (1 km. trail)	6678.	0.0	0.4974	3.3	1.57	-0.00003	"	"	
- Results - Orbits tracked exactly- maintained 1 km. spacing. Delta-v peak =									
2- Chief Orbit (circular).	6678.	0.0	0.4974	3.3	1.57	0.0	Active	Active	
- Deputy Orbit (3 km. trail)	6678.	0.0	0.4974	3.3	1.57	-0.00015	"	"	
- Results - Variation of about 80 m. around orbit.. Delta-v peak = 0.1×10^{-5} km/sec.									
3- Chief Orbit (circular).	6678.	0.0	0.4974	3.3	1.57	0.0	Active	Active	
- Deputy Orbit (1 km. chevrn)	6678.	0.0	0.4974+	3.3	1.57	-0.00003	"	"	
- Results - Delta-v peak = 0.668×10^{-5} km/sec									
4- Chief Orbit (circular).	6678.	0.0	0.4974	3.3	1.57	0.0	Active	Active	
- Deputy Orbit (3 km. chevron)	6678.	0.0	0.4974+	3.3	1.57	-0.00003	"	"	
- Results - Delta-v peak = 2.0×10^{-5} km/sec									

+ indicates that the deputy inclination will not be initialized at same value as chief, for the 3 km lateral spacing.

Delta-v peak was the peak value observed during an orbit. As the orbit completed a cycle the delta- v's would approach zero. If it is desired to maintain a formation for a complete orbit, then "delta-v" in the form of thrust will be required to maintain the desired formation, such as a 3 km chevron, and the above delta-v computations provide as estimate of fuel required, for thrusting purposes. A 3 km. chevron for this study, is defined as the deputy trailing 3 km back, and 3 km to the right, of the chief.

CHAPTER FIVE: CONCLUSIONS

The main purpose of this study was to develop a simulation program that can be used by the UCF KnightSat team to investigate issues and problems related to establishing and maintaining satellite formations in the presence of atmospheric drag and gravity perturbations. Results derived from this program will be useful in defining "delta-v" budgets, and in developing closed-loop control algorithms and control strategies, to help manage a satellite formation. The program developed during this effort includes the following features: 1) two independent satellite orbital models based on the orbit radius, velocity, true anomaly, orbit inclination angle, and angular momentum vector, 2) circular or elliptic may be simulated, 3) each model includes affects of J_2 gravity perturbation, and drag, 4) models are programmed in the MATLAB environment, 5) models use fourth order Runge-Kutta integration for the dynamic "fast variables" with integration step size used from 1 to 10 seconds.

Model performance has only been checked against non-perturbation test cases from reference (8) for an elliptic orbit. The variable structure of the program emphasizes relative orbit variations, similar to Clohessy-Wiltshire or Hill equations, to monitor relative positions and velocities. The variations of deputy with respect to chief, measured with this model were in reasonable agreement for all three-axes. The results obtained during this study demonstrate the following characteristics relative to the maintenance of satellite formations in the presence of perturbations. The addition of J_2 gravity perturbations to the model caused the satellite tracks to drift in a leftward or "negative y" direction, about 7.5 km, during each orbit. However for the Cape Kennedy launched cases, these variations were less, about 3.5 km per orbit, likely due to the differences in inclination of the orbits. Also based on results obtained from this model, the

atmospheric drag perturbation effect was not observable, for the accuracy of the models and time that the models were run. Obviously in the real-world this effect eventually erodes a satellite orbit in LEO, but for the limited scope of this study, it was not observable as to affecting a satellite formation, or an individual satellite for that matter. The drag model was from reference (7).

To demonstrate the satellite formation models reaction to thrust or rocket inputs, a simple three-axis, on-off, thrust capability was added to the simulation of the deputy. One result readily apparent was that the velocity and radial states are dynamically coupled, as would be expected, such that simple thrust inputs in the direction of the velocity vector will require radial thrust compensation to maintain formation positioning, during thrusting.

In addition to the above capability, a delta-v computation was implemented in the program, based in taking the relative differences in "vdot" for the chief and deputy for each time step, and integrating these to obtain a cumulative delta-v. Results indicate that as lateral displacement, by inclination difference, is increased, the required delta-v, to maintain a formation, is increased.

This programmed model provides a means to examine an array of effects including variations in orbital initial conditions, satellite spacing, gravity and drag perturbations, inclination angle, altitude, and eccentricities and the implications for delta-v and control algorithm design. However, it should be recognized that this model has limitations, as all models do, and additional comparative analysis against such programs as Satellite Tool Kit (STK) could be the subject of future research, to develop additional confidence, or point to areas that may need improvement.

APPENDIX: ANALYSIS PROGRAM IN MATLAB

APPENDIX: ANALYSIS PROGRAM IN MATLAB

```
Program KSC_1.m written in MATLAB programming language
By Robert L.Cannaday
% ***** KSC_1.m ***** (11/25/05)
%
% "KSC_1.m" developed to provide UCF KnightSat project simulated check
% cases for an array of chief-deputy formations. J2 and drag active.
% Test Condition Assumptions- Launch KnightSat two-satellite constellation directly
% into orbit from Cape Kennedy, FL.
% Launch Site Coordinates >> Latitude = 28.5 deg, Longitude = -80.55 deg. <<
% --Pre-launch analysis:
% --For Direct Launch into orbit, launch lat = orbit inclination, so inc = 28.5 deg.
% --cos(lambdau)=cos(beta)/sin(i)>>>lambdau = 90.0 deg from Vallado(6-15)p.328
% --so from Vallado Fig 6-8, THTLST= OMG + lambdau>>OMG = -80.55+90.+180=+189.45
% --launch azimuth sin(beta)= cos(inc)/cos(launch lat)>>beta=90.deg?
% No thruster rocket inputs made for KSC cases.
% FORMATIONS TO BE RUN:
% Form(1)- Together, no spacing.(trivial case- same track "delta-v"=0?)
% Form(2)- Chief lead deputy 1 km., same track. (implies dep dMo =
% -0.00014975 radians)
% Form(3)- Chief leads deputy 3 km., same track
% Form(4)- Deputy in 1 km chevron, 1 km to right, 1 km back
% Added rocket thruster to slow up/speed up ("delta-v" related)(11/14/05)
% Added polar coord. format for several "difference variables" vs. true anomaly.(11/11/05)
% Corrected y-lateral (cross-track) variation equations.?(11/03/05)
% Corrected true anomaly by adding J2-precession term to both sats.(11/01/05)
% Added drag perturbation (10/29/05)
% Added capability to do multiple plots on one page(10/26)
% Added simple x,y,z relative computation.(10/24)
% Corrected Runge-Kutta integration and installed for both
% satellites(10/24)
% Added deputy satellite with J2 effects(not verified) (10/10/05)
% Added transform from orbit a,e,i, OMG, arg of perigee, mean anomaly to
% earth inertial X,Y,Z. (10/08/05)
% Added J2 precession effects on arg of perigee, long of ascending node(10/08)
% Added Runge-Kutta fourth order integration for r,v, and w
% Updated 10/06/05
% program j2force.m added J2 gravity perturbation accelerations to
% two-body gravity Keplerian model
```

format compact


```
% ***** >>> USER SUPPLIED <<<<< CHIEF ORBITAL PARAMETERS *****
a = 6678. %km, semi-major axis for ellipse (300 km above Req, spherical earth)
ecc = 0.0 %orbital eccentricity (circular=0.0)
```

```
% ***** >>> USER SUPPLIED <<<<< CHIEF INITIAL CONDITIONS *****
OMG(1) = 189.45/57.2958 %rad,longitd of ascndng node,(mesured in equtrl plane wrt Ix)
inc(1) = 28.5/57.2958 %inclination angle, since launch eastward at max latitude "perigee" pt
M(1)= 0.0 %Mo, initial mean anomaly,rad.
TA(1) = 0.0 % initial true anomaly, rad
gamma = 90.0/57.2958 %rad, initial angle between vel. vctor & radial.(90 deg @ prgee?)
argpg(1)= 90.0/57.2958 %radians, argument of perigee(since launch from KSC)
```

```
w(1) = 0.0 % km^2/sec,initial radial w-state compt? (zero at perigee)(not a velocity)
%ychf(1)= 0.0 %chf initl latrl displcmnt in Hill-like coord.(chf always at origin?)
```

```
% ***** >>>> USER SUPPLIED <<<<<<< CHIEF DRAG PERTURBATION *****
Cd = 2.2 %from Vallado, typical satellite drag coeff in upper atmosphere
Area = .04 % m^2,KnightSat assumed NANOSAT with 8" X 8" >> .2m X .2m = .04m^2
mass = 8.0 % kg, KnightSat target weight.
Hscf= 53.628 % scale height. Valladaotable 8-4(select for each orbit range,see p 537)
rhoref = 2.418e-11 % reference density from Vallado Table 8-4, page 537.(300 km alt)
href = 300. % reference or base altitude, from Vallado, Table 8-4, page 537.
```

```
% ***** >>>> USER SUPPLIED <<<<<<< DEPUTY DRAG PERTURBATION *****
Cddp = 2.2 %from Vallado, typical satellite drag coeff in upper atmosphere
Areadp = .04 %m^2, KnightSat assumed NANOSAT with 8" X 8" >> .2m X .2m = .04m^2
massdp = 8.0 % 8 kilograms KnightSat target weight.
```

```
% *****>>>> USER SUPPLIED <<<<< DEPUTY INITIAL J2 EFFECT VARIABLES **
```

```
argJ2(1) = 0.0
MJ2(1)= 0.0
```

```
% ***** >>>> USER SUPPLIED TIME STEP INFO <<<<<<< *****
T(1)= 0.0
dt = 4.0 % time step, seconds
num = 2716 % integer, (1358= 5431sec/4)(2716 = 2 orbits)
```

```
% ***** >>>> USER SUPPLIED <<<<<< DEPUTY SATELLITE *****
% ***** Initialize ORBIT ELEMENT DIFFERENCE VECTOR (OED)(Deputy w.r.t.
Chief)*****
% ***** OED methodology and notation from Schaub, chapter 14.
```

```
da = 0.0 %given in meters, converted to km, (Table 14.2)
de = 0.0%0095316%0.0001 %dimensionless( Table 14.2)
```

```

di = 0%-0.000149745 %rad, 1 km to right>>requires lower inclintn ang than chf, so must add a
"neg" di
dOmg = 0.0%1/57.2958 %rad (deg in Table 14.2)
darg = 0.0%1/57.2958 %rad (deg in Table 14.2)
dMo = -0.000449236 %rad, >>>> dMo = -3km/6678km = -.000449236 rad <<<<

% **** >>> USER SUPPLIED <<<< (deputy initialing)*****
w_dp(1) = 0.0 %km^2/sec, assumes gamma = 90 at perigee.

% *****>>> USER SUPPLIED <<<< ** DEPUTY INITIAL J2 EFFECT VARIABLES **
argJ2dp(1) = 0.0
MJ2dp(1) = 0.0

% **** CONSTANTS *****
Mu = 3.986E5 %km^3/sec2 Mu = G (Mearth + Msat)
Req = 6378.137 %km, radius of earth
J2 = 1.08263e-3 % earth oblateness coeff, 2nd zonal harmonic
pi = 3.14159

% ***** COMPUTED CHIEF ORBITAL PARAMETERS *****

p = a*(1. - ecc^2) % semiparameter, km (from Vallado)
h = sqrt(Mu*p) % angular momentum, km^2/sec (from Vallado)
n = sqrt(Mu/a^3) % mean motion, rad/sec
L = sqrt(a/Req)
rp = a*(1. - ecc)
ra = a*(1. + ecc)
Pd = 2.*pi/n % period, rad/sec(P= 5431. sec)
hp = rp - Req % km, altitude at perigee??(presumed start at perigee)
eta = sqrt(1 - ecc^2)
r(1) = rp % km, orbit radius at perigee??
hat(1)=r(1) - Req %km, chief height above spherical earth.

% ***** CHIEF ORBIT INITIAL CONDITIONS (computed from input)*****
theta(1) = argpg(1)+TA(1) %radians, true latitude (argpg + true anomaly)
Vp = sqrt((2.*Mu/r(1)) - (Mu/a)) % vel. at perigee, km/sec.(from Vallado eqtn)
v(1) = Vp % km/sec, initial horizontal x-axis sat velocity

% ***** (computed) DEPUTY SATELLITE Orbital Elements = Chief + delta's listed above.
a_dp = a + da % km, where subscript "dp" refers to deputy satellite.
ecc_dp = ecc + de

```

```

inc_dp(1) = inc(1) + di      %rad
OMG_dp(1) = OMG(1) + dOmg   %rad
argpg_dp(1) = argpg(1) + darg %rad
M_dp(1) = M(1) + dMo        % rad

% ***** (computed) DEPUTY ORBITAL PARAMETERS *****

p_dp = a_dp*(1. - ecc_dp^2)
h_dp = sqrt(Mu*p_dp)
n_dp = sqrt(Mu/a_dp^3)
rp_dp = a_dp*(1. - ecc_dp)
ra_dp = a_dp*(1. + ecc_dp)
Pd_dp = 2.*pi/n_dp
eta_dp = sqrt(1 - ecc_dp^2)

% **** (computed) DEPUTY INITIAL CONDITIONS (delta's referenced to CHIEF) ****
TAdp(1) = TA(1) + dMo
r_dp(1) = rp_dp
dephat(1) = r_dp(1) - Req      %km, deputy height above spherical earth.
RDiff(1) = hat(1) - dephat(1) %km, diff between ht. of chief and deputy. (neg if rdep > rchf)
thtdp(1) = argpg_dp(1) + TAdp(1)
Vpdp = sqrt(2.*Mu/r_dp(1) - Mu/a_dp)
v_dp(1) = Vpdp

w_dp(1) = 0.0      %km^2/sec, assumes gamma = 90 at perigee.

% ***** CHIEF DRAG COMPUTATION (if Cd > 0) *****
hellip = r(1) - Req
rho(1) = rhoref*exp(-(hellip - href)/Hsclf)
kdrag = (Cd*Area/mass)
drag(1) = .5*rho(1)*kdrag*v(1)^2      %drag force on chief.

% ***** DEPUTY DRAG COMPUTATION (if Cddp > 0) *****
kdragdp = (Cddp*Areaddp/massdp)
hellipdp = r_dp(1) - Req
rhodp(1) = rhoref*exp(-(hellipdp - href)/Hsclf)
dragdp(1) = .5*rhodp(1)*kdragdp*v_dp(1)^2      %drag force on deputy

% ***** DEPUTY ROCKET ACCELERATION *****
% ***** (rocket triad: thrust components aligned with deputy x-direction
% (along track), deputy y-direction (h-direction or cross-track), and
% z-direction (radial with positive toward earth).
X_rocket(1) = 0.0      % km/sec^2, specif thrust aligned in dep x-direction.

```

Y_rocket(1)= 0.0 % km/sec^2, specif thrust, aligned cross-track (parallel to h)
 Z_rocket(1)=0.0

% ***** Initializing CHIEF J2 force perturbation parameters *****
 % ***** (eqtns from Curtis page 178)*****

kj2 = 1.5*(Mu/r(1)^2)*J2*(Req/r(1))^2

pr(1) = -kj2*(1 - 3.*sin(inc(1))^2*sin(theta(1))^2) %km/sec^2, radial comp of pert.

ptrans(1) = -kj2*sin(inc(1))^2*sin(2*(theta(1))) %km/s^2,transverse (w/vel vector)

ph(1) = -kj2*sin(2*inc(1))*sin(theta(1)) % km/sec^2, where theta = w + TA

%***** J2 ON CHIEF equations below from Schaub 14.133a,b, and c. *****

% *****

OMGJ2dot(1)=-1.5* J2 * n *(Req/p)^2* cos(inc(1)) %J2 ascndng node drift(rad/sec),

argJ2dot(1)=.75* J2 * n *(Req/p)^2*(5.*cos(inc(1))^2 - 1.)%J2 mean drft arg o perige,(rd/sc)

MJ2dot(1)=.75* J2 *n*(Req/p)^2*eta*(3.*cos(inc(1))^2 - 1.)%J2 mean anmly drft(rd/sc)

OMGJ2dotplt(1)= 86400.*57.2957* OMGJ2dot(1) %convert J2 induced drift to deg/day for plot.

argJ2dotplt(1)= 86400.*57.2957* argJ2dot(1) %cnvrt J2 induced arg of perigee drift'deg/day-for plot

MJ2dotplt(1)=86400.*57.2957* MJ2dot(1) % convert J2 induced in mean anomaly rate

%***** Initializing CHIEF Satellite States w/J2 pert. *****

r(1) = w(1)/r(1) % First value of Rdot for deputy.

vdot(1) = -Mu*w(1)/(v(1)*r(1)^3) + ptrans(1)-drag(1) % First value of Vdot.

w(1) = v(1)^2 -Mu/r(1) + r(1)*pr(1) % km^2/sec^2, First value Wdot.

TA(1)=(1/r(1))*sqrt(v(1)^2 -(w(1)/r(1)^2))+ MJ2dot(1)% rad/sec, init tr anmly rate

%***** Initializing CHIEF cross-track velocity and position components due to J2
 (11/03/05)***

h(1) = r(1)*ptrans(1)

idot(1) = h(1)*cos(theta(1))/(n*a^2*eta) % from Vallado eqtn 9-21 (10/25)

vh(1) = idot(1)*r(1)*sin(theta(1))

yJ2chf(1) = vh(1)*dt %km, initial cross-trk displacement from mean trk due to J2.

```

% ***** Initializing DEPUTY J2 force perturbation parameters *****
% *****( eqtns from Curtis page 178)*****
kj2dp = 1.5*(Mu/r_dp(1)^2)*J2*(Req/r_dp(1))^2
prdp(1) = -kj2dp*(1 - 3.*sin(inc_dp(1))^2*sin(thtdp(1))^2) %km/sec^2,radial(+ outward)

ptrnsdp(1) = -kj2dp*sin(inc_dp(1))^2*sin(2*(thtdp(1))) %depty transverse (w/vel vector)

phdp(1) = -kj2dp*sin(2*inc_dp(1))*sin(thtdp(1)) % where theta = w + TA

% Initializing DEPUTY J2 effects on OMG, arg of perigee, and mean anomaly

OMGJ2dotdp(1)=-1.5* J2 * n_dp *(Req/p_dp)^2* cos(inc_dp(1)) %J2 ascndng node
drift(rad/sec),

argJ2dotdp(1)=.75* J2 * n_dp *(Req/p_dp)^2*(5.*cos(inc_dp(1))^2 - 1.)%J2meandrft arg o
perige,(rd/sc)

MJ2dotdp(1)=.75* J2 *n_dp*(Req/p_dp)^2*eta_dp*(3.*cos(inc_dp(1))^2 - 1.)%J2 mean anmly
drft(rd/sc)

OMGJ2dotdpp(1)= 86400.*57.2957* OMGJ2dotdp(1) %convert J2 induced drift to deg/day for
plot.

argJ2dotdpp(1)= 86400.*57.2957* argJ2dotdp(1) %cnvrt J2 induced arg of perigee drift'deg/day-
for plot

MJ2dotdpp(1)=86400.*57.2957* MJ2dotdp(1) % convert J2 induced in mean anomaly rate to
deg/day for plot.

%***** Initializing DEPUTY Satellite States w/J2 pert. *****
rdotdp(1) = w_dp(1)/r_dp(1) % First value of Rdot.
vdotdp(1) = -Mu*w_dp(1)/(v_dp(1)*r_dp(1)^3) + ptrnsdp(1)-dragdp(1) % First value of Vdot.
wdotdp(1) = v_dp(1)^2 -Mu/r_dp(1) + r_dp(1)*prdp(1) % km^2/sec^2, First value Wdot.
TAdotdp(1)=(1/r_dp(1))*sqrt(v_dp(1)^2 -(w_dp(1)/r_dp(1)^2))+MJ2dotdp(1)%rad/sec, init TA
rate

%***** Initializing DEPUTY cross-track velocity and position components due to J2. ***
hdotdp(1) = r_dp(1)*ptrnsdp(1)-r_dp(1)*Y_rocket(1)
hdp(1) = sqrt(Mu*p_dp) %initial angular momentum
idotdp(1) = hdotdp(1)*cos(thtdp(1))/(n_dp*a_dp^2*eta_dp) % from Vallado eqtn 9-21 (10/25)
vhdp(1) = idotdp(1)*r_dp(1)*sin(thtdp(1))
yJ2dp(1) = vhdp(1)*dt

```

yCfDpdiff(1)= yJ2chf(1)- yJ2dp(1)

% ***** Initializing Hill-like parameters ***** (10/24/05)

tadiff(1) = TAdp(1)-TA(1) %rad, difference in true anomaly between chief and dep (neg if chf ahead)

incdiff(1) = inc(1)-inc_dp(1) %rad, difference in chief/deputy inclination angle(s/b neg if deputy on right)

xsep(1) = (2*(r(1) + r_dp(1))/2)*sin(.5*(tadiff(1))) % km, x-axis deputy wrt chief

yHL(1)=(r(1) + r_dp(1))/2*(incdiff(1))*sin(theta(1))%km, y-axis deputy wrt chief (pos deputy@RWng)

zsep(1) = r(1) - r_dp(1) %km, z-axis dep wrt chief (positive for dep below chief)

septn(1) = sqrt(xsep(1)^2 + yHL(1)^2 + zsep(1)^2)

% ***** Initializing Hill-like (?) velocity parameters***** (10/25/05)

xveldiff(1) = v(1) - v_dp(1) % km/sec , tangential velocity diff.

yveldiff(1) = vh(1) - vhd(1) % km/sec , lateral or cross-track vel diff.

zveldiff(1) = rdot(1) - rdotdp(1) % km/sec, vertical or radial vel. diff.

% ***** Total lateral displacement = y(due to incdiff) + y(due to J2)***

yINCdp(1)=-incdiff(1)*r_dp(1)*sin(theta(1))

yINCchf(1)=0.0

yTOTchf(1)=yJ2chf(1)+yINCchf(1)

yTOTdp(1)= yJ2dp(1) + yINCdp(1)

% ***** Initializing Delta-V ***** (11/26/05)

deltaV(1)=(vdot(1) - vdotdp(1))*dt %km/sec, initializing "delta-V" accumulator

% ***** END Initializing *****

% ***** BEGIN LOOPING *****

for i = 1:num

% ***** CHIEF PERTURBATION COMPUTATION ***** (see Curtis p. 178)***

kj2 = 1.5*(Mu/r(i)^2)*J2*(Req/r(i))^2

pr(i) = -kj2*(1 - 3.*sin(inc(i))^2*sin(theta(i))^2)

ptrans(i) = -kj2*sin(inc(i))^2*sin(2*(theta(i)))

ph(i) = -kj2*sin(2*inc(i))*sin(theta(i)) % theta = w + TA

% ***** Computation of J2 EFFECTS on CHIEF orbit parameters OMG, arg of perigee, and

M *****

% ***** equations from Schaub, 14.133 a, b, and c *****

```

OMGJ2dot(i) = -1.5* J2 * n *(Req/p)^2* cos(inc(i)) % J2drift in mean long of ascendg node,
argJ2dot(i)=.75* J2 * n *(Req/p)^2*(5.*cos(inc(i))^2 - 1.)%J2drift rate in mean arg of perigee,
MJ2dot(i)=.75* J2 *n*(Req/p)^2*eta*(3.*cos(inc(i))^2 - 1.)%J2 mean anomaly
drft(rd/sc)(14.133c),Schaub

```

```

OMGJ2dotplt(i) = 86400.*57.2957* OMGJ2dot(i) % convert J2 induced drift into degrees/day
for plot.

```

```

argJ2dotplt(i) = 86400.*57.2957* argJ2dot(i) % convert J2 induced arg of perigee drift
(deg/day) for plot

```

```

MJ2dotplt(i) = 86400.*57.2957* MJ2dot(i) % convert J2 induced in mean anomaly rate to
deg/day for plot.

```

```

%*****
% ***** CHIEF DRAG COMPUTATION (if Cd>0)*****
hellip= r(i)-Req
rho(i)= rhoref*exp(-(hellip - href)/Hsc1f)
drag(i) = .5*rho(i)*kdrag*v(i)^2
% *****

```

```

rdot(i) = w(i)/r(i) %f1
vdot(i) = -Mu*w(i)/(v(i)*r(i)^3) + ptrans(i) - drag(i) %f2 (**includes J2 & drag)
wdot(i) = v(i)^2 - Mu/r(i) + r(i)*pr(i) %f3 (**includes J2perturbation)
TAdot(i) = (1/r(i))*sqrt(v(i)^2 - (w(i)/r(i))^2)+ MJ2dot(i) %f4
vh(i) = r(i)*idot(i)*sin(theta(i))

```

```

% ** CHIEF INTEGRATION SECTION *****
%*****

```

```

j = i + 1

```

```

% ***** Runge-Kutta fourth order *****
% ***** CHIEF RK4 for rdot to r *****
% new RK4 here >>>>>
% ***** RK4 for rdot to r (redone 10/14)*****
% ***
k1r(i) = dt*rdot(i) % k1 for computing r(t(i))

```

```

r_half_est = r(i) + .5 * k1r(i)
rk1slope = (r_half_est - r(i))/(dt/2) %slope at half time step, dt/2.

k2r(i) = dt* rk1slope %k2 for r(t)

r_half_est = r(i) + .5 * k2r(i)

rk2slope = (r_half_est - r(i))/(dt/2) %slope is (delta r)/(delta t)

k3r(i) = dt* rk2slope

r_full_est = r(i) + k3r(i)

rk4slope_full = (r_full_est - r(i))/dt

k4r(i) = dt* rk4slope_full

r(j) = r(i) + (1/6)*(k1r(i) + 2.*k2r(i) + 2 *k3r(i) + k4r(i))

if r(j) < Req, break, end
%*****
hat(j)= r(j)-Req % km, chief height above terrain
% ***** CHIEF RK4 for vdot to v (redone 10/14)*****

k1v(i) = dt*vdot(i) % k1 for computing v(t(i))

v_half_est = v(i) + .5 * k1v(i)
vk1slope = (v_half_est - v(i))/(dt/2) %slope at half time step, dt/2.

k2v(i) = dt* vk1slope %k2 for v(t)

v_half_est = v(i) + .5 * k2v(i)

vk2slope = (v_half_est - v(i))/(dt/2) %slope is (delta r)/(delta t)

k3v(i) = dt* vk2slope

v_full_est = v(i) + k3v(i)

```



```

vk4slope_full = (v_full_est - v(i))/dt

k4v(i) = dt* vk4slope_full

v(j) = v(i) + (1/6)*(k1v(i) + 2.*k2v(i) + 2 *k3v(i) + k4v(i))

% ***** RK4 for wdot to w *****

k1w(i) = dt*wdot(i)

w_half_est = w(i) + .5 * k1w(i)
wk1slope = (w_half_est - w(i))/(dt/2) %slope at half time step, dt/2.

k2w(i) = dt* wk1slope %k2 for r(t)

w_half_est = w(i) + .5 * k2w(i)

wk2slope = (w_half_est - w(i))/(dt/2) %slope is (delta w)/(delta t)

k3w(i) = dt* wk2slope

w_full_est = w(i) + k3w(i)

wk4slope_full = (w_full_est - w(i))/dt

k4w(i) = dt* wk4slope_full

w(j) = w(i) + (1/6)*(k1w(i) + 2.*k2w(i) + 2 *k3w(i) + k4w(i))

% w(j) = w(i) + wdot(i)* dt %old Euler integrator, not used.

% *****
% other variables are considered "slow variables" so
% Euler should be ok.
TAdot(j) = (1/r(j))*sqrt(v(j)^2 - (w(j)/r(j))^2)+MJ2dot(i)
TA(j) = TA(i) + TAdot(j)*dt
argpg(j) = argpg(i) + argJ2dot(i)*dt
theta(j) = argpg(j) + TA(j)

% ***** perturbation terms at j = i + 1 *****
kj2 = 1.5*(Mu/r(j)^2)*J2*(Req/r(j))^2

```

```

pr(j) = -kj2*(1 - 3.*sin(inc(i))^2*sin(theta(j))^2) %note:opposite sign

ptrans(j) = -kj2*sin(inc(i))^2*sin(2*(theta(j)))

ph(j) = -kj2*sin(2*inc(i))*sin(theta(j)) % theta = w + TA(opp sign)

% *****
hdot(j)= r(j)*ptrans(j)
idot(j) = hdot(j)*cos(theta(j))/(n*a^2*eta) % From Vallado eqtn 9-21 (10/25/05)
inc(j) = inc(i) + idot(j)*dt % rad, chief inclination angle
vh(j) = r(j)*idot(j)*sin(theta(j))
yJ2chf(j) = vh(j)*dt + yJ2chf(i) %km, initial cross-trk displacement from mean trk due to J2

OMG(j) = OMG(i) + OMGJ2dot(i)*dt
MJ2(j) = MJ2(i) + MJ2dot(i)*dt

% **** Computation of J2 EFFECTS on CHIEF orbit parameters OMG, arg of perigee, and
M *****
% ***** equations from Schaub, 14.133 a, b, and c *****

OMGJ2dot(j) = -1.5* J2 * n *(Req/p)^2* cos(inc(j)) % J2drift in mean long of ascendg node,
OMG(j) = OMG(i) + OMGJ2dot(j)*dt

argJ2dot(j)=.75* J2 * n *(Req/p)^2*(5.*cos(inc(j))^2 - 1.)%J2drift rate in mean arg of perigee,
argJ2(j) = argJ2(i) + argJ2dot(j)*dt

MJ2dot(j)=.75* J2 *n*(Req/p)^2*eta*(3.*cos(inc(j))^2 - 1.)%J2 mean anomaly
drft(rd/sc)(14.133c),Schaub
MJ2(j) = MJ2(i) + MJ2dot(j)*dt

OMGJ2dotplt(j) = 86400.*57.2957* OMGJ2dot(j) % convert J2 induced drift into degrees/day
for plot.

argJ2dotplt(j) = 86400.*57.2957* argJ2dot(j) % convert J2 induced arg of perigee drift
(deg/day) for plot

MJ2dotplt(j) = 86400.*57.2957* MJ2dot(j) % convert J2 induced in mean anomaly rate to
deg/day for plot.

```

```

%***** END CHIEF CALCULATIONS
*****

% **** DEPUTY COMPUTATION LOOPS **(same loop actually as chief)***** (see Curtis
p. 178)***
% ***** DEPUTY J2 PERTURBATIONS *****

kj2dp = 1.5*(Mu/r_dp(i)^2)*J2*(Req/r_dp(i))^2
prdp(i) = -kj2dp*(1 - 3.*sin(inc_dp(i))^2*sin(thtdp(i))^2) %km/sec^2, radial pert

ptrnsdp(i) = -kj2dp*sin(inc_dp(i))^2*sin(2*(thtdp(i))) %depty transverse (w/vel vector)

phdp(i) = -kj2dp*sin(2*inc_dp(i))*sin(thtdp(i)) % where theta = w + TA

% **** Computation of J2 EFFECTS on DEPUTY orbit parameters OMG_dp, arg of perigee
dp, and M_dp ****
% ***** equations below from Schaub, 14.133 a, b, and c
*****

OMGJ2dotdp(i)=-1.5*J2*n_dp *(Req/p_dp)^2* cos(inc_dp(i)) % J2drift in mean lng of ascndg
node,

argJ2dotdp(i)=.75* J2*n_dp*(Req/p_dp)^2*(5.*cos(inc_dp(i))^2 - 1.)%J2drift rt. mean arg
ofperigee,

MJ2dotdp(i)=.75* J2 *n_dp*(Req/p_dp)^2*eta_dp*(3.*cos(inc_dp(i))^2 - 1.)%J2 mean anmly
drft(rd/sc)

OMGJ2dotdpp(i) = 86400.*57.2957* OMGJ2dotdp(i) % convert J2 induced drift into
degrees/day for plot.

argJ2dotdpp(i) = 86400.*57.2957* argJ2dotdp(i) % convert J2 induced arg of perigee drift
(deg/day) for plot

MJ2dotdpp(i) = 86400.*57.2957* MJ2dotdp(i) % convert J2 induced in mean anomaly rate to
deg/day for plot.

% ***** Deputy Drag computation *****
hellipdp= r_dp(i)-Req
rhodp(i)= rhoref*exp(-(hellipdp - href)/Hsc1f)

```

```
dragdp(i) = .5*rhodp(i)*kdragdp*v_dp(i)^2
```

```
% ***** LOGIC FOR FIRING "X-AXIS" Deputy ROCKET  
*****
```

```
if i < 101,  
    X_rocket(i) = 0.0;  
    Y_rocket(i) = 0.0;  
    Z_rocket(i) = 0.0;  
end  
if i > 101,  
    X_rocket(i) = 0.0%-.00008;          %km/sec2("minus" means deputy breaking wrt chief)  
    Y_rocket(i) = 0.0%0008;  
    Z_rocket(i) = 0.0%0.00006          %km/sec2 (need positive to accel upward.  
end  
if i > 125,  
    X_rocket(i) = 0.0;  
    Y_rocket(i) = 0.0;  
    Z_rocket(i) = 0.0;  
end  
if i > 300,  
    X_rocket(i) = 0.0%0.00006;        %km/sec2 ("positive" value means deputy accel fwrd wrt  
chief)  
    Y_rocket(i) = -0.0%0008;  
  
    Z_rocket(i) = 0.0%0005;  
  
end  
if i > 325,  
    X_rocket(i) = 0.0;  
    Y_rocket(i) = 0.0;  
    Z_rocket(i) = 0.0;  
end  
if i > 1000,  
    X_rocket(i) = 0.000;  
    Y_rocket(i) = 0.0;  
    Z_rocket(i) = 0.0;  
end  
if i > 1025,  
    X_rocket(i) = 0.0;  
    Y_rocket(i) = 0.0;  
    Z_rocket(i) = 0.0;  
end  
if i > 1200,  
    X_rocket(i) = -0.0000;
```

```

    Y_rocket(i) = 0.0;
    Z_rocket(i) = 0.0;
end
if i > 1225,
    X_rocket(i) = 0.0;
    Y_rocket(i) = 0.0;
    Z_rocket(i) = 0.0;
end

%***** DEPUTY Satellite States w/J2 & drag pert. *****
rdotdp(i) = w_dp(i)/r_dp(i) % Deputy Rdot.
vdotdp(i)=-Mu*w_dp(i)/(v_dp(i)*r_dp(i)^3)+ ptrnsdp(i)-dragdp(i)+X_rocket(i)% Deputy Vdot.
wdotdp(i) = v_dp(i)^2 -Mu/r_dp(i) + r_dp(i)*prdp(i)+r_dp(i) * Z_rocket(i)% km^2/sec^2, Dep.
Wdot.
TAdotdp(i)=(1/r_dp(i))*sqrt(v_dp(i)^2 -(w_dp(i)/r_dp(i)^2))+MJ2dotdp(i) %rad/sec, depty
truAnomly.

%***** DEPUTY cross-track velocity and position components. ***
hdotdp(i) = r_dp(i)*ptrnsdp(i) - r_dp(i)*Y_rocket(i) % 11/17/05 Added cross-track rocket
thrust.
idotdp(i) = hdotdp(i)*cos(thtdp(i))/(n_dp*a_dp^2*eta_dp) % from Vallado eqtn 9-21 (10/25)
vhdp(i) = idotdp(i)*r_dp(i)*sin(thtdp(i))

%***** DELTA-V COMPUTATION ***** (added 11/26/05)**
deltaV(j)=(vdot(i)-vdotdp(i))*dt + deltaV(i) %km/sec, cummulative delta-v.

% DEPUTY INTEGRATION SECTION *****
%*****
j = i + 1
% add new RK4 here>>>>>>(10/24)
% ***** RK4 for rdot to r (redone 10/14)***** (fixes 10/24)

k1rdp(i) = dt*rdotdp(i) % k1 for computing rdep(t(i))

rdp_half_est = r_dp(i) + .5 * k1rdp(i)
rk1slopedp = (rdp_half_est - r_dp(i))/(dt/2) %slope at half time step, dt/2.

k2rdp(i) = dt* rk1slopedp %k2 for rdp(t)

rdp_half_est = r_dp(i) + .5 * k2rdp(i)

rk2slopedp = (rdp_half_est - r_dp(i))/(dt/2) %slope is (delta r)/(delta t)

```

```

k3rdp(i) = dt* rk2slopedp

rdp_full_est = r_dp(i) + k3rdp(i)

rk4slopedp_full = (rdp_full_est - r_dp(i))/dt

k4rdp(i) = dt* rk4slopedp_full

r_dp(j) = r_dp(i) + (1/6)*(k1rdp(i) + 2.*k2rdp(i) + 2 *k3rdp(i) + k4rdp(i))

if r_dp(j) < Req, break, end
%*****
dephat(j) = r_dp(j)-Req % km, deputy height above mean spherical earth.
RDiff(j)= hat(j)- dephat(j) % km, diff in radii, (s/b neg if rdep> rchf.)
% ***** RK4 for vdot to v (redone 10/14 & 10/25)*****

k1vdp(i) = dt*vdotdp(i) % k1 for computing vdp(t(i))

vdp_half_est = v_dp(i) + .5 * k1vdp(i)
vk1slopedp = (vdp_half_est - v_dp(i))/(dt/2) %slope at half time step, dt/2.

k2vdp(i) = dt* vk1slopedp %k2 for v(t)

vdp_half_est = v_dp(i) + .5 * k2vdp(i)

vk2slopedp = (vdp_half_est - v_dp(i))/(dt/2) %slope is (delta v)/(delta t)

k3vdp(i) = dt* vk2slopedp

vdp_full_est = v_dp(i) + k3vdp(i)

vdpk4slope_full = (vdp_full_est - v_dp(i))/dt

k4vdp(i) = dt* vdpk4slope_full

v_dp(j) = v_dp(i) + (1/6)*(k1vdp(i) + 2.*k2vdp(i) + 2 *k3vdp(i) + k4vdp(i))

% ***** RK4 for wdot to w *****

k1wdp(i) = dt*wdotdp(i)

```

```

wdp_half_est = w_dp(i) + .5 * k1wdp(i)
wk1slopedp = (wdp_half_est - w_dp(i))/(dt/2) %slope at half time step, dt/2.

k2wdp(i) = dt* wk1slopedp %k2 for wdp(t)

wdp_half_est = w_dp(i) + .5 * k2wdp(i)

wdpk2slope = (wdp_half_est - w_dp(i))/(dt/2) %slope is (delta w)/(delta t)

k3wdp(i) = dt* wdpk2slope

wdp_full_est = w_dp(i) + k3wdp(i)

wdpk4slope_full = (wdp_full_est - w_dp(i))/dt

k4wdp(i) = dt* wdpk4slope_full

w_dp(j) = w_dp(i) + (1/6)*(k1wdp(i) + 2.*k2wdp(i) + 2.*k3wdp(i) + k4wdp(i))

% Euler should be ok for slow variables following.
TAdotdp(j)=(1/r_dp(j))*sqrt(v_dp(j)^2 -(w_dp(j)/r_dp(j))^2)+MJ2dotdp(i)
TAdp(j) = TAdp(i) + TAdotdp(i)*dt
argpg_dp(j) = argpg_dp(i) + argJ2dot(i)*dt
thtdp(j)= argpg_dp(j) + TAdp(j)

% ***** perturbation terms at j = i +1 for DEPUTY *****
kj2dp = 1.5*(Mu/r_dp(j)^2)*J2*(Req/r_dp(j))^2
prdp(j)=-kj2dp*(1 - 3.*sin(inc_dp(i))^2*sin(thtdp(j))^2)% "+" since diff axis definition.

ptrnsdp(j) = -kj2dp*sin(inc_dp(i))^2*sin(2*(thtdp(j))) %depty transverse (w/vel vector)

phdp(j) = -kj2dp*sin(2*inc_dp(i))*sin(thtdp(j)) % "+"(see above),where theta = w + TA

hdotdp(j) = r_dp(j)*ptrnsdp(j)-r_dp(j)*Y_rocket(i) %>>Neg on rocket so y(pos)>>y(pos rate)
idotdp(j) = hdotdp(j)*cos(thtdp(j))/(n_dp*a_dp^2*eta_dp) % from Vallado eqtn 9-21 (10/25)
inc_dp(j) = inc_dp(i) + idotdp(j)*dt
vhdp(j) = r_dp(j)*idotdp(j)*sin(thtdp(j))

OMG_dp(j) = OMG_dp(i) + OMGJ2dotdp(i)*dt

```

```

argJ2dp(j) = argJ2dp(i) + argJ2dotdp(i)*dt
MJ2dp(j) = MJ2dp(i) + MJ2dotdp(i)*dt

yJ2dp(j) = yJ2dp(i) + vhd(i)*dt %km,cross-track y-movement due to J2-h
yCfDpdiff(j)= yJ2chf(j)- yJ2dp(j)
yINCdp(j)=incdiff(i)*r_dp(j)*sin(theta(j))
% ***** Hill-like relative position parameters ***** (10/24/05)
yTOTchf(j)=yJ2chf(j)
yTOTdp(j)= yJ2dp(j) + yINCdp(j)

tadiff(j) = TAdp(j)-TA(j) % rad, difference in true anomaly betwn chf and dep (neg. if chf
ahead)
incdiff(j)=inc(j)-inc_dp(j) %difference in chief/deputy inclination angle
xsep(j) = (2*(r(j) + r_dp(j))/2)*sin(.5*(tadiff(j))) % km, x-axis deputy wrt chief
yHL(j) = ((r(j) + r_dp(j))/2)*(incdiff(j))*sin(theta(j))% km,y-axis dpty wrt chief("+
dpty@rt.wing)
zsep(j) = r(j) - r_dp(j) %km, z-axis dep wrt chief (positive for dep below chief)
septn(j) = sqrt(xsep(j)^2 + yHL(j)^2 + zsep(j)^2)

% ***** Hill-like (?) relative velocity parameters***** (10/25/05)

xveldiff(j) = v_dp(j) - v(j) % km/sec , tangential velocity diff.
yveldiff(j) = vhd(j) - vh(j) % km/sec , lateral or cross-track vel diff.
zveldiff(j) = rdot(i) - rdotdp(i) % km/sec, vertical or radial vel. diff.

% % ***** ROCKET *****
X_rocket(j)= X_rocket(i)
Y_rocket(j)= Y_rocket(i)
Z_rocket(j)= Z_rocket(i)
% *****
T(j) = T(i) + dt
i= i + 1;
end

% ***** PLOTTING SECTION *****
plot(T,deltaV),xlabel('Time,sec'),ylabel('cumulative Dv,km/sec'),title('KSC Dep 3 km Trail, J2
& Drag Act'),
axis([ 0 12000 -.00005 .00005]),grid
pause
%polar(TA,r),title('TrueAnom vs.Chf Radius, J2=Act,Drg=Act, Dep 3 km Rt Chevrn')
%pause
%print
%polar(TA,hat),title('TrueAnom vs.Chf HAT,J2=Act,Drg=Act, Dep 3 km Chevrn')
%pause
%print

```



```

%polar(TAdp,dephat),title('TrueAnom vs.Dep HAT,km,J2=Act,Drg=Act, Dep 3 km Chev')
%pause
%print
%polar(TA,RDiff),title('TrueAnom vs.CHF-DEP Rdiff,km,J2=Act,Drg=Act, Dep 3 km Chev')
%pause
%print
%polar(TA,septn),title('TrueAnom vs.CHF-DEP totdiff,km, J2=Act,Drg=Act, Dep 3 km Chev')
%pause

subplot(3,1,1),plot(TA,xveldiff),xlabel('Time,sec'),ylabel('x-vel diff,km/s'),title('KSC Dep. 3 km
Trail, J2 & Drag Act'),
axis([ 0 13.0 -.001 .001]),grid
subplot(3,1,2),plot(TA,yveldiff),xlabel('Time,sec'),ylabel('y-vel.diff.,km/s'),
axis([ 0 13.0 -.001 .001]),grid
subplot(3,1,3),plot(TA,zveldiff),xlabel('Time,sec'),ylabel('z-vel.diff,km/s'),
axis([ 0 13.0 -.001 .001]),grid
pause
%print
subplot(3,1,1),plot(T,xsep),ylabel('x chf-dep alongtrk,km'),title('KSC Dep. 3 km Trail, J2 & Drag
Act')
axis([0.0 12000 -4.0 -2.0]),grid
subplot(3,1,2),plot(T,yHL),ylabel('y chf-dep crosstrk,km')
axis([0.0 12000 -5. 5.]),grid
subplot(3,1,3),plot(T,zsep),xlabel('Time,sec. '),ylabel('z chf-dep radial sep,km')
axis([0.0 12000 -1.0 1.0]),grid
pause
%print
subplot(3,1,1),plot(T,xveldiff),ylabel('x vel diff,km/sec'),title('KSC Dep. 3 km Trail, J2 & Drag
Act')
axis([0.0 12000 -.001 .001]),grid
subplot(3,1,2),plot(T,yveldiff),ylabel('y cross-trck vel diff,km/sec'),
axis([0.0 12000 -.001 .001]),grid
subplot(3,1,3),plot(T,zveldiff),xlabel('Time,sec. '),ylabel('radial vel diff,km/sec'),
axis([0.0 12000 -.001 .001]),grid
pause
%print
%subplot(3,1,1),plot(T,X_rocket),ylabel('X-dep rocket,km/sec2'),title('Rocket Triad Inputs For 3
km Hold')
%axis([0.0 12000 -.0001 .0001]),grid
%subplot(3,1,2),plot(T,Y_rocket),ylabel('Y-dep rocket,km/sec2'),
%axis([0.0 12000 -.0001 .0001]),grid
%subplot(3,1,3),plot(T,Z_rocket),xlabel('Time,sec'),ylabel('Z-dep rocket,km/sec2'),
%axis([0.0 12000 -.0001 .0001]),grid
%pause
%print

```

```

subplot(3,1,1),plot(T,septn),ylabel('Chf-Dep Separation,km'),title('KSC Dep.3 Km Trail, J2 &
Drag Act')
axis([0.0 12000 0.0 5.]),grid
subplot(3,1,2),plot(T,idotdp),ylabel('dep idot,rad/s')
axis([0.0 12000 -.0001 .0001]),grid
subplot(3,1,3),plot(T,inc_dp),ylabel('dept inclinatr, rad.')
axis([0.0 12000 .49 .50]),grid
pause
subplot(3,1,1),plot(T,yJ2dp),ylabel('y disp/ J2,km'),title('KSC Dep.3 Km Trail, J2 & Drag Act')
axis([0.0 12000 -10. 10.]),grid
subplot(3,1,2),plot(T,yTOTdp),ylabel('y total disp,km')
axis([0.0 12000 -10. 10.]),grid
subplot(3,1,3),plot(T,yTOTchf),ylabel('y chf tot disp,km')
axis([0.0 12000 -10. 10.]),grid
pause
%
polar(TA,xsep),title('TrueAnom vs. CHF-DEP x-axis diff, e=0.03, J2=Act,Drg=Act, Dep Trail
Chf 200 m')
pause
%print
polar(TA,yHL),title('TrueAnom vs. CHF-DEP y-axis diff, e=0.03, J2=Act,Drg=Act, Dep Trail
Chf 200 m')
pause
%print
polar(TA,zsep),title('TrueAnom vs. CHF-DEP z-axis diff, e=0.03, J2=Act,Drg=Act, Dep Trail
Chf 200 m')
pause
%print
polar(TA,xveldiff),title('TrueAnom vs.CHF-DEP x-rel vel, km/s, e=0.03, J2=Act,Drg=Act, Dep
Trail Chf 200 m')
pause
%print
polar(TA,yveldiff),title('TrueAnom vs. CHF-DEP y-axis diff,e=0.03, J2=Act,Drg=Act, Dep Trail
Chf 200 m')
pause
%print
polar(TA,zveldiff),title('TrueAnom vs. CHF-DEP z-axis diff,e=0.03, J2=Act,Drg=Act, Dep Trail
Chf 200 m')
pause
%print
polar(TA,yCfDpdiff),title('TrueAnom vs.CHF-DEP, y-axisJ2diff,e=0.03, J2=Act,Drg=Act, Dep
Trail Chf 200 km')
pause
%print

```

```

subplot(3,1,1),plot(TA,r),ylabel('Orbit Radius, km'),title('chief orbit, J2=Act,drg=Act, e=.03')
axis([0 13.0 6800. 8000.]),grid
subplot(3,1,2),plot(TA,v),ylabel('Velocity, km/sec')
axis([0 13.0 0 10.]),grid
subplot(3,1,3),plot(TA,w),xlabel('True anomaly, rad'),ylabel('w-state, km^2/sec')
axis([0 13.0 -2000. 2000.])
pause
pause
%print

%plot(T,TA),xlabel('TIME,sec'),ylabel('True Anomaly, radians'),title('drag=Act,J2=Act, e=.0')
%axis([0. 7000. 0. 7.0])
%pause
%print %(2)

subplot(3,1,1),plot(TA,yJ2chf),xlabel('TrueAnomly,rad'),ylabel('Chf y-drift wrt track, km'),
axis([ 0 13.0 -20. 20. ]),grid,title('Drag&J2=Act,Chf&Dep y-mvmnt wrt mean,e=0.0')
subplot(3,1,2),plot(TA,yJ2dp),xlabel('TrueAnomly,rad'),ylabel('Depty y-drift wrt track, km'),
axis([ 0 13.0 -20. 20.]),grid
subplot(3,1,3),plot(TA,yCfDpdiff),xlabel('TrueAnomaly,rad'),ylabel('Chf-Dep y(J2)diff, km'),
axis([ 0 13.0 -5. 5.]),grid
pause
%print

plot(TA,yHL),xlabel('TrueAnomaly,rad'),ylabel('Chf-Dep y-sep, km'),title('Drag&J2=Act,Chf-
Dep Diff dueto J2,e=0.0')
axis([ 0 13.0 -0.05 0.05]),grid
pause
%print
%plot(T,TAdot),xlabel('TIME,sec'),ylabel('sigmadot,rad/sec-e=.0')
%axis([ 0 6000. 0 .002])
%pause
%print
%plot(TA,r),xlabel('true anomaly,rad'),ylabel('Orbit Radius, km'),title('J2 =0,e=.00')
%axis([ 0.0 7.0 0 10000.])
%pause
%print
%subplot(3,1,1),plot(TA,pr),ylabel('J2 radial accel'),title('J2=0,drg=act,cicrular')

%subplot(3,1,2),plot(TA,ptrans),ylabel('J2 w/vel vector'),
%subplot(3,1,3),plot(TA,ph),xlabel('true anomaly,rad'),ylabel('J2 norm to orbit plane'),

%print

```

```

subplot(3,1,1),plot(TA,idot),xlabel('Time,sec'),ylabel('incl_rate,rad/sec'),title('Drag&J2=Act,e=.0
')
subplot(3,1,2),plot(TA,inc),ylabel('orbit inclination,rad')
subplot(3,1,3),plot(TA,hdot),xlabel('true anom,rad'),ylabel('hdot,km^2/sec^2')
pause
pause
pause
%print

subplot(3,1,1),plot(TA,OMGJ2dotplt),ylabel('J2 OMGdot,deg/day'),title('Drag&J2=Act., Daily
arg drifts ,e=.0')
axis([0.0 13.0 -10. 10.])
subplot(3,1,2),plot(TA,argJ2dotplt),ylabel('J2 wdot,deg/day')
axis([0.0 13.0 -10. 10.])
subplot(3,1,3),plot(TA,MJ2dotplt),xlabel('true anomaly,rad'),ylabel('J2 Mdot,deg/day')
axis([0.0 13.0 -10. 10.])
pause
pause
%print

subplot(2,1,1),plot(TA,OMG),ylabel('Right ascension,rad'),title('Drag&J2=Act, RtAscen vs
trueAnom,e=.0')
axis([0.0 13.0 .3 .4]),grid
subplot(2,1,2),plot(TA,OMG_dp),xlabel('true anomaly,rad'),ylabel('Dep Right asc,rad')
axis([0.0 13.0 .3 .4]),grid
pause
%print

subplot(2,1,1),plot(TA,argpgg),ylabel('arg of perigee,rad'),title('Drag&J2=Act,..Arg of Prgee Drift
vs trueAnom,e=.0')
axis([0.0 13.0 .1 .2])
subplot(2,1,2),plot(TA,MJ2),xlabel('true anomaly,rad'),ylabel('J2=Act, drift mean anomaly,rad'),
axis([0.0 13.0 0 1.2])
pause
%print

subplot(3,1,1),plot(TA,xsep),ylabel('x chf-dep alongtrk,km'),title('Drag&J2=Act.,Chf-Dep
Seprtn-e=.0')
axis([0.0 13.0 -20. 20.]),grid
subplot(3,1,2),plot(TA,yHL),ylabel('y chf-dep crosstrk,km')
axis([0.0 13.0 -5. 5.]),grid
subplot(3,1,3),plot(TA,zsep),xlabel('true anomaly, rad'),ylabel('z chf-dep radial sep,km')
axis([0.0 13.0 -20. 20.]),grid
pause

```

```

pause
pause
%print

plot(TA,septn),xlabel('true anomaly,rad'),ylabel('Chf-Dep separtn,km'),title('Drag&J2=Act,Chf-
Dep sep,e=.0')
axis([0. 13.0  0. 30.0]),grid
pause
%print
plot(xsep,zsep),xlabel('along track disp,km'),ylabel('radial disp,km'),title('Drag&J2=Act,Orbit
plane chf/dep,e=.0')
axis([-20. 20. -20. 20.]),grid
pause
pause
pause
%print

subplot(3,1,1),plot(TA,xveldiff),ylabel('x vel diff,km/sec'),title('Drag&J2=Act.,Chf/Dep rel.vel
,e=.0')
axis([0.0 13.0  -.01 .01]),grid
subplot(3,1,2),plot(TA,yveldiff),ylabel('cross-trck vel diff,km/sec'),
axis([0.0 13.0  -.01 .01]),grid
subplot(3,1,3),plot(TA,zveldiff),xlabel('true anomaly,rad'),ylabel('radial vel diff,km/sec'),
axis([0.0 13.0  -.01 .01]),grid
pause
%print
plot(zsep,yHL),xlabel('radial distance, chf/dep,km'),ylabel('cross-track dist,
chf/dep,km'),title('Dist to dpt,Drag&J2=Act, e=.0')
axis([-20. 20. -5. 5.]),grid
pause
pause

%print

```

LIST OF REFERENCES

- 1) Campbell and Schetter, "Formation Flying Mission for the UW Dawgstar Satellite", University of Washington, Seattle, WA, IEEE 0-7803-5846-5/00, 2000
- 2) Schweighart & Sedwick, "High-Fidelity Linearized J_2 Model For Satellite Formation Flight", Massachusetts Institute of Technology, Cambridge, MA, May 2002.
- 3) Roberts & Roberts, "The Development of High Fidelity Linearized J_2 Models For Satellite Formation Flying Control.", AAS 04-162, Cranfield University, UK, 2004.
- 4) Inalhan, Tillerson, & How, "Relative Dynamics and Control of Spacecraft Formations In Eccentric Orbits", Stanford and MIT, February 2002.
- 5) F. Brown, R. Johnson, and D. Norris, "Guidance and Control for Aerospace Vehicles ", Hanford House Publishing, London, North Atlantic Treaty Organization (NATO), AGARDograph 131, June 1969.
- 6) Curtis, Orbital Mechanics for Engineering Students, Embry-Riddle Aeronautical University, Elsevier Aerospace Engineering Series, Elsevier Butterworth-Heinemann, Oxford, UK, 2005.
- 7) David A. Vallado, Fundamentals of Astrodynamics and Applications (second edition) , Microcosm Press, El Segundo, CA, 2001.
- 8) Schaub and Junkins, Analytical Mechanics of Space Systems, AIAA Education Series, 2003.